ΠΟΛΥΤΕΧΝΕΙΟ ΚΡΗΤΗΣ

ΣΧΟΛΗ ΗΛΕΚΤΡΟΛΟΓΩΝ ΜΗΧΑΝΙΚΩΝ ΚΑΙ

ΜΗΧΑΝΙΚΩΝ ΥΠΟΛΟΓΙΣΤΩΝ

Διπλωματική Εργασία

Μελέτη Συστήματος Οδήγησης Ηλεκτρικού Κινητήρα με

τη Μέθοδο SPWM

Μιχελακάκης Δ. Παναγιώτης

Εξεταστική Επιτροπή

Αναπληρωτής Καθηγητής Κωνσταντίνος Γυφτάκης (Επιβλέπων)

Καθηγητής Ευτύχιος Κουτρούλης

Επίκουρος Καθηγητής Γεώργιος Πέππας

Χανιά, Σεπτέμβριος 2024

TECHNICAL UNIVERSITY OF CRETE

DEPARTMENT OF ELECTRICAL & COMPUTER ENGINEERING

Diploma Thesis

Study of an Electric Motor Drive System

using the SPWM Method

Michelakakis D. Panagiotis

Supervising Committee

Associate Professor Konstantinos Gyftakis (Supervisor)

Professor Eftichios Koutroulis

Assistant Professor George Peppas

Chania, September 2024

ACKNOWLEDGEMENTS

With the completion of this thesis, I would like to thank all those who helped me and contributed decisively, during its preparation. First of all, my sincere thanks to Professor Mr. Konstantinos Gyftakis for the trust he showed in me by assigning me this topic, his multi-level support and guidance, the excellent cooperation, as well as for the opportunity he gave me to deal with this scientific field, in order to acquire an appropriate theoretical background in the field of Electronics and Energy Systems. A field in which I look forward to joining and contributing with my knowledge, thereby realizing my next professional step of my carrier.

I would also like to thank the distinguished professors Mr. Eftichios Koutroulis and Mr. George Peppas, whose contribution to the Department of Electrical and Computer Engineering of the Technical University of Crete has been unquestionable for years. I am truthfully really honored by their participation in the three-member supervising committee of my thesis.

Separately, I would like to thank my family and friends whose support and patience played a catalytic role in the completion of this work.

Last but not least, a lot of thanks for the discredit and lack of respect, to all of those who consider the quote “Never give up, because it’s never too late” is nothing more than empty words. They just armed me with excessive tenacity and determination in accomplishing my goal.

ABSTRACT

The aim of this diploma thesis is to present the study, analysis and implementation of a DC to AC voltage source inverter (**VSI**), utilizing the beneficial Sinusoidal Pulse Width Modulation (**SPWM**) technique, in order to efficiently control the speed of an AC asynchronous-**induction motor**. For this purpose, the components which make up a motor drive system are briefly explained in general at first, and then, the relevant theory of DC/AC converters (called **inverters**) using the SPWM technique, the basics of AC machinery fundamentals, the relevant theory of induction motors, as well as some generic control strategies of AC motor drive systems are analyzed chapter by chapter. Eventually, a final of two chapters are following, one for simulations and comparisons of experimental results with the respective theory, while the last one stands for indicating the most significant conclusions and possible future work, according to this paper. The overall control system was built-up with **MATLAB/SIMULINK** software package. A variable frequency output waveform of sinusoidal type is produced by the inverter, to run and test a motor at variable speed and load torque conditions, which are directly related to this frequency. The overall circuit was also tested using a typical automatic control system, as constant ratio voltage to frequency **(V/f) scalar** control method, either in an open or in a closed loop configuration. The simulation results, based on a single-phase induction motor drive circuit fed by a single-phase SPWM inverter with a DC Voltage Source (DC is one type of energy found in batteries and AC is a type of energy produced by the power company and found in electrical homes/offices appliances), illustrated that the dynamic speed response of the induction motor is efficient enough, with improved **THD** and power quality (**PF)** factors. The overall results seemed to satisfy and apply to the theoretical conclusions pretty efficiently.

Key Words : Electric drive systems, induction machine, Single-phase inverter, sinusoidal pulse width modulation, scalar control V/f, Capacitor Start – Capacitor Run induction motor

ΠΕΡΙΛΗΨΗ

Σκοπός της παρούσας διπλωματικής εργασίας είναι να παρουσιάσει τη μελέτη, την ανάλυση και την υλοποίηση σε περιβάλλον προσομοίωσης ενός **μετατροπέα πηγής τάσης** (**VSI**) από συνεχές σε εναλλασσόμενο ρεύμα, χρησιμοποιώντας την ευεργετική τεχνική διαμόρφωσης πλάτους ημιτονοειδούς παλμού (**SPWM**), προκειμένου να ελέγχεται αποτελεσματικά η ταχύτητα ενός **ασύγχρονου επαγωγικού κινητήρα** εναλλασσόμενου ρεύματος. Για τον σκοπό αυτό, αρχικά εξηγούνται συνοπτικά οι ηλεκτρομηχανικές συνιστώσες που απαρτίζουν ένα σύστημα οδήγησης κινητήρων και στη συνέχεια, αναλύονται ανά κεφάλαιο η σχετική θεωρία των μετατροπέων DC/AC (που ονομάζονται **αντιστροφείς**) που χρησιμοποιούν την τεχνική SPWM, τα βασικά στοιχεία των θεμελιωδών αρχών των μηχανών εναλλασσόμενου ρεύματος, η σχετική θεωρία των επαγωγικών κινητήρων, καθώς και ορισμένες γενικές στρατηγικές αυτομάτου ελέγχου των συστημάτων οδήγησης κινητήρων εναλλασσόμενου ρεύματος. Ακολουθούν άλλα δύο κεφάλαια, το ένα για προσομοιώσεις και συγκρίσεις πειραματικών αποτελεσμάτων με την αντίστοιχη θεωρία, ενώ το τελευταίο επισημαίνει τα σημαντικότερα συμπεράσματα, καθώς και πιθανές προτάσεις για περαιτέρω διερεύνηση της παρούσας εργασίας. Το συνολικό σύστημα ελέγχου κατασκευάστηκε με το πακέτο λογισμικού **MATLAB/SIMULINK**. Μια κυματομορφή εξόδου μεταβλητής συχνότητας ημιτονοειδούς μορφής παράγεται από τον αντιστροφέα, για να λειτουργήσει και να δοκιμαστεί ένας κινητήρας σε συνθήκες μεταβλητής ταχύτητας και ροπής φορτίου, οι οποίες σχετίζονται άμεσα με τη συχνότητα αυτή. Το συνολικό κύκλωμα δοκιμάστηκε επίσης με τη χρήση ενός τυπικού συστήματος αυτόματου ελέγχου, όπως η μέθοδος **κλιμακωτού ελέγχου** σταθερού λόγου τάσης προς συχνότητα (**V/f**), είτε σε διάταξη ανοικτού είτε κλειστού βρόχου. Τα αποτελέσματα της προσομοίωσης, με βάση ένα μονοφασικό κύκλωμα κίνησης επαγωγικού κινητήρα που τροφοδοτείται από έναν μονοφασικό μετατροπέα SPWM με πηγή συνεχούς τάσης (η συνεχής τάση είναι ένας τύπος ενέργειας που βρίσκεται στις μπαταρίες και η εναλλασσόμενη είναι ένας τύπος ενέργειας που παράγεται από την εταιρεία ηλεκτρισμού και βρίσκεται στις ηλεκτρικές συσκευές των σπιτιών/γραφείων), κατέδειξαν ότι η δυναμική απόκριση ταχύτητας του επαγωγικού κινητήρα είναι αρκετά αποδοτική, με βελτιωμένους συντελεστές **THD** (συνολική αρμονική παραμόρφωση) και ποιότητας ισχύος (**PF**). Τα συνολικά αποτελέσματα φάνηκε να ικανοποιούν και να ταυτίζονται με τα αντίστοιχα θεωρητικά συμπεράσματα αρκετά αποτελεσματικά.

TABLE OF INDEX - CONTENTS

CHAPTER 1 - INTRODUCTION **1**
1.1 Purpose of this diploma thesis 1
1.2 Format of the diploma thesis 2

CHAPTER 2 - INTRODUCTION TO MOTOR DRIVE SYSTEMS **4**
2.1 Power Source 4
2.2 Power Processor (Converter) 5
2.3 Electric Machine (Motor) 7
2.4 The Load 8
2.5 Control Unit (Feedback Controller) 9

CHAPTER 3 - SWITCH-MODE DC-AC CONVERTERS (INVERTERS) **10**
3.1 Introduction of Switch-mode dc-to-ac Inverters 10
3.2 Basic Concepts of Single-Phase Switch-Mode Inverters 11
3.3 Introduction of H-Bridge Inverters 12
3.4 Sinusoidal - Pulse - Width - Modulated Switching Scheme (SPWM) explained 13
3.5 SPWM with Bipolar Voltage Switching (in Half-Bridge inverter) 15
3.6 True Sine Wave Generation in the Output of the Inverter 21
3.7 Full-Bridge Inverter employing SPWM Bipolar voltage switching 23
3.8 Full-Bridge Inverter employing SPWM Unipolar voltage switching 24

CHAPTER 4 - AC MACHINERY FUNDAMENTALS **27**
4.1 Introduction to Machinery Principles 27
4.1.1 The Magnetic Field Production in A Magnetic Circuit 27
4.1.2 Magnetic Behavior of Ferromagnetic Materials 29
4.1.3 Faraday's Law - Induced Voltage from A Time-Changing Magnetic Field 30
4.1.4 Production of Induced Force on A Wire 31
4.1.5 Induced Voltage on A Conductor Moving in A Magnetic Field 32
4.1.6 Real, Reactive and Apparent Power in Single-Phase AC Circuits 32
4.2 A Simple Loop in a Uniform Magnetic Field 34
4.2.1 The Voltage Induced in a Simple Rotating Loop 34
4.2.2 The Torque Induced in a Current-Carrying Loop 35
4.3 The Rotating Magnetic Field 36
4.3.1 Proof of the Rotating Magnetic Field Concept 36
4.3.2 The Relationship between Frequency and Speed of the Magnetic Field Rotation 39
4.3.3 Reversing the Direction of Magnetic Field Rotation 40
4.4 Magnetomotive Force and Flux Distribution on AC Machines 41
4.5 Induced Voltage in AC Machines 42
4.5.1 The Induced Voltage in a Coil on a Two-Pole Stator 42
4.5.2 The Induced Voltage in a Three-Phase Set of Coils 44
4.5.3 The RMS Voltage in a Three-Phase Stator 45
4.6 Induced Torque In An AC Machine 46

CHAPTER 5 - AC MACHINES (INDUCTION MOTORS) **48**
5.1 Introduction of Induction Motors 48
5.1.1 The Development of Induced Torque in an Induction Motor 49
5.1.2 The Concept of Rotor Slip 50

5.1.3 The Electrical Frequency on the Rotor ... 51
5.2 Losses, Power and Torque in Induction Motors ... 51
5.3 Introduction To Single-Phase Induction Motors ... 54
5.3.1 The Double-Revolving-Field Theory of Single-Phase Induction Motors ... 56
5.3.2 The Cross-Field Theory of Single-Phase Induction Motors ... 58
5.4 Starting Single-Phase Induction Motors ... 60
5.4.1 Split-Phase Windings ... 61
5.4.2 Capacitor-Start Motors ... 63
5.4.3 Permanent Split-Capacitor and Capacitor-Start, Capacitor-Run Motors ... 64
5.4.4 Shaded-Pole Motors ... 66
5.5 Speed Control of Single-Phase Induction Motors ... 67
5.6 The Circuit Model of A Single-Phase Induction Motor ... 69
5.7 Circuit Analysis with the Single-Phase Induction Motor Equivalent Circuit ... 70

CHAPTER 6 - CONTROL STRATEGIES OF AC MOTOR DRIVE SYSTEMS ... 74
6.1 Introduction to Basic Control Methods of Induction Motors ... 74
6.2 Scalar Control with Constant Voltage to Frequency Ratio (V/f) ... 75
6.2.1 Open-Loop Control Circuit in PWM-VSI Drives ... 75
6.2.2 Scalar Control in a Closed-loop Circuit ... 77

CHAPTER 7 - IMPLEMENTATION AND SIMULATION RESULTS ... 79
7.1 A Single-Phase SPWM-VSI with Bipolar and Unipolar Voltage Switching Technique ... 79
7.2 Scalar Control of an SPWM Single-Phase VSI Motor Drive System (open-loop) ... 86
7.3 Scalar Control of an SPWM Single-Phase VSI Motor Drive System (closed-loop) ... 94

CHAPTER 8 - GENERAL CONCLUSIONS AND FUTURE WORK ... 96
8.1 General Conclusions According to Theory and Simulation Results ... 96
8.2 Future Work ... 97

REFERENCES ... 98

1. INTRODUCTION

1.1 Purpose of this diploma thesis

The purpose of this diploma thesis is to present the study, analysis, and implementation of a **DC** to **AC voltage source inverter** (**VSI**), utilizing the beneficial **Sinusoidal Pulse Width Modulation** (**SPWM**) technique, in order to efficiently control the speed of an **AC motor**. A VSI is a type of power inverter that converts direct current (DC) into alternating current (AC). Unlike current source inverters (CSI), which output a current waveform, VSIs output a voltage waveform. The primary advantage of a VSI is its ability to provide a stable and controllable AC voltage output from a DC power source, making it highly suitable for applications that require precise voltage regulation and control, such as driving induction motors. VSIs are widely used in various power electronic applications due to their robust performance and efficiency **[1]**. **Induction motors**, also known as **asynchronous motors**, are a type of AC motor where power is supplied to the rotor by electromagnetic induction, rather than by direct electrical connections. They are widely used in industrial and domestic applications due to their robustness, reliability, and simplicity. Induction motors operate on the principle of electromagnetic induction, where a rotating magnetic field induces a current in the rotor, which in turn produces torque. These motors are known for their durability and low maintenance requirements, making them ideal for heavy-duty applications **[2]**.

The **SPWM** technique operates by modulating the width of the pulses in a pulse train, in a way that the average voltage follows a sine wave. This modulation is achieved by comparing a sinusoidal reference signal with a high-frequency triangular carrier signal. When the reference signal is greater than the carrier signal, the output is high, and when it is lower, the output is low. This method results in a series of pulses that can be filtered to produce a smooth AC waveform, which is essential for driving AC motors. One of the primary advantages of SPWM is its ability to significantly reduce harmonic distortion in the output waveform. Harmonics are undesirable frequencies that can cause additional heating in motors, leading to inefficiency and potential damage. By minimizing these harmonics, SPWM ensures smoother and more efficient motor operation **[3]**. **Total Harmonic Distortion** (**THD**) is a measure of the harmonic distortion present in a signal and is defined as the ratio of the sum of the powers of all harmonic frequencies above the fundamental frequency to the power of the fundamental frequency. In the context of power systems and inverters, THD quantifies the distortion of the output voltage or current waveform due to the presence of harmonics. High THD can lead to inefficiencies, overheating, and potential damage to electrical equipment. Therefore, reducing THD is a key objective in the design of inverters and motor drives, making SPWM an attractive technique due to its effectiveness in minimizing harmonic content **[4]**. Additionally, the SPWM technique achieves fine control over the motor speed and torque, which is critical in applications requiring precise motor performance.

Efficiency is a critical factor in the design of any power electronic system. The SPWM technique contributes to higher efficiency in several ways. Firstly, it allows for better utilization of the DC input voltage, ensuring that more of the input power is converted into useful AC power. Secondly, the reduction in harmonics means less energy is wasted as heat, which not only improves efficiency but also enhances the longevity of the motor and the inverter components **[1]**. **Power factor (PF)** is a measure of how effectively electrical power is being used by a system and is defined as the ratio of real power (measured in watts) to apparent power (measured in volt-amperes). It ranges from 0 to 1, with a power factor of 1 indicating that all the power is being effectively converted into useful work. In AC power systems, a low power factor indicates poor efficiency, as more power is required to achieve the same amount of useful work. Induction motors, especially when lightly loaded, can have a low power factor, which necessitates the use of techniques like SPWM to improve efficiency and reduce energy losses **[1]**.

Reliability is another significant advantage of SPWM-based inverters. The technique's inherent ability to produce a high-quality output waveform reduces the stress on the motor and inverter components. This reduction in stress leads to lower failure rates and longer operational lifespans for the system. Furthermore, modern implementations of SPWM are often enhanced with advanced digital control techniques, which provide robust protection mechanisms against overcurrent, overvoltage, and thermal overload conditions **[5]**.

The versatility and efficiency of SPWM-based inverters have led to their widespread adoption across various industries. In industrial automation, these inverters are used to control the speed and torque of conveyor belts, pumps, and fans, enabling precise control of production processes. In the renewable energy sector, SPWM inverters are critical for converting DC power from solar panels and wind turbines into AC power suitable for the grid or for local consumption **[6]**. Electric vehicles (EVs) also heavily rely on SPWM-inverters to drive their AC motors. The precise speed control and high efficiency provided by SPWM are essential for the performance and range of EVs, making this technology a cornerstone of modern electric transportation. In home appliances, SPWM inverters are used in applications such as air conditioners and washing machines, where they contribute to energy savings and improved appliance performance.

In conclusion, the study, analysis, and implementation of a DC to AC VSI using the SPWM technique provide a robust and efficient solution for controlling the speed of AC asynchronous-induction motors. The ability of SPWM to reduce harmonics, improve efficiency, provide precise control and enhance reliability, makes it an indispensable technology in the power electronics industry. Its widespread application across industrial automation, renewable energy, electric vehicles, and home appliances underscores its significance and ensures its continued relevance in advancing modern technological solutions.

1.2 Format of diploma thesis

Initially, the paper presents the theoretical background required for the implementation of an overall motor drive system. Then, it gradually analyzes the main components needed for the construction process of the thesis (inverters and induction motors), concluding, finally, in designing the proper system and obtaining results, as well as experimental confirmations, during the simulation of system's operation. Below, is a brief description of the chapters that compose the present project.

- **Chapter 2:** This chapter discusses the subsystems that make up the overall electric drive system and the most important applications of electric motor drive systems in industry.

- **Chapter 3:** The third chapter provides a detailed analysis of switch-mode **dc**-**ac** converters, called inverters, explains both cases of the SPWM technique (**bipolar** and **unipolar** voltage-switching) on voltage source inverters (VSIs) and describes the construction and topology of a proper VSI, capable of feeding inductive-type of loads, such as AC machines.

- **Chapter 4:** The fourth chapter mediates between chapter of inverters and the chapter of induction motors and was written, in order to provide an intermediate theoretical stepping stone for the understanding of basic **AC machinery fundamentals**, as we bring the system analysis from electric to mechanical basis, including useful and worth mentioning concepts, such as the rotating magnetic field, Faraday's Law, the induced voltage and torque on AC machines, magnetomotive force and flux distribution on AC machines etc..

- **Chapter 5:** This chapter provides a detailed analysis of AC machines (**induction motors**), illustrates the manufacturing configuration of asynchronous motors (stator and the two types of rotors) and explains in the beginning the operation of induction motors as a three-phase set of currents. Then, the analysis of single-phase induction motors is carried out, in order to emphasize the significance of the starting techniques end eventually the starting currents at the windings of a **single-phase motor** (such as **split-phase** windings, **capacitor-type** windings, **shaded stator poles**).

- **Chapter 6:** This chapter delves into the complexities and advancements in automatic control strategies for AC motor drive systems. It reviews the most common control techniques (such as V/f scalar control, Field Oriented Control and Direct Torque Control), states briefly some more modern strategies and finally, it discusses in further detail , the method of scalar control with constant voltage-to-frequency ratio, either in an open-loop or in a closed-loop circuit configuration.

- **Chapter 7:** In the seventh chapter, the design of the overall system is implemented and its operation is simulated with the use of Simulink/MATLAB software package. Basically, three main experiments have taken place, to underline the differences, as long as the respective efficiency between the two types of voltage switching by SPWM in inverters-VSIs (bipolar and unipolar) and subsequently, to confirm a satisfactory operation of a complete single-phase motor driving system using SPWM, under various load circumstances, either as an open-loop or as a closed-loop circuit configuration.

- **Chapter 8:** The final chapter of the present paper, contains the summary of the results and conclusions extracted from the previous simulating processes, in order to confirm those practical results with the relative theoretical ones. It makes a short assessment of the overall work and points out its impact in both industrial and research applications, as well as in simple practical devices of everyday life. Finally, some guidelines are given for possible future work that can extend and improve this thesis.

2. INTRODUCTION TO MOTOR DRIVE SYSTEMS

In today's era, electric motor drives are assumed as one of the most important and most useful fields of Electrical and Computer Engineering, while they are playing a vital role in a wide range of applications, from simple everyday life's tasks to applications in science and research. From high-performance position-controlled drives in robotics to a simple adjustment of the speed of an electric hand drill **[7]**.

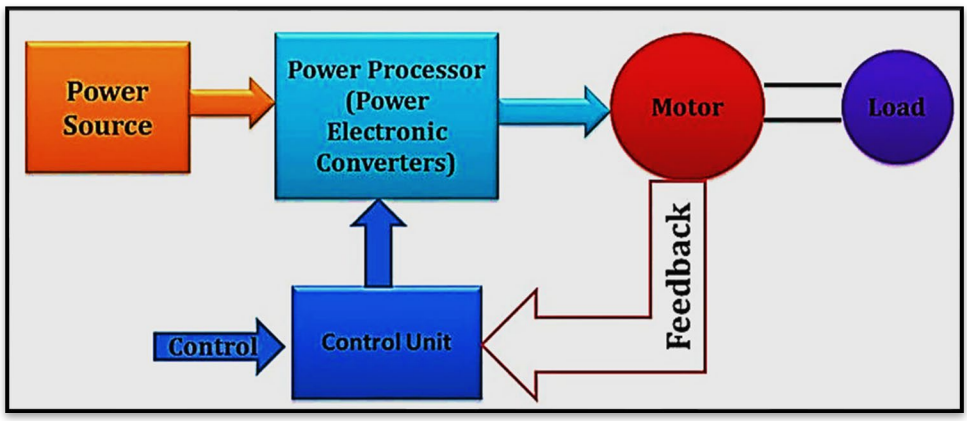

Figure 2.1 – A general diagram of motor drives [8]

In their general form as shown above in **Figure 2.1**, they appear as integrated electromechanical circuits, which consist of the following components **[9]**, **[10]**, **[12]**;

2.1 Power source

The power source can provide alternating voltage coming from the grid (PPC-Δ.Ε.Η.) and it can be achieved either with single-phase or with symmetrical three-phase. This trend is mainly produced by thermal power stations and in less cases by renewable energy sources (e.g. wind, solar, etc.). Also, direct voltages can be produced by power sources, coming from accumulators (batteries), photovoltaic arrays, rectified alternating grid voltage, etc.

Choosing the right power source depends on each time desirable application that needs to be implemented. In recent years and within the increase of interest in electromobility, the research on battery and electric accumulator technologies has greatly increased, due to the fact that they are considered as the biggest obstacle on electric motor drives. The main requirements are to provide high energy density, multi-cycle charge-discharge capability and high-power supply capability. The most developed battery technologies nowadays, are those of lithium ion (Li-ON) and lead-acid. The following **Fig 2.2** indicates the most common types of batteries with their related energy density per weight, as a function of the energy density per volume.

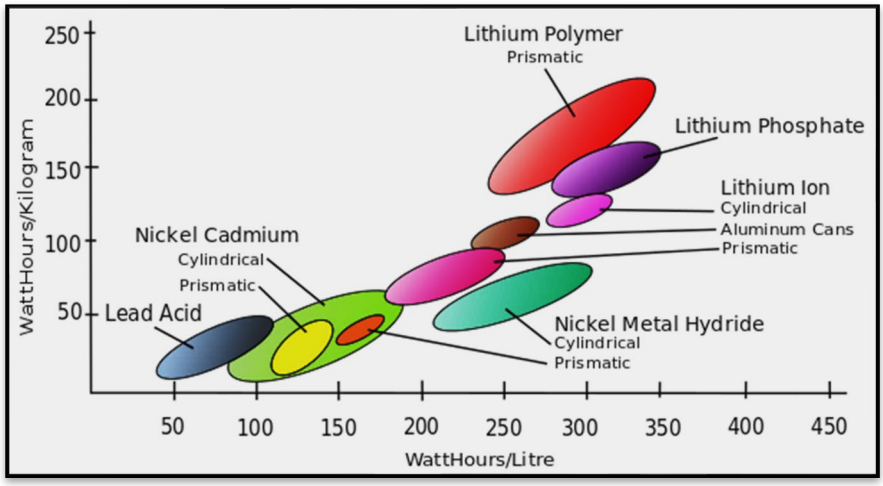

Figure 2.2 - Energy density diagram for most common types of batteries [11]

2.2 Power Processor (Converter)

A power processor is an electric device inserted between a power source and an electric machine. Its purpose is to enable the operation and manage the control of the machine and is achieved by changing the magnitude and form (frequency) of its voltage or of its current output. It will output a voltage or current capable of driving the motor according to the requirements of each application.

The power processors usually consist of more than one power conversion stage (as shown in **Fig 2.3**), where the operation of these stages is decoupled on an instantaneous basis by means of energy storage elements such as capacitors and inductors. Therefore, the instantaneous power input does not have to equal the instantaneous power output. Each power conversion stage is referred to as a power converter **[12]**.

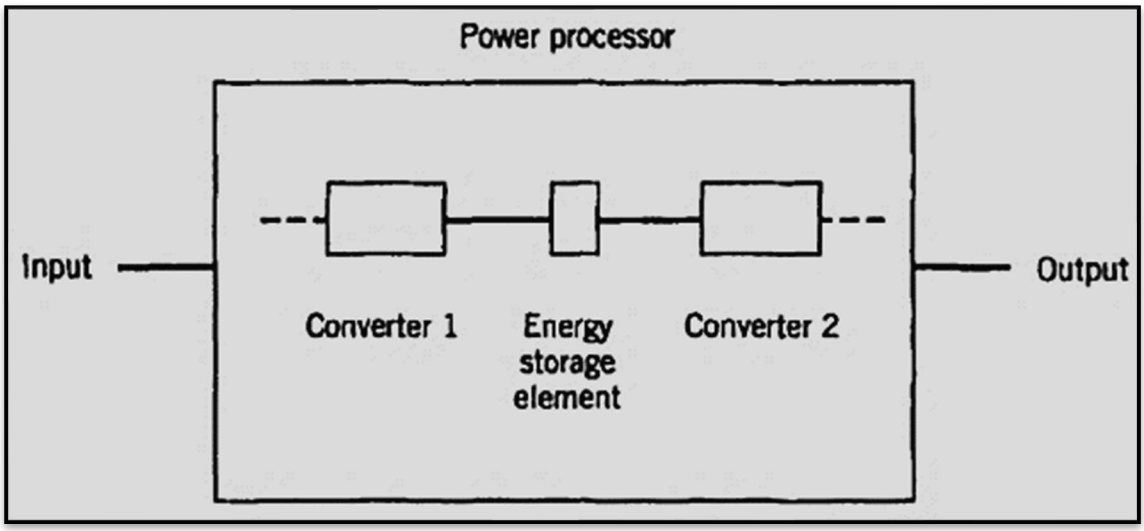

Figure 2.3 - Power processor block diagram [7]

Thus, a converter is a basic module (building block) of power electronic systems. It utilizes power semiconductor devices controlled by signal electronics (integrated circuits) and possibly energy storage elements such as inductors and capacitors. Based on the form (frequency) on the two sides, converters can be divided into the following broad categories:

• ***DC-DC power converter (Buck-Boost Converter)***. This converter provides the output with step-down or step-up DC input voltage.

• ***DC-AC power converter (or inverter)***. The inverter accepts a direct voltage as input and converts it into an alternating voltage three-phase or single-phase. The specific paper focuses especially on this particular type of converters due to their advantages, which follow below with further analysis.

• ***AC-DC power converter (or rectifier)***. The rectifier accepts as input a three-phase or single-phase alternating voltage and turns it into continuous **[12]**.

Various use cases of power converters are shown below in **Fig 2.4** :

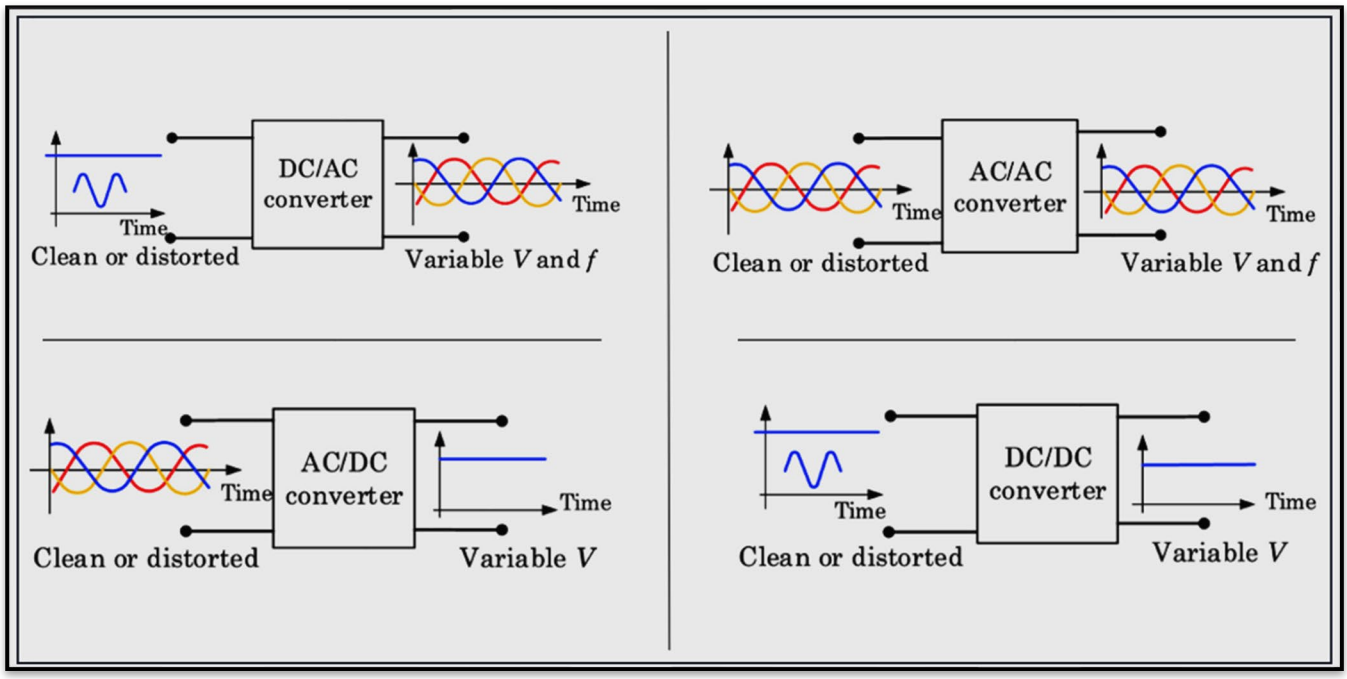

Figure 2.4 – Different use cases of power converters [13]

These converters have basically different topologies, but all of them consist of semiconductor elements that act as switches (diodes, thyristors or controlled switches). Controlled switches can be of many types, some of which are shown below:

• Bipolar Junction Transistors (BJTs)
• Metal-Oxide Semiconductor Field Effect Transistors (MOSFETs)
• Insulated Gate Bipolar Transistors (IGBTs)
• Gate Turn Off Thyristors (GTOs)

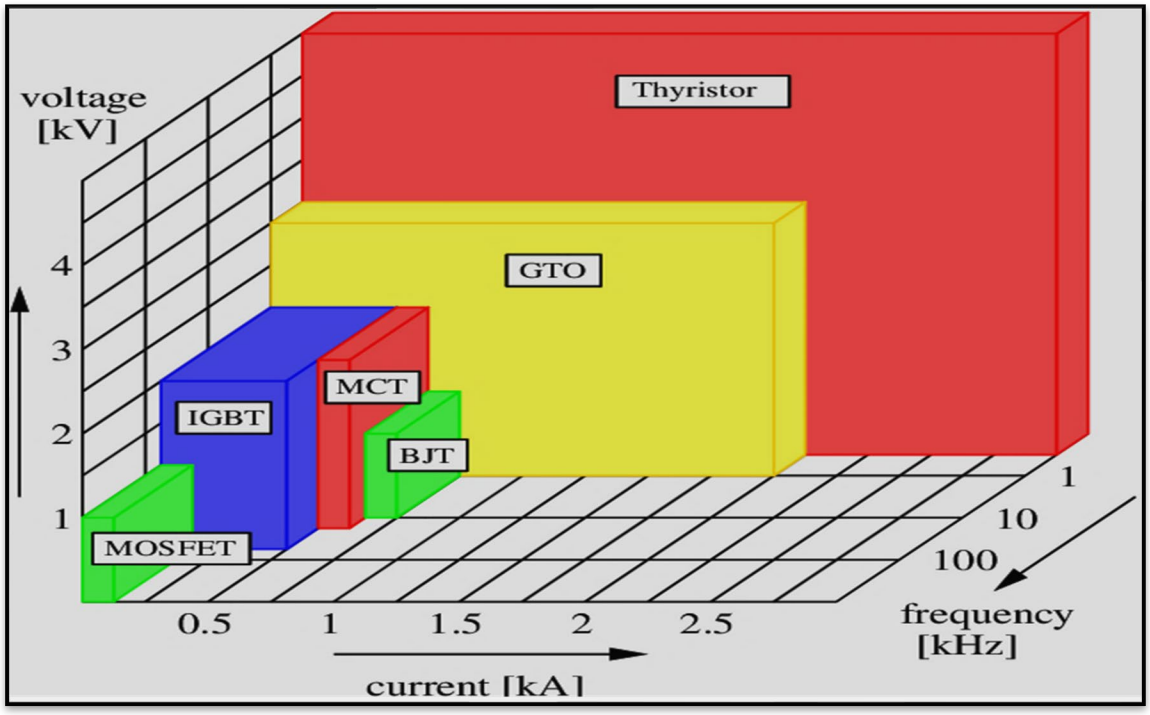

Figure 2.5 - Areas of correct operation for semiconductor elements [14]

Therefore, according to the type of application and its requirements, the selection of the appropriate semiconductor elements is based on the **Fig 2.5** above.

2.3 Electric Machine (Motor)

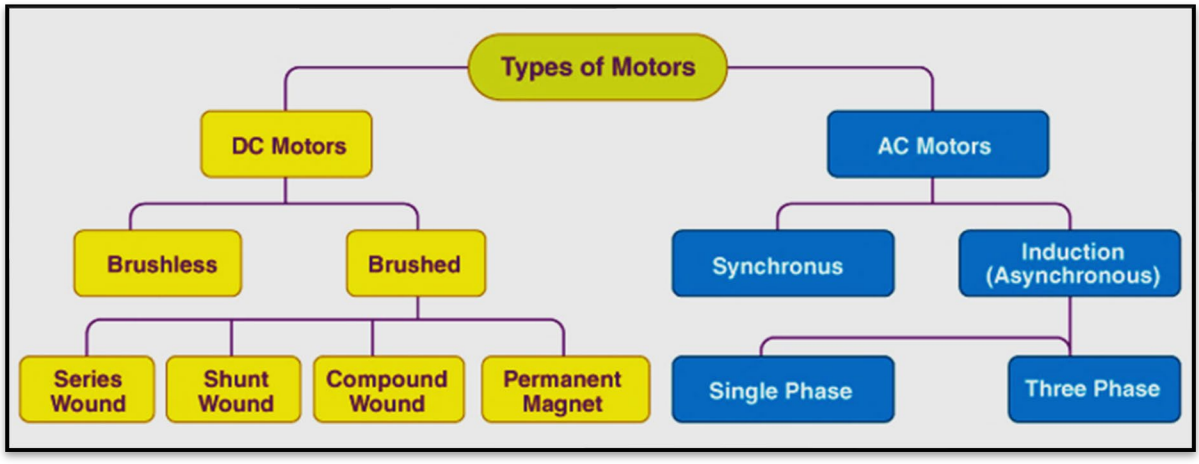

Figure 2.6 - A general classification of motor drives [15]

The electric machine or motor is the next part of the electric drive system and its function is to convert electrical energy into mechanical energy or vice versa. There are different types of motors with different properties, advantages and disadvantages to each other, which in general, are classified into two main categories, as in **Fig 2.6**.

- **DC Motors**

In direct current machines, the excitation field is located in the stator, while the field of the armature is in the rotor. Collectors and brushes equipped by a system of permanent magnets are used to maintain a stable field in the armature. Their control is simple and can be done by regulating the excitation and armature direct currents. This had made them irreplaceable in variable speed applications until about 30 years ago, when induction machines began to gain ground thanks to advanced control techniques. However, in applications where an extremely low maintenance is not required, dc drives continue to be used because of their low initial cost and excellent drive performance **[7]**.

- **AC Motors**

In general, AC machines are generators that convert mechanical energy to AC electrical energy and motors that convert AC electrical energy to mechanical energy. There are two major classes of ac machines. **Synchronous machines** are motors and generators whose magnetic field current is supplied by a separate dc power source, while **induction machines** are motors and generators whose field current is supplied by magnetic induction (transformer action) into their field windings. The field circuits of most synchronous and induction machines are located on their rotors.

Synchronous motors are used as servo drives in applications such as computer peripheral equipment, robotics, and adjustable-speed drives in a variety of applications such as load-proportional capacity-modulated heat pumps, large fans, and compressors. Instead of an excitation winding in the rotor, synchronous motors employ either permanent magnets, salient poles (having projecting magnetic poles), or an independently excited rotor winding to generate the excitation field. This resolves the issue of the machine's continuous power supply, while avoiding copper losses in the rotor winding. It is highly promising at the research level, and its use is expanding continuously in electromobility, due to its high efficiency and reliability. Some drawbacks include the constant excitation and the high cost of magnets.

The asynchronous type of AC machines is the most widespread both in industry and in electromobility. The reason for its common use is that induction motors can provide low complexity, low construction and maintenance costs, and high efficiency. Their name derives from its basic operating principle, which is always to rely on a small difference in speed between the stator rotating magnetic field and the rotor shaft speed called slip, in order to induce rotor current in the rotor AC winding. As a result, the induction motor cannot produce torque near synchronous speed where induction (or slip) is irrelevant or ceases to exist **[7]**, **[12]**.

2.4 The Load

The load is the primary element of the system, and the entire design is based on the requirements it imposes on each application. It is a mechanical system connected to the machine's shaft, exchanging energy with it (either receiving, if it is a motor, or delivering, if it is a generator). There are four typical cases of loads **[12]**:

Constant Power Load : The torque of the load is inversely proportional to the speed. The mechanical power of the load is constant. Examples of such loads include machine tools.

Constant Torque Load : The torque of the load is constant, while the mechanical power is a linear function of the speed. Examples of such loads include conveyors.

Linear Torque Load : The torque of the load is linear, and the mechanical power is a quadratic function of the speed. Examples of such loads include certain fans and centrifugal pumps, depending on their impeller type.

Parabolic Torque Load : The torque of the load is parabolic, while the mechanical power is a third-degree function of the speed. Examples of such loads include some other types of fans and centrifugal pumps, depending on their impeller type.

Fig 2.7 below, indicates the speed-torque and power-speed characteristics of typical loads.

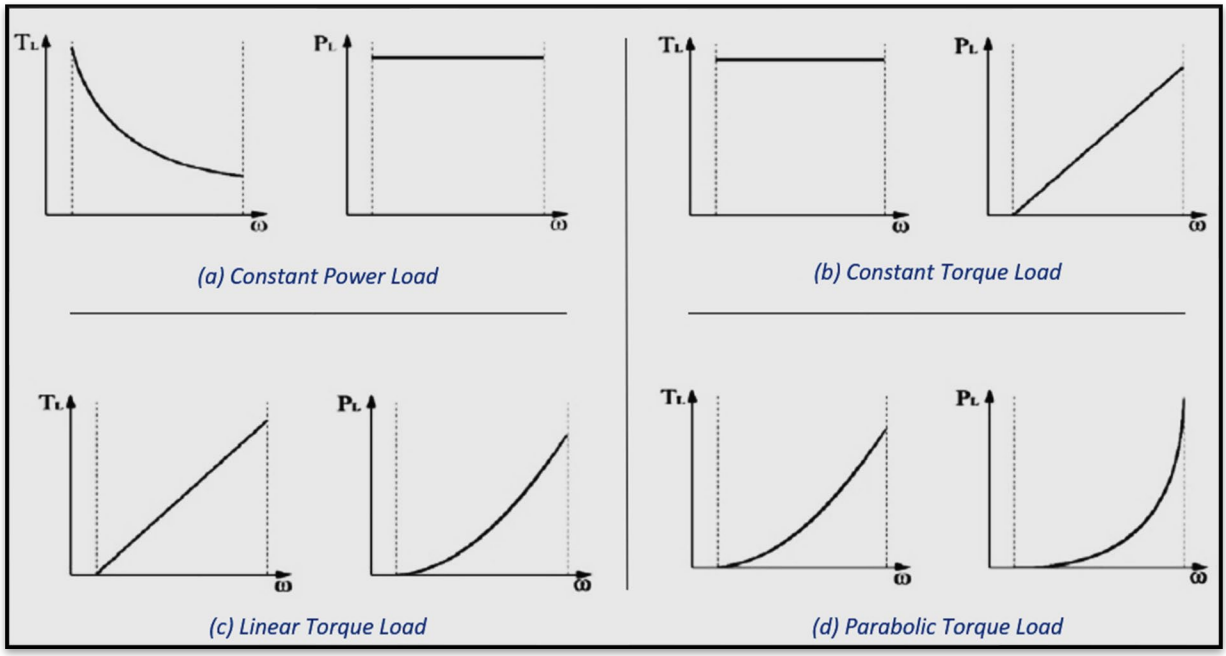

Figure 2.7 - Speed-torque and power-speed characteristics of typical loads [12]

2.5 Control Unit (Feedback Controller)

The control unit refers to the subsystem that monitors the operation of the entire system and takes actions to provide each time the desired response at the output.

Normally, a feedback controller compares the output of the power processor unit with a desired (or a reference) value, and the error between the two is minimized by the controller. The power flow through such systems may be reversible, thus interchanging the roles of the input and the output.

In recent years, the field of power electronics has experienced a large growth due to confluence of several factors. The controller in the block diagram of **Fig 2.1** consists of linear integrated circuits and/or digital signal processors. Revolutionary advances in microelectronics methods have led to the development of such controllers. Moreover, these advances in semiconductor fabrication technology have made it possible to significantly improve the voltage- and current-handling capabilities and the switching speeds of power semiconductor devices, which make up the power processor unit of **Fig 2.1**.

In many occasions, mathematical models, estimators, or observers are developed to perform as meters and sensors, calculating previously measured quantities and replacing them. This avoids distortion of measurements that may be due to environmental disturbances and makes the arrangement more reliable **[7]**.

3. SWITCH-MODE DC-AC CONVERTERS (INVERTERS)

3.1 Introduction of Switch-mode dc-to-ac Inverters

Switch-mode dc-to-ac inverters are used in ac motor drives and uninterruptible ac power supplies (UPS), where the objective is to produce a sinusoidal ac output whose magnitude and frequency can both be controlled. As an example, an ac motor drive, is shown in **Fig 3.1** in a block diagram form.

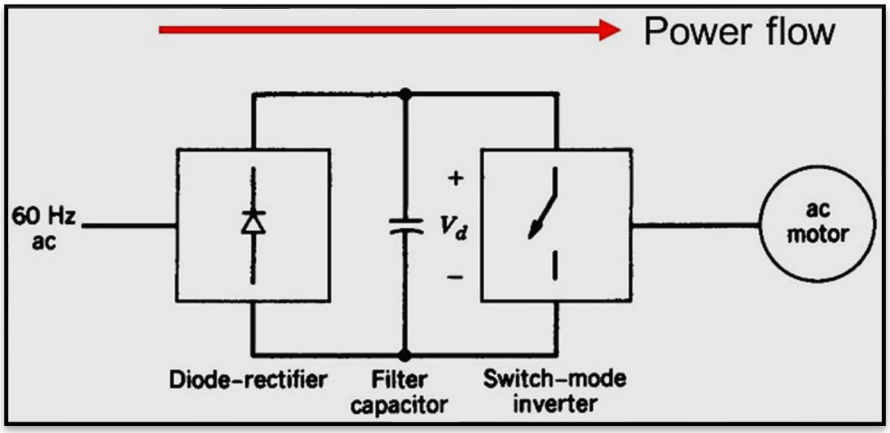

Figure 3.1 - Switch-mode inverter in AC motor drive [7]

The dc voltage is obtained by rectifying and filtering the line voltage, most often by the diode rectifier circuits. In an ac motor load, the voltage at its terminals is desired to be sinusoidal and adjustable in its magnitude and frequency. This is accomplished by means of the switch-mode dc-to-ac inverter of **Fig 3.1**, which accepts a dc voltage as the input and produces the desired ac voltage input. To be precise, the switch-mode inverter in **Fig 3.1** is a converter through which the power flow is reversible. However, most of the time the power flow is from the dc side to the motor on the ac side, requiring an inverter mode of operation. Therefore, these switch-mode converters are often referred to as **switch-mode inverters [7]**.

But in motor applications, where the so-called braking of the motor needs to be performed frequently, a better alternative is regenerative braking, where the energy recovered from the motor load inertia is fed back to the utility grid, as shown in the system of **Fig 3.2**.

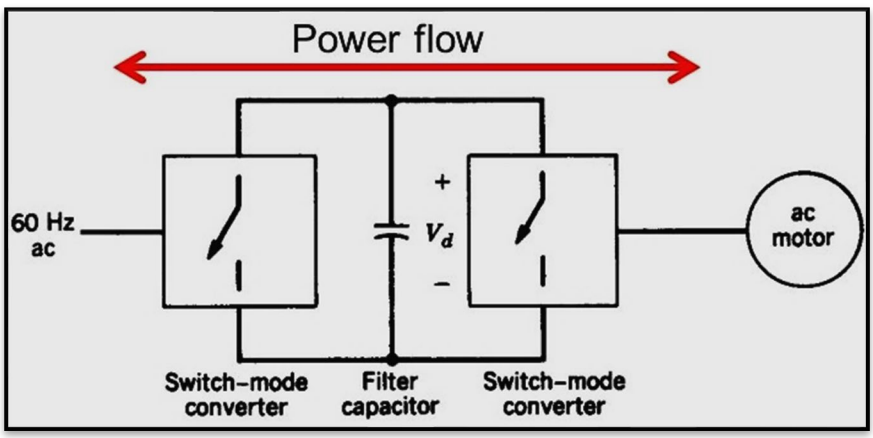

Figure 3.2 - Switch-mode converters for motoring and regenerative braking in AC motor drive [7]

This requires, that the converter connecting the drive to the utility grid be a two-quadrant converter with a reversible dc current, which can operate as a rectifier during the motoring mode of the ac motor and as an

inverter during the braking of the motor. Such a reversible-current two-quadrant converter can be realized by means of switch-mode converter as shown in **Fig 3.2**.

The input to switch-mode inverters is assumed to be a dc voltage source, in which the dc source has small or negligible impedance. The voltage at the input terminals is constant. Such inverters are referred to as voltage source inverters (**VSIs**). In this paper, we will analyze inverters with single-phase ac output.

In one of VSIs general categories, such as in circuit of **Fig 3.1**, the input dc voltage is essentially constant in magnitude**,** where a diode rectifier was used to rectify the line voltage. Therefore, the inverter must control the magnitude and the frequency of the ac output voltages. This is achieved by the **Pulse Width Modulation technique** of the inverter switches and hence such inverters are called **PWM inverters**.

Concerning PWM inverters, there are various schemes to pulse-width modulate the inverter switches in order to shape the output ac voltages to be as close to a sine wave as possible. Out of these various PWM schemes, the scheme **sinusoidal - PWM** will be discussed in further detail.

3.2 Basic Concepts of Single-Phase Switch-Mode Inverters

A single-phase inverter is shown in block diagram form in **Fig 3.3(a)**, where the output voltage of the inverter is filtered so that v_o can be assumed to be sinusoidal. Since the inverter supplies an inductive load such as an ac motor, i_o will lag v_o , as shown in **Fig 3.3(b)**.

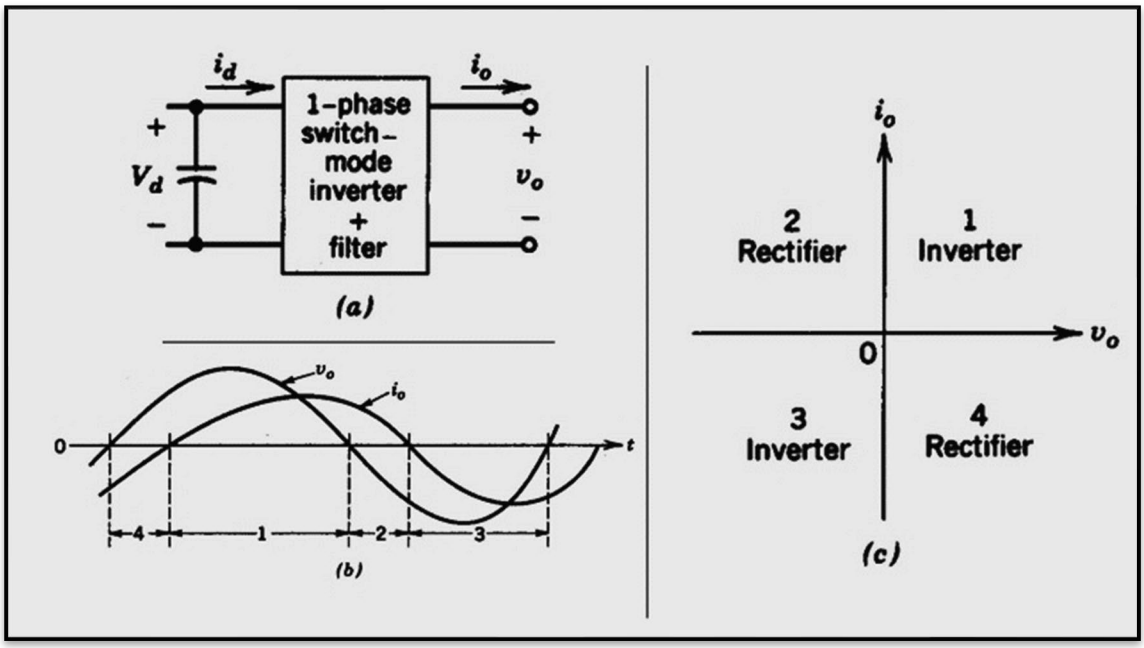

Figure 3.3 - Single-Phase Switch-Mode Inverter [7]

The output waveforms of the specific figure, show that during interval 1, v_o and i_o are both positive, whereas during interval 3, v_o and i_o are both negative. Therefore, during intervals 1 and 3, the instantaneous power flow p_o (= $v_o i_o$) is from the dc side to the ac side, corresponding to an inverter mode of operation.

In contrast, v_o and i_o are of opposite signs during intervals 2 and 4, and therefore p_o flows from the ac side to the dc side of the inverter, corresponding to a rectifier mode of operation. Thus, the switch-mode inverter of **Fig 3.3(a)** must be capable of operating in all four quadrants of the i_o-v_o plane, as shown in **Fig 3.3(c)** during each cycle of the ac output.

3.3 Introduction of H-Bridge Inverters

A VSI can be in the half-bridge or full-bridge configuration. The single-phase units can be joined to have three-phase or multiphase topologies **[16]**.

The half-bridge inverter in **Fig 3.4(a)**, consists of a one-leg of two switches, ***T+*** and ***T-*** . The two switches are switched in such a way that when one of them is in its OFF state, the other switch is ON. Therefore, they are never off simultaneously and the output voltage v_{Ao} , shown in **Fig 3.4(c)** in purple color, fluctuates between two values ($\frac{1}{2} V_d$ and $-\frac{1}{2} V_d$). These switches may be BJT, Thyristor, IGBT, etc. . ***D+*** and ***D-*** are called freewheeling diodes, also known as feedback diodes, as they feedback the load reactive power **[7]**.

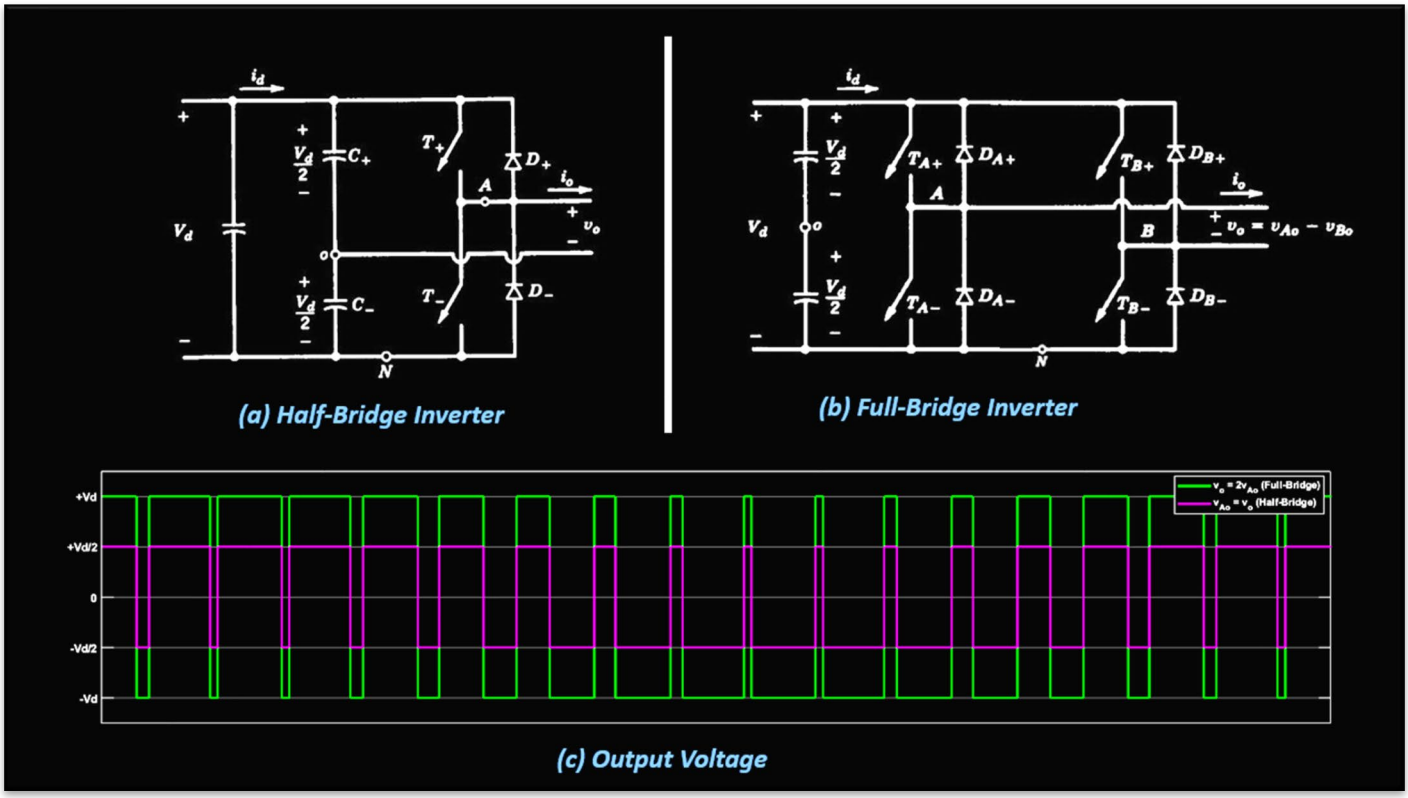

Figure 3.4 - Single-Phase H-Bridge Inverters

A full-bridge inverter is shown in **Fig 3.4(b)**, where the (green-colored) output voltage v_{AB} in **Fig 3.4(c)** fluctuates between two values (V_d and $-V_d$). This inverter consists of two one-leg inverters and is preferred over other arrangements in higher power ratings. With the same dc input voltage, the maximum output voltage of the full-bridge inverter is twice that of the half-bridge inverter. This implies that for the same power, the output current and the switch currents are one-half of those for a half-bridge inverter. At high power levels, this is a distinct advantage, since it requires less paralleling of devices **[17]**, **[18]**.

In the single-phase inverters of **Fig 3.4**, the input is a fixed-magnitude dc voltage V_d. The output of the inverter is a dc voltage v_o, which can be controlled in magnitude, as well as polarity. Similarly, the magnitude and the direction of the output current i_o can be controlled and the power flow through the converter can be in either direction. Thus, the full-bridge inverter must be capable of operating in all four quadrants of the i_o-v_o plane and hence bridge inverters meet the switch-mode inverter requirements **[7]**, **[18]**.

3.4 Sinusoidal - Pulse - Width - Modulated Switching Scheme (SPWM) explained

In a dc-dc converter with a given input voltage, the average output voltage is controlled by controlling the switch on and off durations (t_{on} and t_{off}). The average value Vo of the output voltage v_o depends on t_{on} and t_{off}. One of the methods for controlling the output voltage employs switching at a constant frequency (hence, a constant switching time period $T_s = t_{on} + t_{off}$) and adjusting the on duration of the switch to control the average output voltage. In this method, called **pulse-width modulation (PWM) switching**, the switch duty ratio D, which is defined as the ratio of the on duration to the switching time period, is varied.

In the PWM switching at a constant switching frequency, the switch control signal, which controls the state (ON or OFF) of the switches, is generated by comparing a signal-level control signal $v_{control}$ with a repetitive waveform v_{tri}, as block diagram shows in **Fig 3.5(a)**. The voltage signal $v_{control}$ (constant or slowly varying in time) is generally obtained by amplifying the error, or the difference between the actual output voltage and its feedback desired value **[7]**.

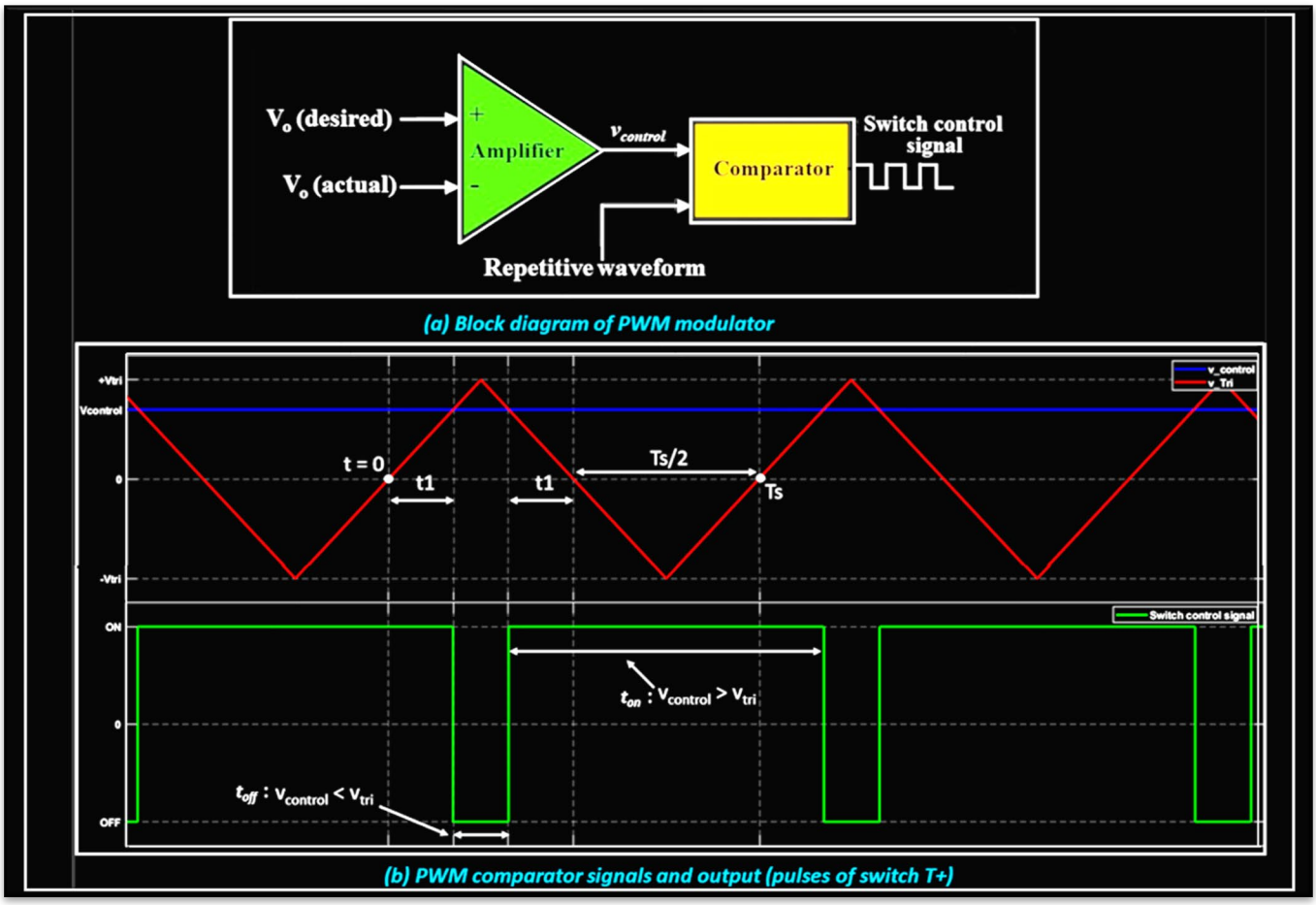

Figure 3.5 - Pulse-Width Modulation

The frequency of the repetitive (or carrier) waveform with a constant peak, which is shown to be in a triangular form, establishes the switching frequency. This frequency is kept constant in a PWM control and is chosen to be from a few kilohertz to a few hundred kilohertz range.

When the amplified error signal, which varies very slowly with time relative to the switching frequency, is greater than the repetitive waveform, the switch control signal becomes high, causing the switch to turn on.

Otherwise, the switch is off (**Fig 3.5(b)**). In terms of $v_{control}$ and the peak of the repetitive waveform $\hat{V}_{tri}$, the switch duty ratio can be expressed as

$$D = \frac{t_{on}}{T_s} = \frac{v_{control}}{\hat{V}_{tri}} \quad \text{…….. (3.1)}$$

where $T_s (= 1/f_s)$ is usually kept constant and t_{on} is adjusted. Controlling the switch duty ratios in this way allows the average dc voltage output to be controlled **[7]**.

However, as mentioned earlier, we would like the inverter output to be sinusoidal with magnitude and frequency controllable. In order to produce a sinusoidal output voltage waveform at a desired frequency, the PWM in inverter circuits gets a bit more complex. In particular, a sinusoidal control signal at the desired frequency is compared with a triangular waveform, as shown in **Fig 3.6(a)**.

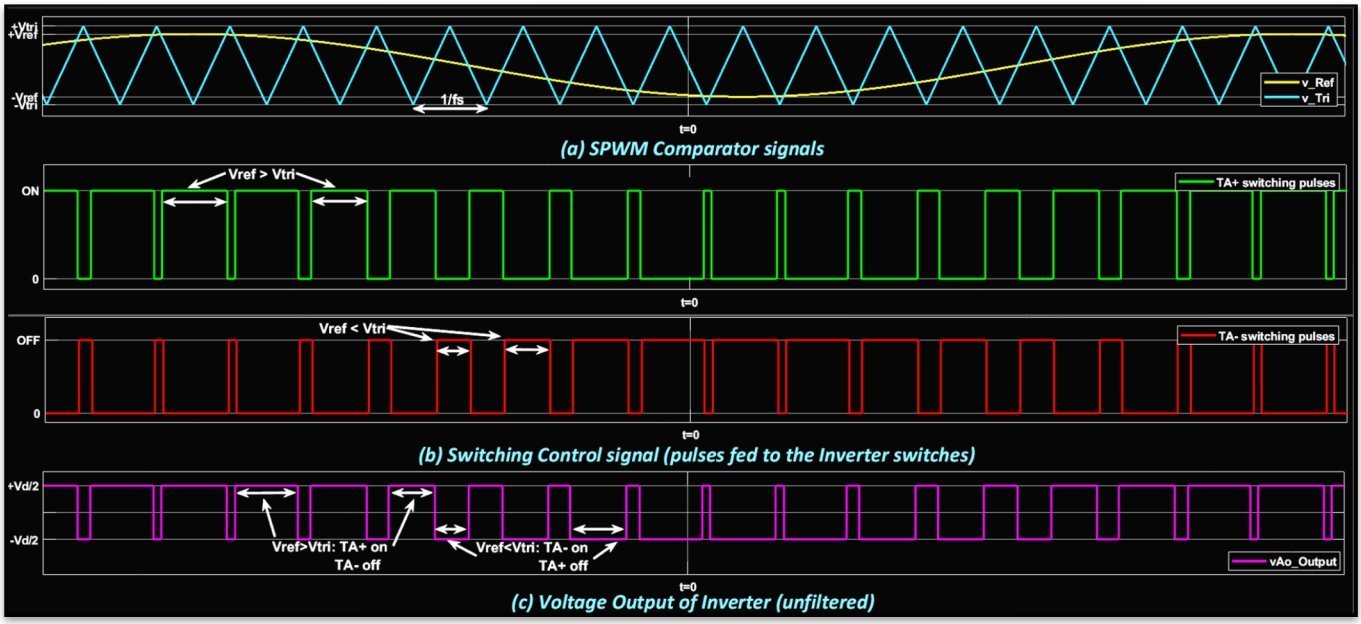

Figure 3.6 - Sinusoidal Pulse Width Modulation (SPWM)

This **sinusoidal PWM (SPWM) method** also known as the triangulation, sub harmonic, or suboscillation method, is very popular in industrial applications, especially in ac motor drives **[7]**.

The SPWM is explained with reference to **Fig 3.4(a)**, which is the half-bridge circuit topology for a single-phase inverter. The frequency of the triangular waveform establishes the inverter switching frequency and is generally kept constant along with its amplitude $\hat{V}_{tri}$.

The triangular waveform v_{tri} in **Fig 3.6(a)** is at a switching frequency f_s, which establishes the frequency with which the inverter switches are switched. The reference (or modulating or control) signal v_{ref} is used to modulate the switch duty ratio and has a frequency f_{ref} (or f_1), which is the desired fundamental frequency of the inverter voltage output, recognizing that the inverter output voltage will not be a perfect sine wave and will contain voltage components at harmonic frequencies of f_1.

The amplitude modulation ratio m_a and the frequency modulation ratio m_f are defined as

$$m_a = \frac{\hat{V}_{ref}}{\hat{V}_{tri}} \quad \text{…….. (3.2)} \qquad m_f = \frac{f_s}{f_1} \quad \text{…….. (3.3)}$$

where $\hat{V}_{ref}$ is the peak amplitude of the reference signal v_{ref}.

3.5 SPWM with Bipolar Voltage Switching (in a Half-Bridge inverter)

In the Half-Bridge inverter of **Fig 3.4(a)** , the switches T+ and T- are controlled based on the comparison of v_{ref} and v_{tri} which are mixed in a comparator as in **Fig 3.5(a)**. When the sinusoidal wave has magnitude higher than the triangular wave, the comparator output is high, causing T+ to turn on, otherwise it is low, causing T- to turn on (**Fig 3.6(b)**). Therefore, and independently of the direction of i_o , output voltage has the following results:

$$v_{ref} > v_{tri}, \text{ T+ is ON}, \quad v_{Ao} = \frac{1}{2} V_d \quad \text{..... (3.4)}$$

or

$$v_{ref} < v_{tri}, \text{ T- is ON}, \quad v_{Ao} = -\frac{1}{2} V_d \quad \text{..... (3.5)}$$

Since the two switches are never off simultaneously, voltage v_{Ao} fluctuates between two values ($\frac{1}{2} V_d$ and $-\frac{1}{2} V_d$) and is shown in **Fig 3.6(c)**. That is the reason why this type of switching is called SPWM with bipolar voltage switching.

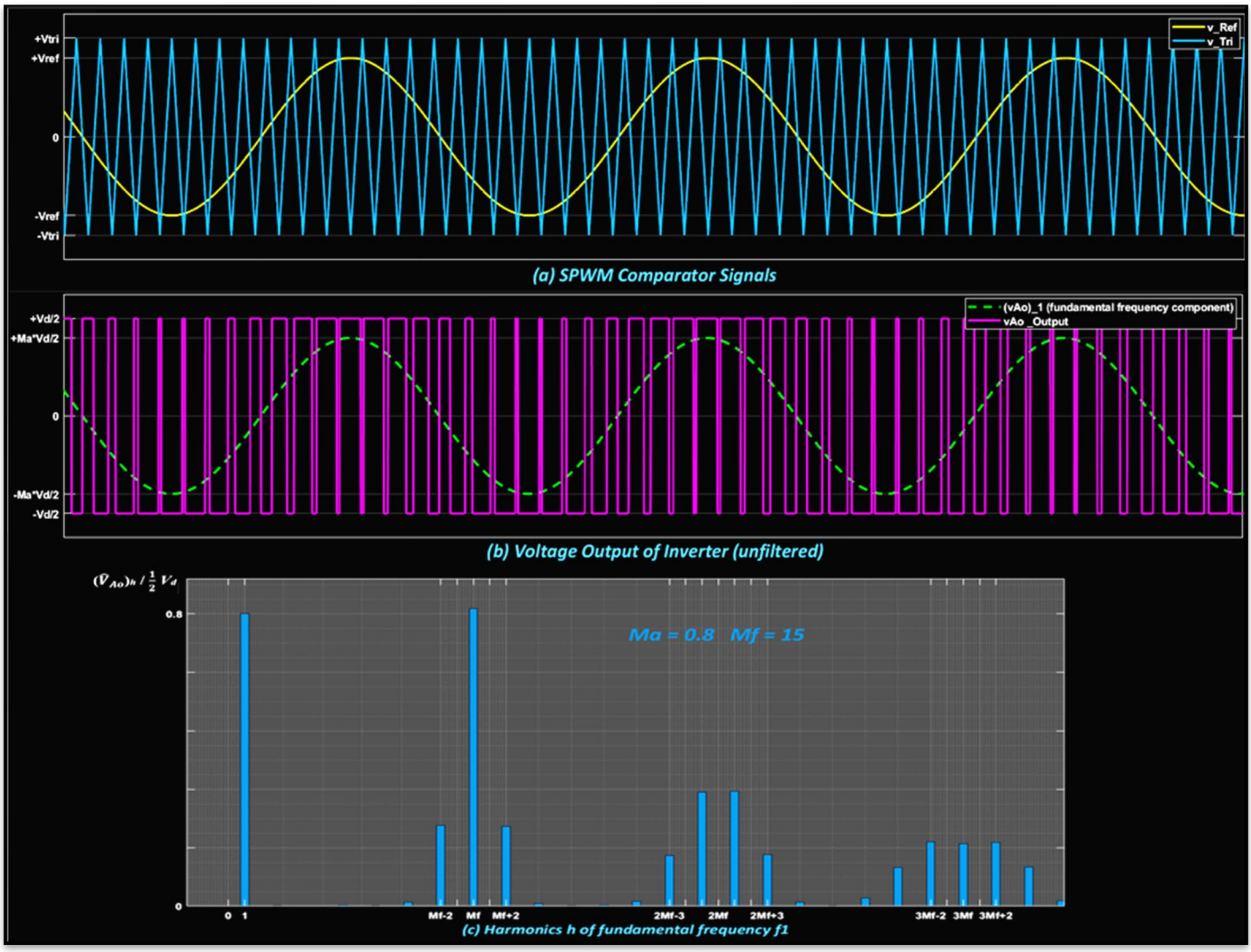

Figure 3.7 - SPWM with Bipolar voltage switching (Single-Phase)

Output voltage v_{Ao} is also shown in **Fig 3.7(b)** along with its fundamental frequency component (dashed curve), which are drawn for m_a = 0.8 and m_f = 15. The harmonic spectrum of v_{Ao} is shown in **Fig 3.7(c)**, where the normalized harmonic voltages $(\hat{V}_{Ao})_h / \frac{1}{2} V_d$ having significant amplitudes are plotted.

For an amplitude modulation ratio $m_a \leq 1.0$, we conclude that **the peak amplitude of the fundamental-frequency component $(\hat{V}_{Ao})_1$ is m_a times $\frac{1}{2} V_d$ [7], [9], [17], [18]**.

This can be explained by first considering a constant $v_{control}$ as shown in **Fig 3.5(b)** and then, by arbitrarily selecting the zero-time instant $t = 0$, which is also shown in the specific diagram, yielding **[19]**:

$$v_{tri} = \hat{V}_{tri} \frac{t}{T_s/4}, \quad 0 < t < \frac{T_S}{4} \quad \text{…….. (3.6)}$$

At $t = t_1$ in **Fig 3.5(b)** , $v_{control} = v_{tri}$, therefore from **Eq 3.6** :

$$t_1 = \frac{v_{control}}{\hat{V}_{tri}} \frac{T_S}{4} \quad \text{…….. (3.7)}$$

According to the operating conditions of the switches, the on-duration t_{on} of switch T+ is

$$t_{on} = 2t_1 + \frac{1}{2} T_s \quad \text{…….. (3.8)}$$

Therefore, its duty ratio is

$$D_1 = \frac{t_{on}}{T_S} = \frac{1}{2}\left(1 + \frac{v_{control}}{\hat{V}_{tri}}\right) \quad \text{…….. (3.9)}$$

Therefore, the duty ratio $D2$ of the switch T- is

$$D_2 = \frac{t_{off}}{T_s} = \frac{1 - t_{on}}{T_s} = 1 - D_1 \quad \text{…….. (3.10)}$$

Hence, the average value of the output voltage is obtained as:

$$V_{Ao} = \frac{1}{T_S} \int_0^{Ts} v_{A_o} dt =$$

$$= \frac{1}{T_s} \frac{V_d}{2} \left(\int_0^{t_1} dt + \int_{\frac{T_s}{2} - t_1}^{T_s} dt - \int_{t_1}^{\frac{T_s}{2} - t_1} dt \right) = \frac{1}{T_s} \frac{V_d}{2} \left[2t_1 + \frac{T_s}{2} - \left(\frac{T_s}{2} - 2t_1 \right) \right] =$$

$$= \frac{1}{T_s} \frac{V_d}{2} (t_{on} - t_{off}) = \frac{V_d}{2} (D_1 - D_2) = \frac{V_d}{2} (2D_1 - 1) = \frac{V_d}{2} \left[2 \left(\frac{1}{2} + \frac{v_{control}}{\hat{V}_{tri}} \right) - 1 \right]$$

$$V_{Ao} = \frac{V_d}{2} \frac{v_{control}}{\hat{V}_{tri}} \quad \text{…….. (3.11)}$$

Therefore, the average output voltage (or more specifically, the output voltage averaged over one switching time period $T_s = 1/f_s$) V_{Ao} depends on the switch duty ratio of v_{ref} to $\hat{V}_{tri}$ for a given V_d and so

$$V_{Ao} = \frac{v_{ref}}{\hat{V}_{tri}} \frac{V_d}{2} \quad , \qquad v_{ref} \leq \hat{V}_{tri} \quad \text{…….. (3.12)}$$

Eq 3.12 indicates how the "instantaneous average" value of v_{Ao} (averaged over one switching time period T_s) varies from one switching time period to the next. This "instantaneous average" is the same as the fundamental-frequency component of v_{Ao} **[7]**.

The foregoing argument shows why v_{ref} is chosen to be sinusoidal to provide a sinusoidal output voltage with fewer harmonics. Now, let the control voltage vary sinusoidally at the frequency $f_1 = \omega_1/2\pi$ which is the desired (or the fundamental) frequency of the inverter output:

$$v_{ref} = \hat{V}_{ref} \sin \omega_1 t \text{ , where } \hat{V}_{ref} \leq \hat{V}_{tri} \quad \text{…….. (3.13)}$$

Using **Eq 3.12** and **Eq 3.13** and the foregoing arguments, which show that the fundamental frequency component $(v_{Ao})_1$ varies sinusoidally and in phase with v_{ref} as a function of time, results in

$$(v_{Ao})_1 = \frac{\hat{V}_{ref}}{\hat{V}_{tri}} \sin \omega_1 t \frac{V_d}{2} =$$

$$= m_a \sin \omega_1 t \frac{V_d}{2} \text{ , for } m_a \leq 1.0 \quad \text{…….. (3.14)}$$

Therefore,

$$(\hat{V}_{Ao})_1 = m_a \frac{V_d}{2} \text{ , for } m_a \leq 1.0 \quad \text{…….. (3.15)}$$

which shows that in a sinusoidal PWM, the amplitude of the fundamental-frequency component of the output voltage varies linearly with m_a (provided $m_a \leq 1.0$). Therefore, the range of m_a from **0** to **1** is referred to as the linear range [19].

The harmonics in the inverter output voltage waveform appear as sidebands, centered around the switching frequency and its multiples, that is, around harmonics m_f, $2m_f$, $3m_f$ and so on **[7]**, **[9]**. This general pattern holds true for all values of m_a in the range **0 - 1**. For a frequency modulation ratio $m_f \leq 9$ (which is always the case, except in very high-power ratings), the harmonic amplitudes are almost independent of m_f, though m_f defines the frequencies at which they occur. Theoretically, the frequencies at which voltage harmonics occur can be indicated as

$$f_h = (jm_f \pm k) f_s$$

that is, the harmonic order h corresponds to the k^{th} sideband of j times the frequency modulation ratio m_f:

$$h = (jm_f) \pm k \quad \text{…….. (3.16)}$$

where the fundamental frequency corresponds to $h = 1$. For odd values of j, the harmonics exist only for even values of k. For even values of j, the harmonics exist only for odd values of k.

It will be useful later on to recognize that in the inverter circuit of **Fig 3.4(a),** the relation between ac-output voltage v_{AN} and dc-input voltage V_d is

$$v_{AN} = v_{Ao} + \frac{1}{2} V_d \quad \text{…….. (3.17)}$$

Therefore, the harmonic voltage components in v_{AN} and v_{Ao} are the same:

$$\left(\hat{V}_{AN}\right)_h = \left(\hat{V}_{Ao}\right)_h \quad \text{…….. (3.18)}$$

In **Table 1** the normalized harmonics $(\hat{V}_{Ao})_h / \frac{1}{2} V_d$ are tabulated as a function of m_a, assuming $m_f \geq 9$. Only those with significant amplitudes up to $j = 4$ in **Eq 3.16** are shown.

m_a / h	0.2	0.4	0.6	0.8	1.0
1 fundamental	0.2	0.4	0.6	0.8	1.0
mf	1.242	1.15	1.006	0.818	0.601
mf ± 2	0.016	0.061	0.131	0.220	0.318
mf ± 4					0.018
2mf ± 1	0.190	0.326	0.370	0.314	0.181
2mf ± 3		0.024	0.071	0.139	0.212
2mf ± 5				0.013	0.033
3mf	0.335	0.123	0.083	0.171	0.113
3mf ± 2	0.044	0.139	0.203	0.176	0.062
3mf ± 4		0.012	0.047	0.104	0.157
3mf ± 6				0.016	0.044
4mf ± l	0.163	0.157	0.008	0.105	0.068
4mf ± 3	0.012	0.070	0.132	0.115	0.009
4mf ± 5			0.034	0.084	0.119
4mf ± 7				0.017	0.050

Table 1 . Generalized harmonics of vAo for a large mf (≥ 9) [7]

From **Table 1**, the **rms** voltage at any value of h is given as

$$(V_{Ao})_h = \frac{1}{\sqrt{2}} \frac{V_d}{2} \frac{\left(\hat{V}_{A0}\right)_h}{V_d/2} \quad \text{…….. (3.19)}$$

The foregoing arguments show that **Eq 3.15** is followed almost exactly and the amplitude of the fundamental component in the output voltage varies linearly with amplitude modulation ratio m_a.

So far, it was assumed that $m_a \leq 1.0$, corresponding to a sinusoidal PWM in the linear range. Therefore, the amplitude of the fundamental-frequency voltage varies linearly with m_a , as derived in **Eq 3.15**. In this range of $m_a \leq 1.0$, PWM pushes the harmonics into a high-frequency range around the switching frequency and its multiples. Despite this desirable feature of a sinusoidal PWM in the linear range, one of the drawbacks is that the maximum available amplitude of the fundamental-frequency component is not as high as we wish.

To increase further the amplitude of the fundamental-frequency component in the output voltage, m_a is increased beyond **1.0**, resulting in what is called **overmodulation [7], [9], [20]**. Overmodulation causes the output voltage to contain many more harmonics in the side-bands as compared with the linear range (with $m_a \leq 1.0$), as shown in **Fig 3.8**.

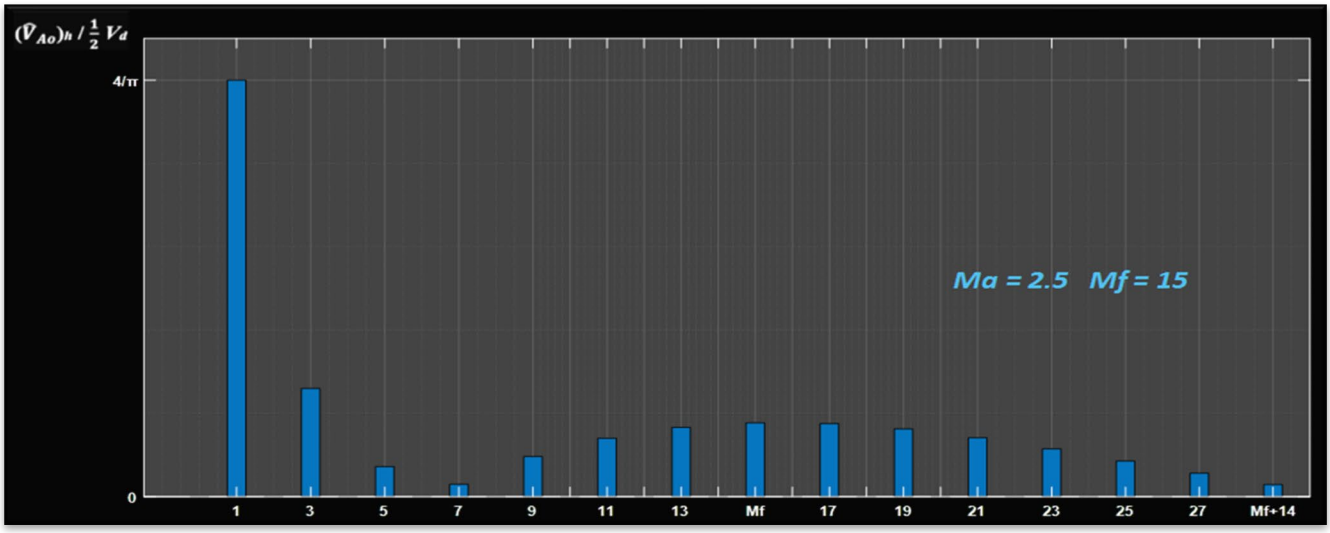

Figure 3.8 - Harmonic Spectrum of v_{Ao} due to Overmodulation

The harmonics with dominant amplitudes in the linear range may not be dominant during overmodulation. More significantly, with overmodulation, the amplitude of the fundamental-frequency component does not vary linearly with the amplitude modulation ratio m_a . Even at reasonably large values of m_f , $(\hat{V}_{Ao})_1 / \frac{V_d}{2}$ depends on m_f in the overmodulation region. This is contrary to the linear range, where $(\hat{V}_{Ao})_1 / \frac{V_d}{2}$ varies linearly with m_a , almost independent of m_f **[7]**.

For sufficiently large values of m_a , the inverter voltage waveform degenerates from a pulse-width-modulated waveform into a square wave **[20]**. It should be noted that the square-wave switching is also a special case of the sinusoidal PWM switching, when m_a becomes so large that the control voltage waveform v_{ref} intersects with the triangular waveform v_{tri} in **Fig 3.7(a)** only at the zero crossing of control signal. Therefore, the output voltage is independent of m_a in the square-wave region.

It can be concluded that in the overmodulation region,

$$\frac{V_d}{2} < (\hat{V}_{Ao})_1 < \frac{4}{\pi}\frac{V_d}{2} \quad , \text{ for } m_a > 1 \quad \text{..... (3.20)}$$

The overmodulation region is avoided in uninterruptible power supplies (UPS) because of a stringent requirement on minimizing the distortion in the output voltage. However, it should be mentioned, because in induction motor drives overmodulation is normally used **[7]**.

Now, concerning the selection of the switching frequency f_s and the frequency modulation ratio m_f, due to the relative ease in filtering harmonic voltages at high frequencies, it is desirable to use as high a switching frequency as possible. However, switching losses in the inverter switches increase proportionally with the switching frequency f_s. Therefore, in most applications, the switching frequency is selected to be either less than 6 kHz or greater than 20 kHz to be above the audible range **[7]**. If the optimum switching frequency (based on the overall system performance) turns out to be somewhere in the 6-20-kHz range, then the disadvantages of increasing it to 20 kHz are often outweighed by the advantage of no audible noise with f_s equal or greater than 20 kHz.

Therefore, in 50/60 Hz type applications, such as ac motor drives (where the fundamental frequency of the inverter output may be required to be as high as 200 Hz), the frequency modulation ratio m_f may be 9 or even less for switching frequencies of less than 2 kHz. On the other hand, m_f will be larger than 100 for switching frequencies higher than 20 kHz. The desirable relationships between the triangular waveform signal and the control voltage signal are dictated by how large m_f is **[7]**.

More specifically, for small values of m_f, the triangular waveform signal v_{tri} and the control signal v_{ref} should be synchronized to each other (the frequency of the control signal f_1 stays constant along with the carrier switching frequency f_s) as shown in **Fig 3.6(a)**. This **synchronous PWM** requires that m_f be an **integer**. The reason for using the synchronous PWM is that the asynchronous PWM (where m_f is **not an integer**) results in subharmonics of the desired fundamental frequency, which are very unwanted in most applications.

The harmonic m_f **should be an odd integer** (except in single-phase inverters with SPWM unipolar voltage switching, which follows with extra analysis) **[21]**. Choosing m_f as an odd integer, results in an odd symmetry $[f(-t) = -f(t)]$ as well as a half-wave symmetry $[f(t) = -f(t + 1/2T_s)]$ with the time origin shown in **Fig 3.6(c)**, which is plotted for odd $m_f (= 15)$. Therefore, only odd harmonics are present and the even harmonics disappear from the waveform of v_{Ao} **[22]**. Moreover, only the coefficients of the sine series in the Fourier analysis are finite; those for the cosine series are zero. The harmonic spectrum is plotted in **Fig 3.7(c)**.

The amplitudes of subharmonics due to **asynchronous PWM** are small at large values of m_f. Therefore, at large values of m_f the asynchronous PWM can be used, where the switching frequency f_s is kept constant, whereas the frequency f_1 of control signal v_{ref} varies, resulting in non-integer values of m_f (so long as they are large). However, if the inverter is supplying a load such as an ac motor, the subharmonics at zero or close to zero frequency, even though small in amplitude, will result in large currents that will be highly undesirable. Therefore, the asynchronous PWM should be avoided.

*** A general assumption: For all the above conclusions, m_f = 21 is treated as the borderline between large and small, though its selection is somewhat arbitrary but very enlightening as well. * [7]**

3.6 True Sine Wave Generation in the Output of the Inverter

The switching frequency is assumed to be remarkably high, approaching infinity. Therefore, to filter out the high-switching-frequency components in v_o and i_d , filter components L and C are required in both ac- and dc-sides. For simplicity, fictitious L-C high-frequency filters are used at the dc-side as well as at the ac side, as shown in **Fig 3.9**. This implies that the energy stored in the filters is negligible **[20]**. Since the converter itself has no energy storage elements, the instantaneous power input must equal the instantaneous power output**[7]**.

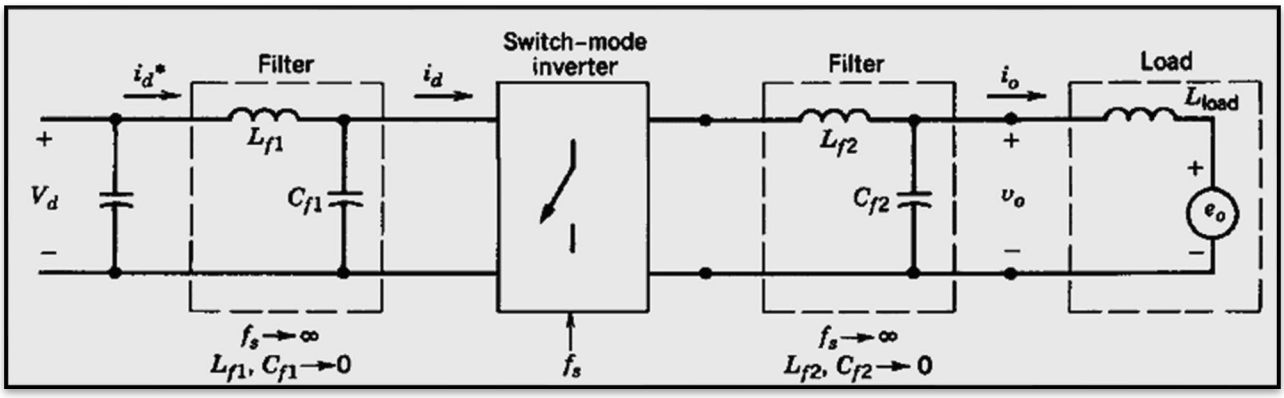

Figure 3.9 - Inverter with "fictitious" filters in both dc and ac side [7]

Having made these assumptions, v_o in **Fig 3.9** is a pure sine wave at the fundamental output frequency ω_1,

$$v_{o1} = v_o = \sqrt{2}\, V_o \sin\omega_1 t \quad \ldots\ldots\ldots (3.21)$$

If the load is as shown in **Fig 3.9**, where e_o is a sine wave at frequency ω_1 , then the output current would also be sinusoidal and would lag v_o for an inductive load such as an ac motor **[7]**, **[9]**, **[20]**, **[21]**:

$$i_o = \sqrt{2}\, I_o \sin(\omega_1 t - \varphi) \quad \ldots\ldots\ldots (3.22)$$

where φ is the angle by which i_o lags v_o.

On the dc side, the L-C filter will filter the high-switching-frequency components in i_d , and i_d^* would only consist of the low-frequency and dc components.

Assuming that no energy is stored in the filters,

$$V_d\, i_d^*(t) = v_o(t) i_o(t) = \sqrt{2}\, V_o \sin\omega_1 t \sqrt{2}\, I_o \sin(\omega_1 t - \varphi) \quad \ldots\ldots\ldots (3.23)$$

Therefore,

$$i_d^*(t) = \frac{V_o I_o}{V_d} \cos\varphi - \frac{V_o I_o}{V_d} \cos(2\omega_1 t - \varphi) = I_d + i_{d2} \quad \ldots\ldots\ldots (3.24)$$

$$\Rightarrow V_d\, i_d^*(t) = I_d - \sqrt{2}\, I_{d2} \cos(2\omega_1 t - \varphi) \quad \ldots\ldots\ldots (3.25)$$

where

$$I_d = \frac{V_o I_o}{V_d} \cos\varphi \quad \ldots\ldots\ldots (3.26) \qquad \text{and} \qquad I_{d2} = \frac{1}{\sqrt{2}} \frac{V_o I_o}{V_d} \quad \ldots\ldots\ldots (3.27)$$

Eq 3.25 for i_d^* shows that it consists of a dc component I_d, which is responsible for the power transfer from V_d on the dc side of the inverter to the ac side. Also, i_d^* contains a sinusoidal component at twice the fundamental frequency. The inverter input current i_d consists of i_d^* and the high-frequency components due to inverter switchings, as shown in **Fig 3.10(b)**.

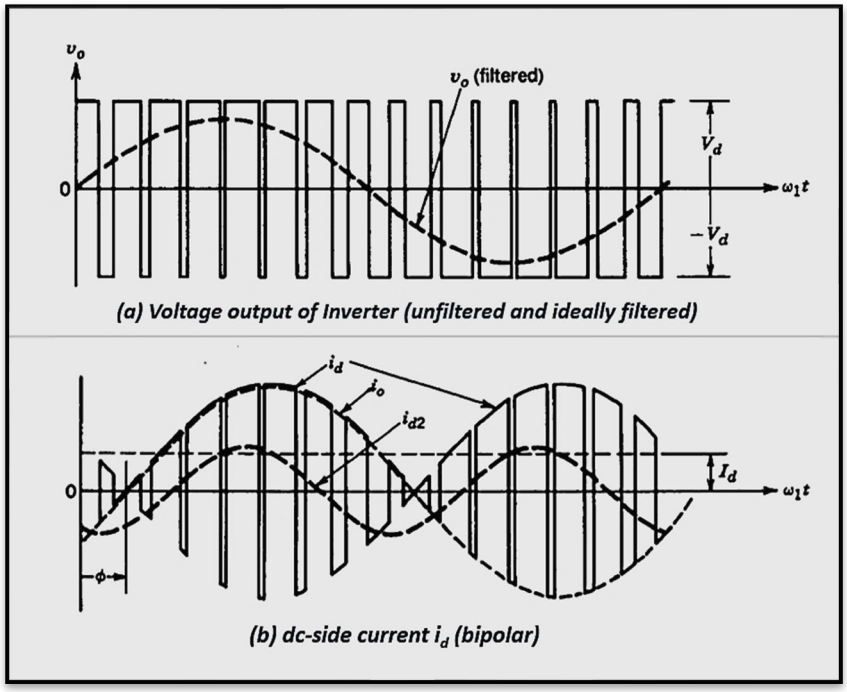

Figure 3.10 - The dc-side current in a Single-Phase inverter with bipolar SPWM [7]

In practical systems, the previous assumption of a constant dc voltage as the input to the inverter is not entirely valid. Normally, this dc voltage is obtained by rectifying the ac utility line voltage. A large capacitor is used across the rectifier output terminals to filter the dc voltage. The ripple in the capacitor voltage, which is also the dc input voltage to the inverter, is due to two reasons **[7]**:

(1) The rectification of the line voltage to produce dc does not result in a pure dc, dealing with the line-frequency rectifiers.

(2) As shown above by **Eq 3.25**, the current drawn by a single-phase inverter from the dc side is not a constant dc but has a second harmonic component (of the fundamental frequency at the inverter output) in addition to the high-switching-frequency components. The second harmonic current component results in a ripple in the capacitor voltage, although the voltage ripple due to the high switching frequencies is essentially negligible.

The filtered output v_o of the inverter is normally specified to contain very little harmonic distortion in real practical systems, even though most loads are highly nonlinear and, hence, inject larger harmonic currents. Therefore, the inverter must allow almost instantaneous control over its output ac waveform. The output voltage harmonic content is specified by means of a term called **total harmonic distortion** (***THD***) as

$$\%THD = 10 \cdot \frac{\left(\sum_{h=2}^{\infty} V_h^2\right)^{1/2}}{V_1} \quad \text{…….. (3.28)}$$

where V_1 is the fundamental-frequency rms value of the output voltage and V_h is the rms magnitude at the harmonic of order h. Typically, THD is specified to be less than 5%, while each harmonic voltage as a ratio of V_1 is specified to be less than 3% **[17]**, **[20]**, **[24]**.

Furthermore, concerning the designing of the L-C filter at the output terminal of a VSI, the cut-off frequency is chosen such that most of the low order harmonics is eliminated. To operate as an ideal voltage source, that means no additional voltage distortion even though under the load variation or a nonlinear load, the output impedance of the inverter must be kept zero. Therefore, the capacitance value should be maximized and the inductance value should be minimized at the selected cut-off frequency of the low-pass filter **[20]**. However, it is worth noting, that particularly in applications where the load is an engine, there is usually no need for a filter at the output of the inverter, as its large inductance acts as a filter and the current tends to become almost a pure sine wave **[12]**.

3.7 Full-Bridge Inverter employing SPWM Bipolar voltage switching

In the full-bridge single phase inverter in **Fig 3.4(b)**, the diagonally opposite switches T_{A+}_T_{B-} and T_{A-}_T_{B+} from the two **legs A** and **B**, are switched as switch pairs 1 and 2, respectively, the same way as it was shown in **Fig 3.6(b)** for the half-bridge inverter switches T+_T- . The output voltage waveform of **leg A** is identical to the output of the basic half-bridge inverter in **Fig. 3.6(c)**, with which SPWM switching scheme was previously explained. The output of inverter **leg B** is negative of the **leg A** output **[7]**. For example, when T_{A+} is ON and v_{Ao} is equal to $+\frac{1}{2}V_d$, T_{B-} is also ON and $v_{Bo} = -\frac{1}{2}V_d$. Therefore

$$v_{Bo}(t) = -v_{Ao}(t) \quad \text{…….. (3.29)}$$

and

$$v_o(t) = v_{Ao}(t) - v_{Bo}(t) = 2v_{Ao}(t) \quad \text{…….. (3.30)}$$

The v_o waveform switches between $-V_d$ and $+V_d$ voltage levels and is shown in **Fig 3.4(c)** or in **Fig 3.6(c)** but with peak voltages $\pm V_d$, not $\pm V_d/2$). The bipolar analysis carried out for the basic one-leg inverter (Half-Bridge) completely applies to this type of SPWM switching with Full-Bridge topology. Therefore, the peak of the fundamental-frequency component in the output voltage $(\hat{V}_o)_1$ can be obtained from **Eq 3.15**, **Eq 3.20** and **Eq 3.30** as

$$\hat{V}_{o1} = m_a V_d \quad (m_a \leq 1.0) \quad \text{…….. (3.31)}$$

and

$$V_d < \hat{V}_{o1} < \frac{4}{\pi}V_d \quad (m_a > 1.0) \quad \text{…….. (3.32)}$$

In a Full-Bridge VSI the **rms** voltage at any harmonic h can be obtained by multiplying **Eq 3.19** by a factor of 2. Therefore,

$$(V_o)_h = 2\frac{1}{\sqrt{2}}\frac{V_d}{2}\frac{\left(\hat{V}_{A0}\right)_h}{V_d/2} =$$

$$= \frac{V_d}{\sqrt{2}}\frac{\left(\hat{V}_{A0}\right)_h}{V_d/2} \quad \text{…….. (3.33)}$$

One leg of switching can be used to obtain bipolar inverter. However, one leg cannot achieve the unipolar inverter **[7]**.

3.8 Full-Bridge Inverter employing SPWM Unipolar voltage switching

In SPWM with unipolar voltage switching, the switches in the two legs of the full-bridge inverter of **Fig 3.4(b)** are not switched simultaneously, as in the previous SPWM scheme. Here, the **legs A** and **B** of the full-bridge inverter are controlled separately by comparing v_{tri} with v_{ref} and $-v_{ref}$ respectively.

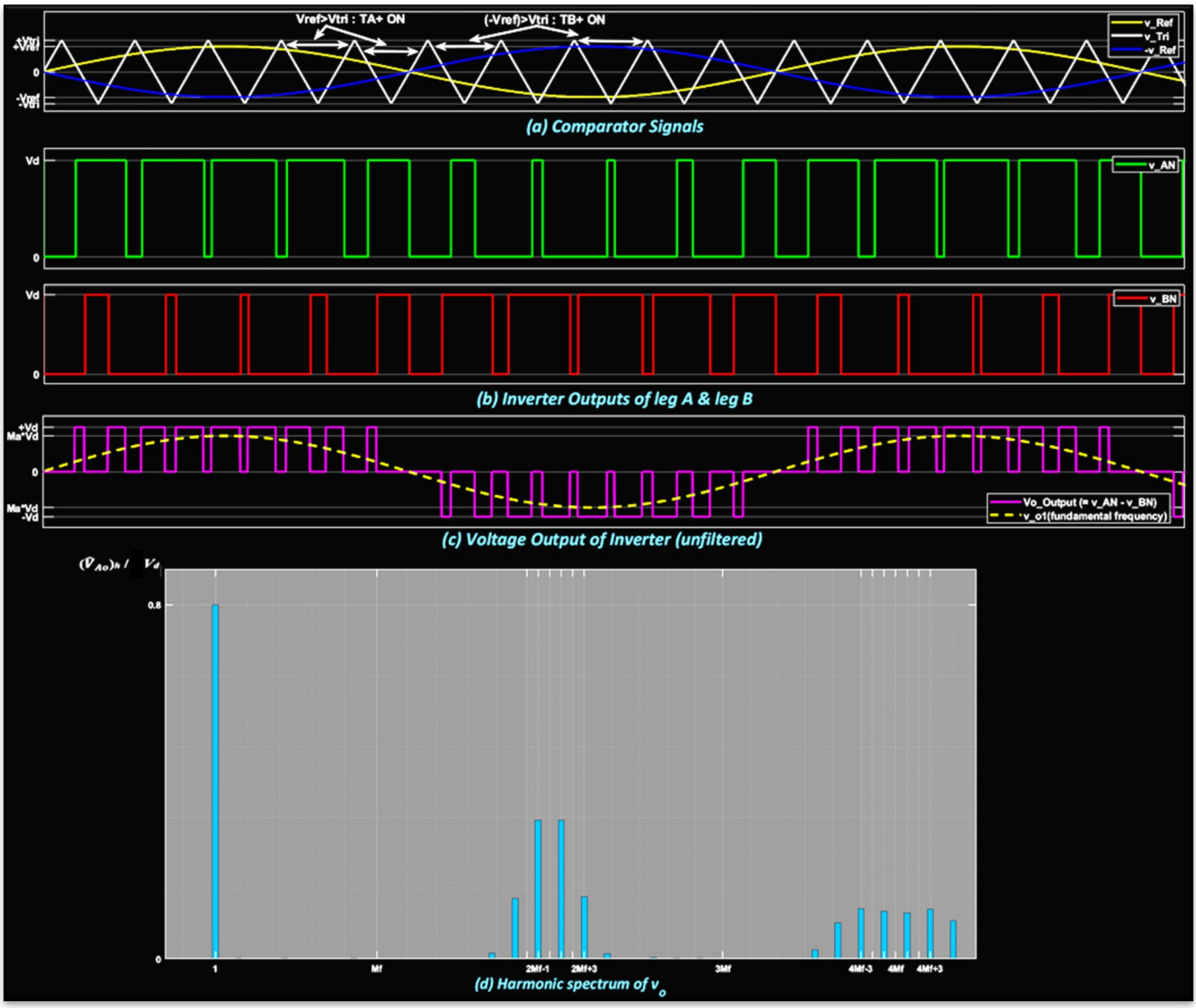

Figure 3.11 - SPWM with Unipolar voltage switching (Single-Phase)

As shown in **Fig 3.11(a)**, the comparison of the reference signals with the triangular waveform results in the following logic signals to control the switches in **leg A**:

$$v_{ref} > v_{tri}: \quad T_{A+} \text{ ON and } V_{AN} = V_d \qquad \text{…….. (3.34)}$$

$$v_{ref} < v_{tri}: \quad T_{A-} \text{ ON and } V_{AN} = 0$$

For controlling the **leg B** switches, $-v_{ref}$ is compared with the same triangular waveform, which yields the following:

$$(-v_{ref}) > v_{tri}: \quad T_{B+} \text{ ON and } V_{BN} = V_d$$
$$(-v_{ref}) < v_{tri}: \quad T_{B-} \text{ ON and } V_{BN} = 0 \qquad \ldots\ldots\ldots (3.35)$$

The output voltages of inverter **leg A** and **leg B** with respect to the negative dc bus **N** are shown in **Fig 3.11(b)**.

Because of the feedback diodes in antiparallel with the switches, the foregoing voltages given by **Eq 3.34** and **Eq 3.35** are independent of the direction of the output current i_o. The waveforms of **Fig 3.11** show that there are four combinations of switch on-states and the corresponding voltage levels **[23]**:

1. T_{A+} and T_{B-} are ON: $v_{AN} = V_d$, $v_{BN} = 0$ → $v_o = V_d$
2. T_{A-} and T_{B+} are ON: $v_{AN} = 0$, $v_{BN} = V_d$ → $v_o = -V_d$
3. T_{A+} and T_{B+} are ON: $v_{AN} = V_d$, $v_{BN} = V_d$ → $v_o = 0$
4. T_{A-} and T_{B-} are ON: $v_{AN} = 0$, $v_{BN} = 0$ → $v_o = 0$ ……. (3.36)

We notice that when both the upper switches are on, the output voltage is zero. The output current circulates in a loop through T_{A+} and D_{B+} or D_{A+} and T_{B+} depending on the direction of i_o. During this interval, the input current i_d is zero. A similar condition occurs when both bottom switches T_{A-} and T_{B-} are ON.

In this type of SPWM scheme, when a switching occurs, the output voltage changes between 0 and $+V_d$ or between 0 and $-V_d$ voltage levels (**Fig 3.11(c)**). For this reason, this type of SPWM scheme is called SPWM with a unipolar voltage switching, as opposed to the SPWM with bipolar voltage-switching scheme described earlier. This scheme has the advantage of "effectively" doubling the switching frequency as far as the output harmonics are concerned, compared to the bipolar voltage-switching scheme. Also, the voltage jumps in the output voltage at each switching are reduced to V_d, as compared to $2V_d$ in the previous scheme **[7]**.

The advantage of "effectively" doubling the switching frequency appears in the harmonic spectrum of the output voltage waveform, shown in **Fig 3.11(d)**, where the lowest harmonics (in an idealized circuit) appear as sidebands of twice the switching frequency. It is easy to understand this if we choose the frequency modulation ratio m_f to be even (m_f should be odd for SPWM with bipolar voltage switching) in a single-phase inverter **[7]**. The voltage waveforms v_{AN} and v_{BN} are displaced by 180° of the fundamental frequency f_{ref} with respect to each other. Therefore, the harmonic components at the switching frequency in v_{AN} and v_{BN} have the same phase ($\varphi_{AN} - \varphi_{BN} = 180^\circ \cdot m_f = 0^\circ$, since the waveforms are 180° displaced and m_f is assumed to be even). This results in the cancellation of the harmonic component at the switching frequency in the output voltage $v_o = v_{AN} - v_{BN}$. In addition, the sidebands of the switching-frequency harmonics disappear. In a similar manner, the other dominant harmonic at twice the switching frequency cancels out, while its sidebands do not. Here also

$$\hat{V}_{o1} = m_a V_d \quad , \quad \text{for } m_a \leq 1.0 \qquad \ldots\ldots\ldots (3.37)$$

and

$$V_d < \hat{V}_{o1} < \frac{4}{\pi} V_d \quad , \quad \text{for } m_a > 1 \qquad \ldots\ldots\ldots (3.38)$$

Based on the analysis of unipolar voltage switching, the harmonic order h can be written as

$$h = 2(jm_f) \pm k \quad \text{…….. (3.39)}$$

where the harmonics exist as sidebands around $2m_f$ and the multiples of $2m_f$. Since h is odd, k in **Eq 3.39** attains only odd values **[23]**.

Comparison of the unipolar voltage switching with the bipolar voltage switching shows that, in both cases, the fundamental-frequency voltages are the same for equal m_a. However, with unipolar voltage switching, the dominant harmonic voltages centered around m_f disappear, thus resulting in a significantly lower harmonic content.

Under conditions similar to those in the circuit of **Fig 3.9** for the PWM with bipolar voltage switching, **Fig 3.12(b)** shows the dc-side current i_d for the SPWM unipolar voltage-switching scheme (where m_f = 14 instead of m_f = 15 for the bipolar voltage switching).

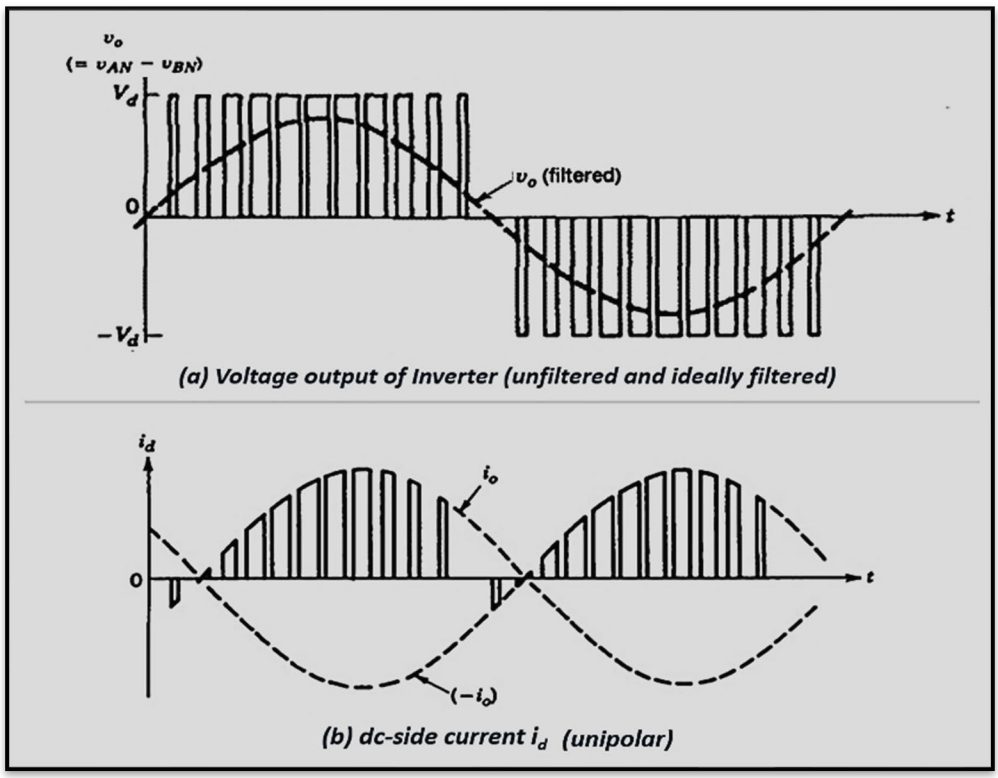

Figure 3.12 - The dc-side current in a single-phase inverter with unipolar SPWM [7]

By comparing **Fig 3.12(b)** with **Fig 3.10(b)**, it is clear that using PWM with unipolar voltage switching results in a smaller ripple in the current on the dc side of the inverter **[45]**.

4. AC MACHINERY FUNDAMENTALS

4.1 Introduction to Machinery Principles

4.1.1 The Magnetic Field Production in A Magnetic Circuit

Magnetic fields are the fundamental mechanism by which energy is converted from one form to another in motors, generators, and transformers. A loop of wire (an exciting coil) and a ferromagnetic core constitute the simplest possible electromagnetic system, which essentially produces a constant magnetic field. The direction of the produced flux density is perpendicular to the plane of the coil and is given by the right-hand rule. The basic law governing the production of a magnetic field $\boldsymbol{H}$ by a current $\boldsymbol{i}$ is Ampere's law:

$$\oint \boldsymbol{H} \cdot \boldsymbol{dl} = \boldsymbol{I_{net}} \quad \text{..... (4.1)}$$

$\boldsymbol{H}$ is the magnetic field intensity produced by the current $\boldsymbol{I_{net}}$, and $\boldsymbol{dl}$ is a differential element of length along the path of integration. In SI units, $\boldsymbol{H}$ is measured in **ampere-turns per meter [2]**.

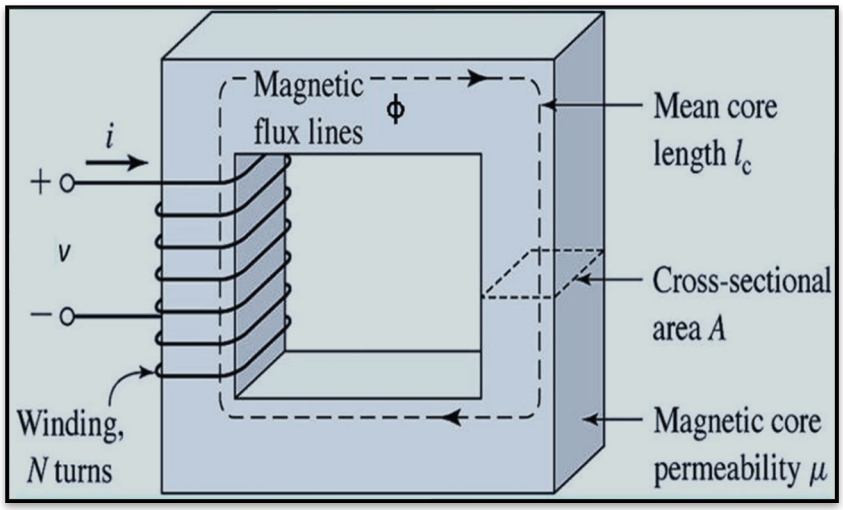

Figure 4.1 - A simple magnetic core [25]

Fig. 4.1 shows a rectangular core with a winding of $\boldsymbol{N}$ turns of wire wrapped around one leg of the core. If the core is composed of iron or certain other similar metals (collectively called **ferromagnetic materials**), essentially, all the magnetic field produced by the current will remain inside the core so the path of integration in Ampere's law is the mean path length of the core $\boldsymbol{l_c}$. The current passing within the path of integration $\boldsymbol{I_{net}}$ is then $\boldsymbol{N_i}$, since the coil of wire cuts the path of integration $\boldsymbol{N}$ times, while carrying current $\boldsymbol{i}$. Therefore, the magnitude of the magnetic field intensity in the core due to the applied current is

$$\boldsymbol{H} = \frac{\boldsymbol{Ni}}{\boldsymbol{l_c}} \quad \text{..... (4.2)}$$

The magnetic field intensity $\boldsymbol{H}$ is in a sense a measure of the "effort" that a current is putting into the establishment of a magnetic field. The strength of the magnetic field flux produced in the core also depends

on the material of the core. The relationship between the magnetic field intensity H and the resulting magnetic flux density ***B*** produced within a material, is given by

$$B = \mu H \quad \text{..... (4.3)}$$

where ***H*** represents the effort exerted by the current to establish a magnetic field and μ represents the relative ease of establishing a magnetic field in a given material. The units of **magnetic field intensity** are **ampere-turns per meter**, the units of **permeability** are **henrys per meter** and the units of the resulting **flux density** are **webers per square meter**, known as **teslas (T) [26]**.

The permeability of any material compared to the permeability of free space $\mu_0 \ (= 4\pi \times 10\text{-}7 \ H/m)$ is called **relative permeability** $\mu_r \ (= \mu / \mu_0)$. Obviously, because the permeability of the metals in a motor is much higher than that of air, the great majority of the flux in a core remains inside the core instead of traveling through the surrounding air. The small leakage flux that does leave the iron core is very important in determining the flux linkages between coils and the self-inductances of coils in transformers and motors.
In a core such as the one shown in **Fig 4.1**, the magnitude of the flux density is given by

$$B = \mu H = \frac{\mu N i}{l_c} \quad \text{..... (4.4)}$$

Now the total flux in a given area is given by

$$\phi = \int_A B \cdot dA \quad \text{..... (4.5)}$$

where ***dA*** is the differential unit of area. If the flux density vector is perpendicular to a plane of area ***A*** and if the flux density is constant throughout the area, then the equation of total flux in the core due to the current i in the winding reduces to

$$\phi = BA = \frac{\mu N i A}{l_c} \quad \text{..... (4.6)}$$

where ***A*** is the cross-sectional area of the core **[2]**, **[26]**.

In an electric circuit, the relationship between voltage and current is Ohm's law ($V = IR$). It is the applied voltage **or electromotive force** ***(emf)*** that drives the current ***I*** around the circuit through a resistance ***R***. By analogy, the corresponding quantity in the magnetic circuit is called the magnetomotive force ***F*** (or ***mmf***). The applied magnetomotive force causes **flux** ϕ to be produced **[26]**. The relationship between magnetomotive force and flux is

$$F = \phi R \quad \text{..... (4.7)}$$

where ***R*** is the reluctance of a magnetic circuit and its units are **ampere-turns per weber**.

4.1.2 Magnetic Behavior of Ferromagnetic Materials

Assuming that a direct current is applied to the core of **Fig 4.1**, by starting with **0** ***A*** and slowly working up to the maximum permissible current. The flux produced in the core is plotted versus the magnetomotive force producing it and looks like **Fig 4.2(a)** below.

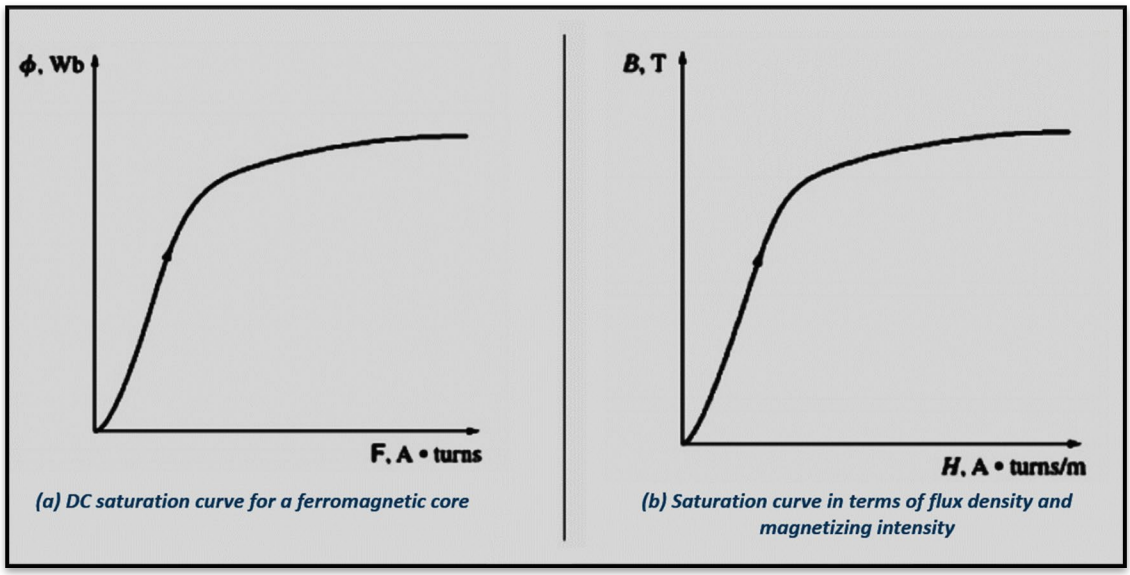

Figure 4.2 - Saturation curve of a typical ferromagnetic material [2]

This type of plot is called a **saturation curve** or **a magnetization curve**. At first, a small increase in the magnetomotive force produces a huge increase in the resulting flux. After a certain point, though, further increases in the magnetomotive force produce relatively smaller increases in the flux. Finally, an increase in the magnetomotive force produces almost no change at all. The region of this figure in which the curve flattens out is called the **saturation region**, and the core is said to be saturated. In contrast, the region where the flux changes very rapidly, is called the **unsaturated region** of the curve, and the core is said to be unsaturated. The transition region between the unsaturated region and the saturated region is sometimes called the **knee of the curve**. Note that the flux produced in the core is linearly related to the applied magnetomotive force in the unsaturated region and approaches a constant value regardless of magnetomotive force in the saturated region **[2], [26]**.

Fig 4.2(b) is a plot of magnetic flux density ***B*** to magnetizing intensity ***H*.** From **Eq 4.2** and **Eq.4.6**, it is easy to see that magnetizing intensity ***H*** is directly proportional to magnetomotive force ***F*** and magnetic flux density ***B*** is directly proportional to flux ϕ for any given core. Therefore, the relationship between ***B*** and ***H***, has the same shape as the relationship between flux ϕ and magnetomotive force ***F***. The slope of the curve of flux density ***B*** versus magnetizing intensity at any value of ***H*** in **Fig 4.2(b)** is by definition the permeability of the core at that magnetizing intensity. The curve shows that the permeability is large and relatively constant in the unsaturated region and then gradually drops to a very low value as the core becomes heavily saturated **[2]**.

Since real generators and motors depend on magnetic flux to produce voltage and torque, they are designed to produce as much flux as possible. As a result, most real machines operate near the knee of the saturation curve and the flux in their cores is not linearly related to the magnetomotive force producing it.

4.1.3 Faraday's Law - Induced Voltage from A Time-Changing Magnetic Field

There are various ways in which an existing magnetic field can affect its surroundings. The first major effect to be considered is called **Faraday's law**. It is the basis of **transformer operation [2]**, **[27]**. Faraday's law states that if a flux passes through a turn of a coil of wire, a voltage e_{ind} will be induced in the turn of wire that is directly proportional to the rate of change in the flux ϕ with respect to time. If a coil has N turns and if the same flux passes through all of them, then the voltage induced across the whole coil is given by

$$e_{ind} = -N\frac{d\phi}{dt} \quad \text{..... (4.8)}$$

In practical problems, the foregoing equation assumes that exactly the same flux is present in each turn of the coil. If the windings were tightly coupled, so that the vast majority of the flux passing through one turn of the coil does indeed pass through all of them, then **Eq 4.8** could give valid answers. However, the flux leaking out of the core into the surrounding air prevents this from being true. If leakage is quite high or if extreme accuracy is required, a different expression is needed. Thus, if there are N turns in the coil of wire, the total voltage on the coil can be re-expressed in terms of flux ϕ as

$$e_{ind} = \sum_{i=1}^{N} e_i \quad \text{..... (4.9)}$$

$$= \sum_{i=1}^{N} \frac{d\phi_i}{dt} \quad \text{..... (4.10)}$$

$$= \frac{d}{dt}\left(\sum_{i=1}^{N} \phi_i\right) \quad \text{..... (4.11)}$$

where e_i is the magnitude of the voltage in the ith turn of the coil. The term in parentheses in **Eq 4.11** is called the **flux linkage** λ of the coil, and Faraday's law can be rewritten in terms of flux linkage as

$$e_{ind} = \frac{d\lambda}{dt} \quad \text{..... (4.12)}$$

Faraday's law is the fundamental property of magnetic fields involved in transformer operation. The effect of Lenz's law in transformers (the minus sign in **Eq 4.8**) is to predict the polarity of the voltages induced in transformer windings. Faraday's law also explains the **eddy current losses**. A time-changing flux induces voltage within a ferromagnetic core in just the same manner as it would in a wire wrapped around that core. These voltages cause swirls of current to flow within the core, much like the eddies seen at the edges of a river. It is the shape of these currents that gives rise to the name eddy currents. These eddy currents are flowing in a resistive material (the iron of the core), so lost energy is dissipated by them, which goes into heating the iron core**[26]**.

4.1.4 Production of Induced Force on A Wire

A second major effect of a magnetic field on its surroundings is that it induces a force on a current-carrying wire within the field. The basic concept involves a conductor present in a uniform magnetic field of flux density B, illustrated in **Fig 4.3**.

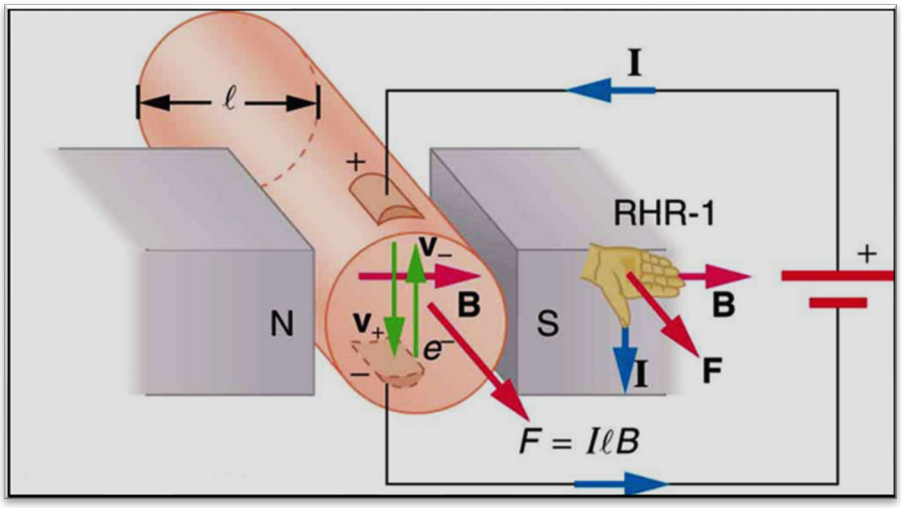

Figure 4.3 - Force on a current-carrying conductor in a magnetic field [28]

The conductor itself is l meters long and contains a current of i amperes. The force induced on the conductor is given by

$$F = i(l \times B) \quad \text{..... (4.13)}$$

The direction of the force is given by the right-hand rule. If the index finger of the right hand points in the direction of the vector l (which is always defined to be in the direction of current i flow) and the middle finger points in the direction of the flux density vector B, then the thumb points in the direction of the resultant F on the wire. The magnitude of the force is given by the equation

$$F = i\, l\, B \sin\theta \quad \text{..... (4.14)}$$

where θ is the angle between the wire and the flux density vector.

The induction of a force in a wire by a current, in the presence of a magnetic field, is the basis of **motor action.** Almost every type of motor depends on this basic principle for the forces and torques which make it move **[2]**, **[29]**.

4.1.5 Induced Voltage on A Conductor Moving in A Magnetic Field

There is a third major way in which a magnetic field interacts with its surroundings. If a wire with the proper orientation moves through a magnetic field, a voltage is induced in it. This idea is shown in **Fig 4.4**.

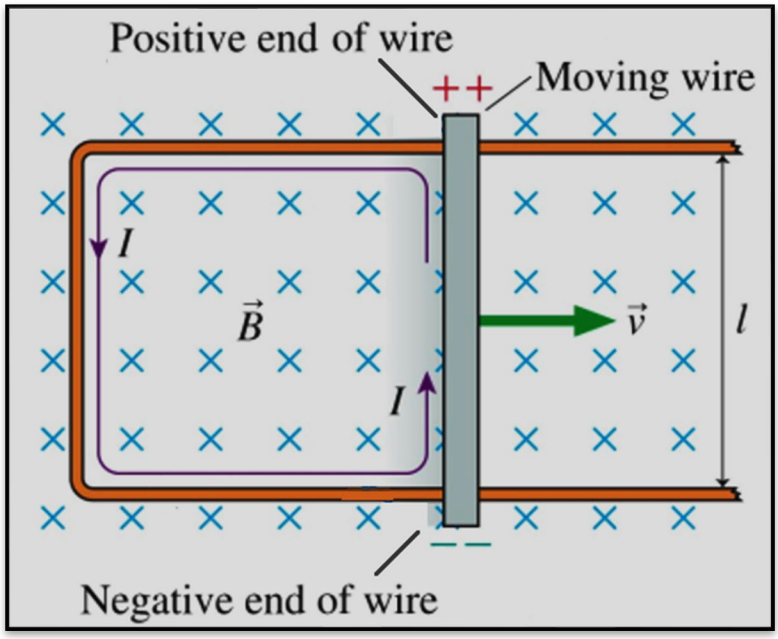

Figure 4.4 - A moving conductor in the presence of a magnetic field [30]

The voltage induced in the wire is given by

$$e_{ind} = (\boldsymbol{v} \times \boldsymbol{B}) \cdot \boldsymbol{l} \quad \text{..... (4.15)}$$

where $\boldsymbol{v}$ = velocity of the wire
$\boldsymbol{B}$ = magnetic flux density vector
$\boldsymbol{l}$ = length of conductor in the magnetic field

Vector $\boldsymbol{l}$ points along the direction of the wire toward the end, making the smallest angle with respect to the vector $\boldsymbol{v} \times \boldsymbol{B}$. The voltage in the wire will be built up so that the positive end is in the direction of the vector $\boldsymbol{v} \times \boldsymbol{B}$. The induction of voltages in a wire moving in a magnetic field is fundamental to the operation of all types of generators. For this reason, it is called **generator action [2], [29]**.

4.1.6 Real, Reactive and Apparent Power in Single-Phase AC Circuits

In a dc circuit, the **power** supplied to the dc load is simply the product of the voltage across the load and the current flowing through it ***(P = VI)***. The situation in sinusoidal ac circuits is a bit more complex, as there can be a phase difference between the ac voltage and the ac current supplied to the load. The **instantaneous power** supplied to an ac load will still be the product of the instantaneous voltage and the instantaneous current, but the **average power** supplied to the load will be affected by the phase angle between the voltage and the current. If a single-phase voltage source supplying power to a single-phase inductive load with impedance $\boldsymbol{Z} = \boldsymbol{Z} < \boldsymbol{\theta}°$, then the impedance angle $\boldsymbol{\theta}$ of the load will be positive, and the current will lag the voltage by $\boldsymbol{\theta}°$. The voltage applied to this load is

$$v(t) = \sqrt{2} V \cos \omega t \quad \text{..... (4.16)}$$

where V is the **rms value** of the voltage applied to the load, and the resulting current flow is

$$i(t) = \sqrt{2}I \cos(\omega t - \theta) \quad \text{..... (4.17)}$$

where I is the **rms value** of the current flowing through the load. For inductive loads, the impedance angle is positive and the current waveform lags the voltage waveform by $\theta°$. Applying trigonometric identities, the instantaneous power supplied to this load at any time t, can be expressed as

$$p(t) = v(t)\, i(t) = 2VI \cos \omega t \cos(\omega t - \theta) \quad \text{..... (4.18)}$$

$$\Rightarrow p(t) = VI \cos\theta\,(1 + \cos 2\omega t) + VI \sin\theta \sin 2\omega t \quad \text{..... (4.19)}$$

The first term of this equation represents the power supplied to the load by the component of current that is in phase with the voltage, while the second term represents the power supplied to the load by the component of current that is 90° out of phase with the voltage. Note that the first term of the instantaneous power expression is always positive, but it produces pulses of power instead of a constant value. The **average value** of this term is

$$P = VI \cos\theta \quad \text{..... (4.20)}$$

which is the **average** or **real power** (P) supplied to the load by the first term of **Eq 4.19**. The units of real power are watts W, where $1\ W = 1\ V \times 1\ A$.

The second term of the instantaneous power expression is positive half of the time and negative half of the time, so that the average power supplied by this term is zero. This term represents power that is first transferred from the source to the load, and then returned from the load to the source. The power that continually bounces back and forth between the source and the load is known as **reactive power** *(Q)* **[2]**,**[7]**. Reactive power represents the energy that is first stored and then released in the magnetic field of an inductor, or in the electric field of a capacitor. The reactive power of a load is given by

$$Q = VI \sin\theta \quad \text{..... (4.21)}$$

where θ is the impedance angle of the load. By convention, Q is positive for inductive loads and negative for capacitive loads, because the impedance angle θ is positive for inductive loads and negative for capacitive loads. The units of reactive power are **volt-amperes reactive** *(var)*, where $1\ var = 1\ V \times 1\ A$.

For simplicity in computer calculations, real and reactive power are sometimes represented together as a **complex power** S**,** where

$$S = P + jQ \quad \text{..... (4.22)}$$

The complex power S supplied to a load can be calculated from the equation

$$S = VI^* \quad \text{..... (4.23)}$$

where the * represents the complex conjugate operator.

A loop of wire in a uniform magnetic field is the simplest possible machine that produces a sinusoidal ac voltage. This case is not representative of real ac machines, since the flux in real ac machines is not constant in either magnitude or direction. However, the factors that control the voltage and torque on the loop can be applied equally to control the voltages and torques in real ac machines **[2]**.

4.2 A Simple Loop in a Uniform Magnetic Field

4.2.1 The Voltage Induced in a Simple Rotating Loop

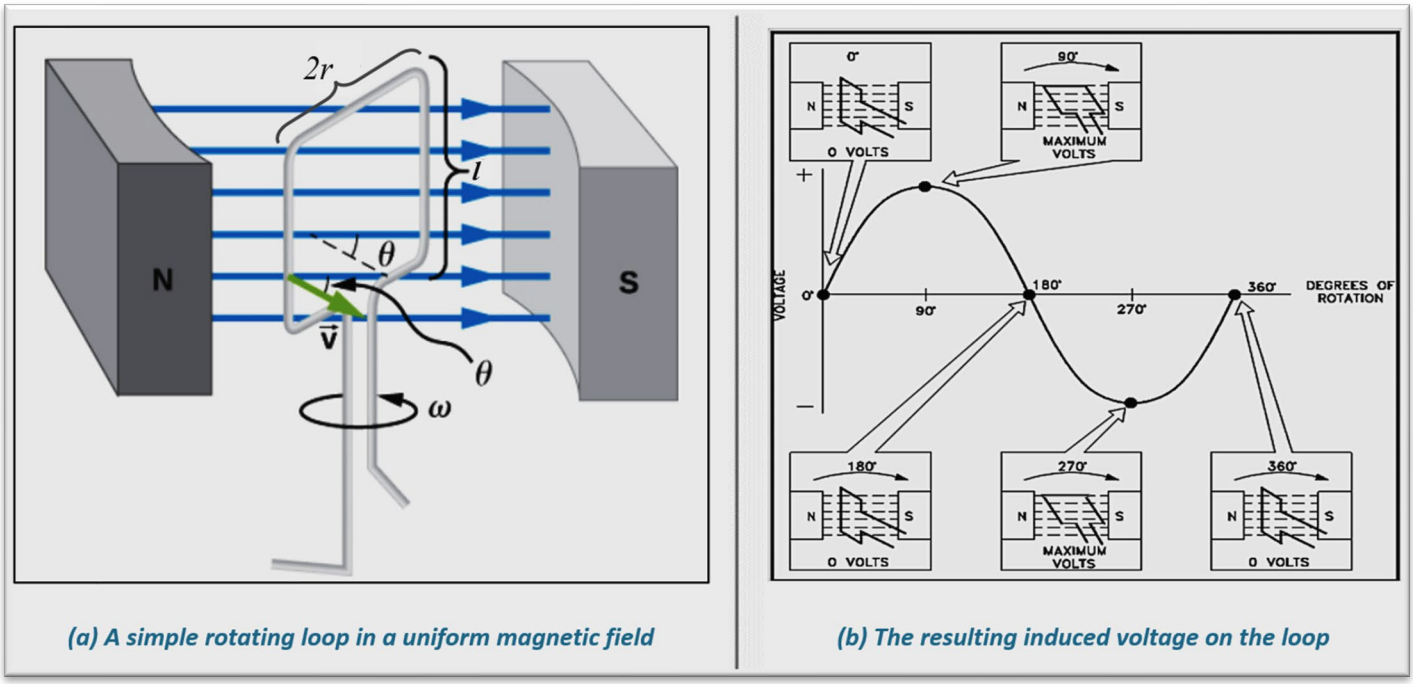

(a) A simple rotating loop in a uniform magnetic field *(b) The resulting induced voltage on the loop*

Figure 4.5 - Simple rotating loop and induced voltage output of a uniform magnetic field [31],[32]

Fig 4.5(a) shows a simple machine consisting of a large stationary magnet producing an essentially constant and uniform magnetic field $\boldsymbol{B}$ (the blue arrows) and a rectangular rotating loop of wire within that field. The rotating part of the machine is called the **rotor** and the stationary part of the machine is called the **stator**. Also, from **Fig 4.5(a)** it is observable that the **area of the loop** is just equal to $\boldsymbol{A = 2rl}$. If the loop is rotating at a constant **angular velocity** $\boldsymbol{\omega}$, then the angle $\boldsymbol{\theta}$ of the loop will increase linearly with time. In other words, $\boldsymbol{\theta = \omega t}$. Also, the tangential velocity $\boldsymbol{v}$ of the edges of the loop can be expressed as $\boldsymbol{v = \omega r}$, where $\boldsymbol{r}$ is the radius from axis of rotation out to the edge of the loop. The sum of the resulting voltages on each side of the loop determines the **total induced voltage** on the loop $\boldsymbol{e_{ind}}$. Therefore, it can be noted that the induced voltage, with the use of trigonometric identities along with the foregoing arguments, becomes

$$\boldsymbol{e_{ind} = 2vBl \sin\theta} \quad \text{..... (4.24)}$$

$$\boldsymbol{\Rightarrow e_{ind} = 2r\,\omega Bl \sin\omega t} \quad \text{..... (4.25)}$$

$$\boldsymbol{\Rightarrow e_{ind} = AB\omega \sin\omega t} \quad \text{..... (4.26)}$$

and is shown if **Fig 4.5(b)**. The maximum flux $\boldsymbol{\phi_{max}}$ through the loop occurs when the loop is perpendicular to the magnetic flux density lines. This flux is just the product of the loop's surface area $\boldsymbol{A}$ and the flux density $\boldsymbol{B}$ through the loop.

$$\boldsymbol{\phi_{max} = AB} \quad \text{..... (4.27)}$$

Therefore, the final form of the voltage equation is

$$e_{ind} = \phi_{max}\,\omega \sin \omega t \quad \text{..... (4.28)}$$

Thus, the voltage generated in the loop is in a sinusoidal form with magnitude equal to the product of the flux inside the machine and the speed of rotation of the machine. This is also true of real ac machines. In general, the voltage in any real machine will depend on three factors: **(a)** the flux in the machine, **(b)** the speed of rotation and **(c)** a constant representing the construction of the machine (the number of loops, etc.) **[2]**.

4.2.2 The Torque Induced in a Current-Carrying Loop

Now assume that the rotor loop of **Fig 4.5** is at some arbitrary angle θ with respect to the magnetic field and a current i is flowing in the loop, as shown in **Fig 4.6**. If a current flows in the loop, then a torque will be induced on the wire loop. The total induced torque on the τ_{ind} is the sum of the torques on each of its sides, resulting in

$$\tau_{ind} = 2rilB \sin \theta \quad \text{..... (4.29)}$$

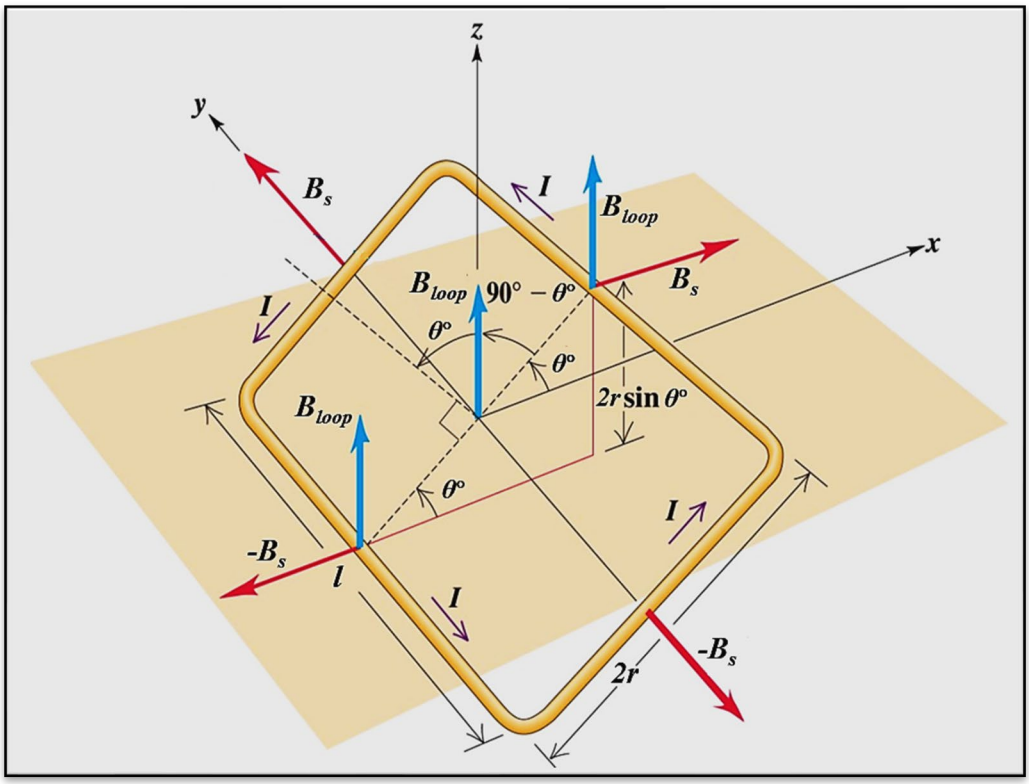

Figure 4.6 - A current-carrying loop in a uniform magnetic field [33]

If the current in the loop is as shown in the figure, that current will generate a magnetic flux density B_{loop} with direction perpendicular to the plane of the loop. The magnitude of B_{loop} will be

$$B_{loop} = \frac{\mu_i}{G} \quad \text{..... (4.30)}$$

where G is a factor that depends on the geometry of the loop (if the loop was a circle, then $G = 2r$, where r is the radius of the circle, so $B_{loop} = \mu_i/2r$. For a rectangular loop, the value of G will vary, depending on the exact length-to-width ratio of the loop.). Substituting **Eq 4.30** into **Eq 4.29** yields the result

$$\tau_{ind} = \frac{AG}{\mu} B_{loop} B_s \sin\theta \quad \text{..... (4.31)}$$

$$= k B_{loop} B_s \sin\theta \quad \text{..... (4.32)}$$

where $k = AG/\mu$ is a factor depending on the construction of the machine, B_s is used for the stator magnetic field to distinguish it from the magnetic field generated by the rotor, and θ is the angle between B_{loop} and B_s. The angle between B_{loop} and B_s can be seen by trigonometric identities to be the same as the angle θ in **Eq 4.29**. Both the magnitude and the direction of the induced torque can be determined by expressing **Eq 4.32** as a cross product:

$$\tau_{ind} = k B_{loop} \times B_s \quad \text{..... (4.33)}$$

Thus, the torque induced in the loop is proportional to the strength of the loop's magnetic field, the strength of the external magnetic field, and the sine of the angle between them. In general, the torque in any real machine will depend on four factors: **(a)** the strength of the rotor magnetic field, **(b)** the strength of the external magnetic field, **(c)** the sine of the angle between them and **(d)** a constant representing the construction of the machine (geometry, etc.) **[2]**.

4.3 The Rotating Magnetic Field

4.3.1 Proof of the Rotating Magnetic Field Concept

So far it has been shown that, if two magnetic fields are present in a machine, then a torque will be created which will tend to line up the two magnetic fields. If one magnetic field is produced by the stator of the machine and the other one is produced by the rotor of the machine, then a torque will be induced in the rotor which will cause the rotor to turn and align itself with the stator magnetic field. If there was some way to make the stator magnetic field rotate, then the induced torque in the rotor would cause it to constantly "chase" the stator magnetic field around in a circle. This is basically, the fundamental ac motor operation principle. So that, if a three-phase set of currents, each of equal magnitude and differing in phase by 120°, flows in a three-phase winding, then it will produce a rotating magnetic field of constant magnitude **[2]**.

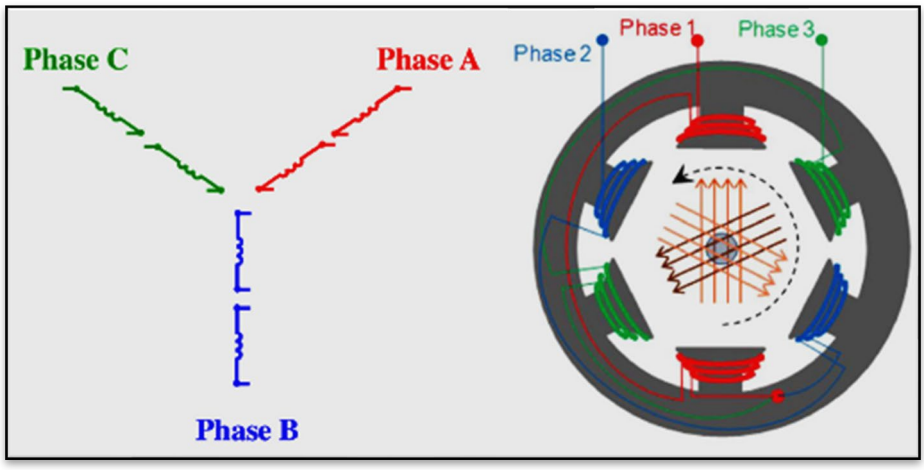

Figure 4.7 - A simple three-phase stator with a two-pole winding assembly [34]

The three-phase winding consists of three separate windings spaced 120 electrical degrees apart, around the stator of the machine, as shown in **Fig 4.7** above. Since such a winding produces only one north and one south magnetic pole, it is a two- pole winding. Currents in this stator are assumed positive if they flow from the unprimed end to the primed end of the coils **[2]**. By applying such a set of currents (expressed in Amperes ***A***) in the three coils at specific instants of time according to equations

$$i_{AA'}(t) = I_M \sin \omega t \quad \text{..... (4.34-a)}$$

$$i_{BB'}(t) = I_M \sin (\omega t - 120°) \quad \text{..... (4.34-b)}$$

$$i_{CC'}(t) = I_M \sin (\omega t - 240°) \quad \text{..... (4.34-c)}$$

the respective magnetizing intensities (expressed in $A \bullet turns / m$) are produced by each coil, given by equations

$$H_{AA'}(t) = H_M \sin \omega t \angle 0° \quad \text{..... (4.35-a)}$$

$$H_{BB'}(t) = H_M \sin (\omega t - 120°) \angle 120° \quad \text{..... (4.35-b)}$$

$$H_{CC'}(t) = H_M \sin (\omega t - 240°) \angle 240° \quad \text{..... (4.35-c)}$$

where $0°$, $120°$ and $240°$ are the **spatial angle** of the magnetic field intensity vector. The direction of each magnetic field intensity vector is given by the right-hand rule: if the fingers of the right-hand curl in the direction of the current flow in the coil, then the resulting magnetic field is in the direction that the thumb points. The magnitude of any of the magnetic field intensity vectors varies sinusoidally in time and its direction stays always constant. The flux densities (expressed in ***Teslas T***) resulting from these magnetic field intensities are given by **Eq 4.4** $(B = \mu H)$. They are

$$B_{AA'}(t) = B_M \sin \omega t \angle 0° \quad \text{..... (4.36-a)}$$

$$B_{BB'}(t) = B_M \sin (\omega t - 120°) \angle 120° \quad \text{..... (4.36-b)}$$

$$B_{CC'}(t) = B_M \sin (\omega t - 240°) \angle 240° \quad \text{..... (4.36-c)}$$

where $B_M = \mu H_M$. The currents and their corresponding flux densities can be examined at specific times to determine the resulting net magnetic field in the stator **[2]**.

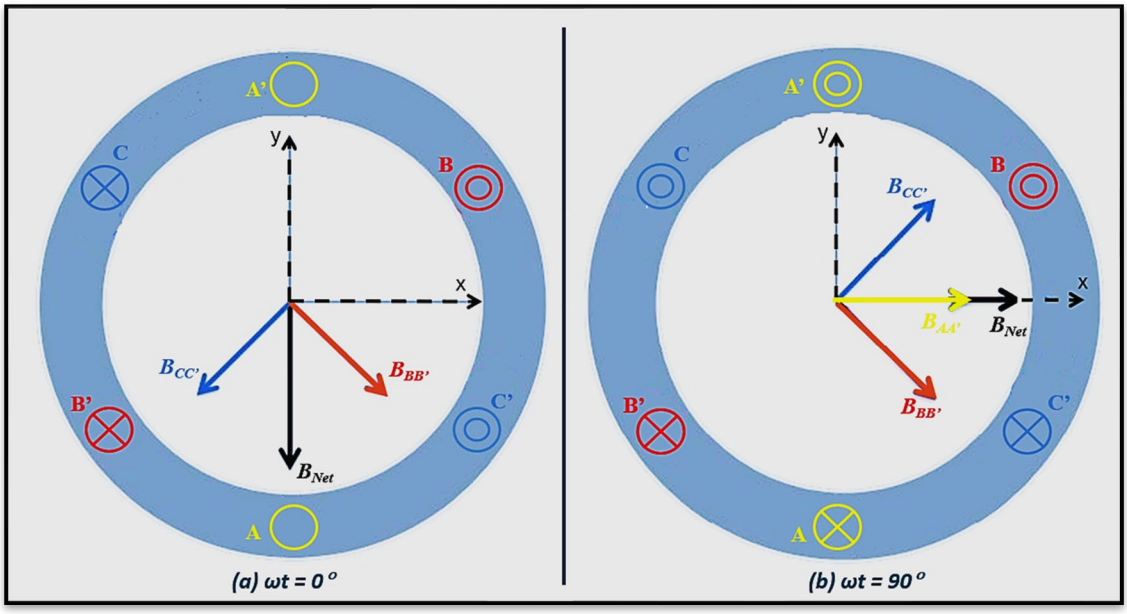

Figure 4.8 - The magnetic field vector B_{net} in a stator at specific instants of time

For example, at time $\omega t = 0°$ the net magnetic field $\boldsymbol{B}_{net}$, from all three coils added together, is shown in **Fig 4.8(a)** and it can be calculated as follows:

$$\boldsymbol{B}_{net} = \boldsymbol{B}_{AA'} + \boldsymbol{B}_{BB'} + \boldsymbol{B}_{CC'} =$$

$$= 0 + \left(-\frac{\sqrt{3}}{2}\boldsymbol{B}_M\right)\angle 120° + \left(\frac{\sqrt{3}}{2}\boldsymbol{B}_M\right)\angle 240°$$

$$= \left(\frac{\sqrt{3}}{2}\boldsymbol{B}_M\right)[-(\cos 120°\hat{x} + \sin 120°\hat{y}) + (\cos 240°\hat{x} + \sin 240°\hat{y})]$$

$$= \left(\frac{\sqrt{3}}{2}\boldsymbol{B}_M\right)\left(\frac{1}{2}\hat{x} - \frac{\sqrt{3}}{2}\hat{y} - \frac{1}{2}\hat{x} - \frac{\sqrt{3}}{2}\hat{y}\right)$$

$$= \left(\frac{\sqrt{3}}{2}\boldsymbol{B}_M\right)(-\sqrt{3}\,\hat{y})$$

$$= -1.5\,\boldsymbol{B}_M\,\hat{y}$$

$$\Rightarrow \boldsymbol{B}_{net} = 1.5\,\boldsymbol{B}_M\,\angle -90° \quad \text{..... (4.37)}$$

where $\hat{x}$ is the unit vector in the x direction, and $\hat{y}$ is the unit vector in the y direction.

In perspective, **Fig 4.8(b)** indicates the magnetic field at time $\omega t = 90°$, where the resulting $\boldsymbol{B}_{net}$ becomes

$$\boldsymbol{B}_{net} = \boldsymbol{B}_{AA'} + \boldsymbol{B}_{BB'} + \boldsymbol{B}_{CC'} =$$

$$= \ \ldots\ = 1.5\,\boldsymbol{B}_M\,\angle -90°$$

The magnetic field has the same magnitude $\mathbf{1.5}B_M$ and continues to rotate in a counterclockwise direction at angular velocity ω at any time t. Eventually, the total magnetic flux density in the stator is simply the sum of the three component magnetic fields added vectorially and the final expression for B_{net} is given by

$$B_{net} = (1.5\, B_M \sin \omega t)\, \hat{x} - (1.5\, B_M \cos \omega t)\, \hat{y} \quad \text{..... (4.38)}$$

4.3.2 The Relationship between Frequency and Speed of the Magnetic Field Rotation

Fig 4.9(a) below, shows that the rotating magnetic field in this stator can be represented as a north pole (where the flux leaves the stator) and a south pole (where the flux enters the stator). These magnetic poles complete one mechanical rotation around the stator surface for each electrical cycle of the applied current. Therefore, the mechanical speed of rotation of the magnetic field in revolutions per second is equal to the electric frequency in hertz **[2]**, **[7]**, **[9]**:

$$f_{se} = f_{sm} \quad \text{two poles} \quad \text{..... (4.39)}$$

$$\omega_{se} = \omega_{sm} \quad \text{two poles} \quad \text{..... (4.40)}$$

where f_{sm} and ω_{sm} are the mechanical speed of the stator magnetic fields in **revolutions per second** and **radians per second**, while f_{se} and ω_{se} are the electrical frequency of the stator currents in hertz and **radians per second**. The windings on the two-pole stator in **Fig 4.9(a)** occur in the order ***a-c'-b-a'-c-b'*** (taken counterclockwise).

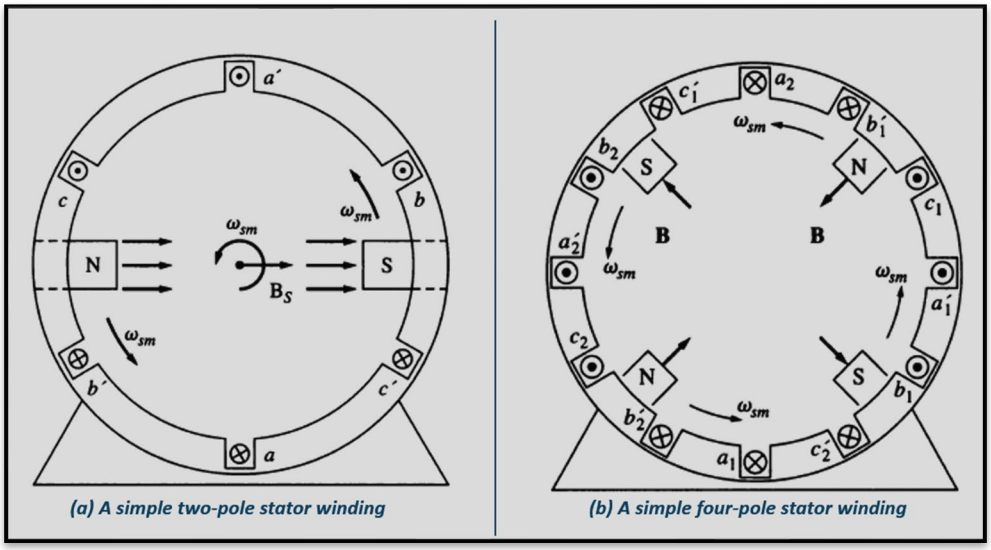

Figure 4.9 - The Rotating magnetic field represented as moving north and south stator poles [2]

When a three-phase set of currents is applied to this stator, two north poles and two south poles of alternating polarity every **90°** around the stator surface are produced in the stator winding, as shown in **Fig 4.9(b)**. In this winding, a pole moves only halfway around the stator surface in one electrical cycle. Since one electrical cycle is **360 electrical degrees**, and since the mechanical motion is **180 mechanical degrees**, the relationship between the stator electrical angle θ_{se} and the mechanical angle θ_{sm} in this stator is

$$\theta_{se} = 2\theta_{sm} \quad \text{..... (4.41)}$$

Thus, for the four-pole winding, the electrical frequency of the current is twice the mechanical frequency of rotation:

$$f_{se} = 2f_{sm} \quad \text{four poles} \quad \text{..... (4.42)}$$

$$\omega_{se} = 2\omega_{sm} \quad \text{four poles} \quad \text{..... (4.43)}$$

In general, if the number of magnetic poles on an ac machine stator is P, then there are $P/2$ repetitions of the winding sequence $a\text{-}c'\text{-}b\text{-}a'\text{-}c\text{-}b'$ around its inner surface, and the electrical and mechanical quantities on the stator are related by

$$f_{se} = \frac{P}{2} f_{sm} \quad \text{..... (4.44)}$$

$$\omega_{se} = \frac{P}{2} \omega_{sm} \quad \text{..... (4.45)}$$

Also, noting that $f_{sm} = n_{sm}/60$, it is possible to relate the electrical frequency of the stator in hertz to the resulting mechanical speed of the magnetic fields in revolutions per minute. This relationship is

$$f_{se} = \frac{n_{sm} P}{120} \quad \text{..... (4.46)}$$

4.3.3 Reversing the Direction of Magnetic Field Rotation

Another interesting fact which can be taken into consideration is that if the current in any two of the three coils is swapped, the direction of the magnetic field's rotation will be reversed. This means that it is possible to reverse the direction of rotation of an ac motor just by switching the connections on any two of the three coils. This reversible direction of rotation can be proved, by switching phases bb' and cc' in **Fig 4.9(a)** and calculating the resulting flux density B_{net}. Then, the net magnetic flux density B_{net} will eventually result in

$$B_{net} = (1.5\, B_M \sin \omega t)\, \hat{x} + (1.5\, B_M \cos \omega t)\, \hat{y} \quad \text{..... (4.47)}$$

This time the magnetic field has the same magnitude but rotates in a clockwise direction. Therefore, switching the currents in two stator phases reverses the direction of magnetic field rotation in an ac machine **[2]**.

4.4 Magnetomotive Force and Flux Distribution on AC Machines

In the previous section, the flux produced inside a simple ac machine, was treated as if it was in free space. The direction of the flux density produced by a coil of wire was assumed to be perpendicular to the plane of the coil, with the direction of the flux given by the right-hand rule. However, this case is not representative, since the flux in real ac machines is not constant in either magnitude or direction, as long as there is a ferromagnetic rotor in the center of the machine with a small air gap between the rotor and the stator. The rotor can be cylindrical or it can have pole faces projecting out from its surface, like the ones shown in **Fig 4.10**. If the rotor is cylindrical, the machine is said to have **nonsalient poles**. If the rotor has pole faces projecting out from it, the machine is said to have **salient poles [2]**.

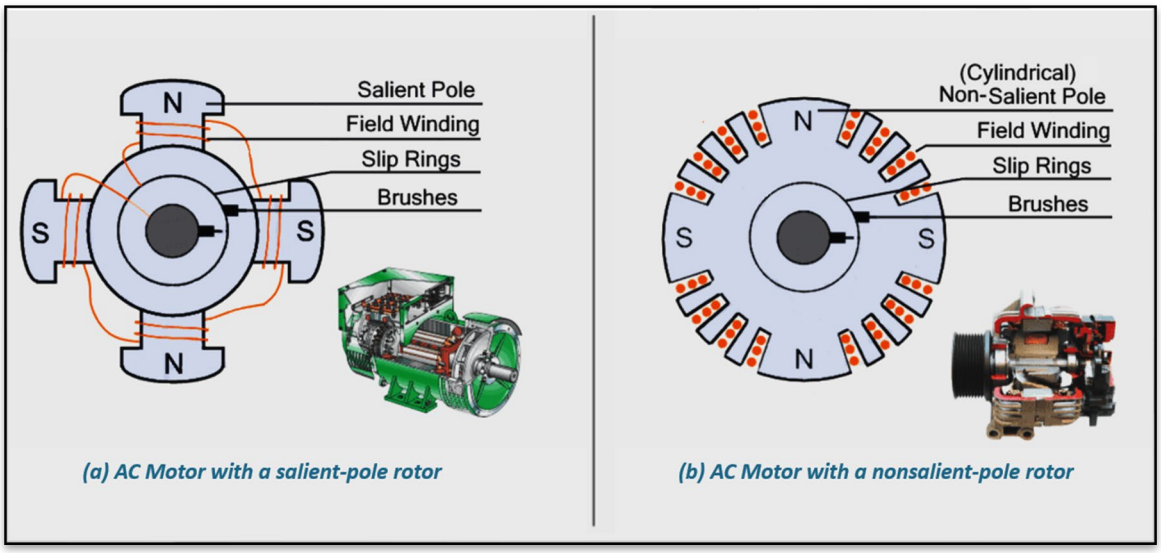

Figure 4.10 - The two types of AC machine rotors [35],[36]

The reluctance of the air gap in the cylindrical-rotor machine in **Fig 4.10(b)** is much higher than the reluctances of either the rotor or the stator, so the flux density vector ***B*** takes the shortest possible path across the air gap and jumps perpendicularly between the rotor and the stator **[2]**.

To produce a sinusoidal voltage in a machine like this, the magnitude of the flux density vector ***B*** must vary in a sinusoidal manner along the surface of the air gap. The flux density will vary sinusoidally only if the magnetizing intensity ***H*** and so the magnetomotive force ***F*** **(or *mmf*)**, varies in a sinusoidal manner along the surface of the air gap. The most direct way to achieve a sinusoidal variation of magnetomotive force along the surface of the air gap is to distribute the turns of the winding that produces the ***F*** in closely spaced slots around the surface of the machine and to vary the number of conductors in each slot in a sinusoidal manner. **Fig 4.11(a)** shows such a winding, and **Fig 4.11(b)** shows the magnetomotive force resulting from the winding.

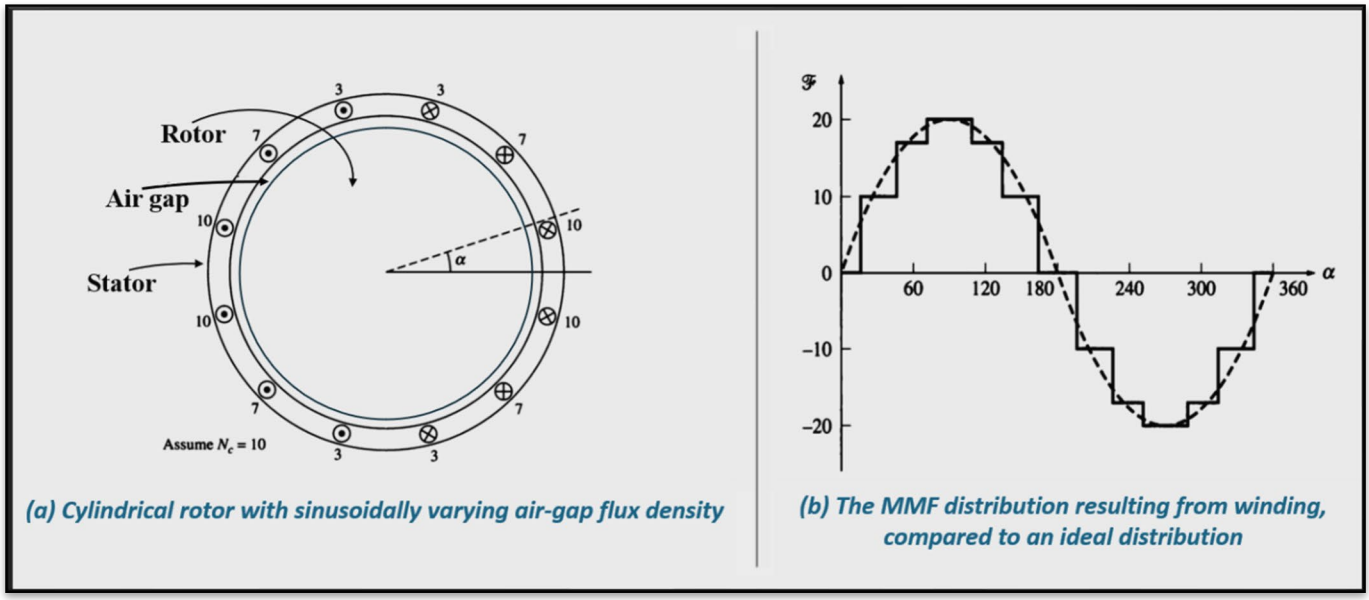

Figure 4.11 - AC machine with a distributed stator winding and its mmf distribution output [2]

The number of conductors in each slot is given by the equation

$$n_c = N_c \cos \alpha \quad \text{..... (4.48)}$$

where N_C is the number of conductors at an angle of **0°**.

As **Fig 4.11(b)** shows, this distribution of conductors produces a close approximation to a sinusoidal distribution of magnetomotive force. Furthermore, the more slots there are around the surface of the machine and the more closely spaced the slots are, the better this approximation becomes **[2]**.

In practice, it is not possible to distribute windings exactly in accordance with **Eq 4.48**, since there are only a finite number of slots in a real ac motor and since only integral numbers of conductors can be included in each slot. The resulting magnetomotive force distribution F is only approximately sinusoidal and higher-order harmonic components are present. Fractional-pitch windings are used to suppress these unwanted harmonic components.

Furthermore, it is often convenient for the machine designer to include equal numbers of conductors in each slot, instead of varying the number. Windings of this type have stronger high-order harmonic components than the designed windings in accordance with **Eq 4.48**.

4.5 Induced Voltage in AC Machines

Just as a three-phase set of currents in a stator can produce a rotating magnetic field, a rotating magnetic field can produce a three-phase set of voltages in the coils of a stator. By looking at just one single-turn coil and then expanding the results to a more general three-phase stator, makes the development much easier to begin.

4.5.1 The Induced Voltage in a Coil on a Two-Pole Stator

Fig 4.12 shows a rotating rotor with a sinusoidally distributed magnetic field in the center of a stationary coil. Notice that this is the reverse of the foregoing situation in Section **4.2**, which involved a stationary magnetic field and a rotating loop.

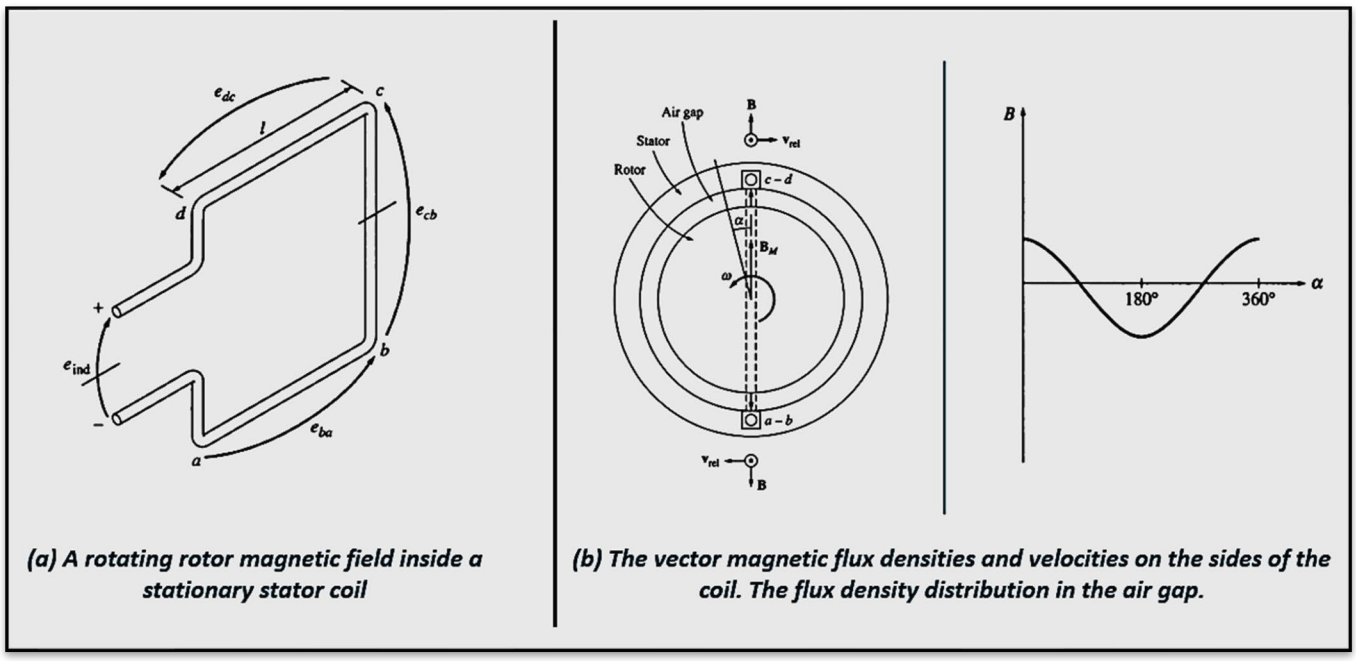

(a) A rotating rotor magnetic field inside a stationary stator coil

(b) The vector magnetic flux densities and velocities on the sides of the coil. The flux density distribution in the air gap.

Figure 4.12 - Rotating rotor in the center of a stationary coil [2]

The magnitude of the flux density vector $\boldsymbol{B}$ in the air gap between the rotor and the stator is assumed to vary sinusoidally with mechanical angle, while the direction of $\boldsymbol{B}$ is always radially outward. If α is the angle measured from the direction of the peak rotor flux density, then the magnitude of the flux density vector $\boldsymbol{B}$ at a point around the rotor is given by

$$B = B_M \cos \alpha \quad \text{..... (4.49-a)}$$

At some locations around the air gap, the flux density vector will really point in toward the rotor. In those locations, the sign of **Eq 4.49-a** is negative. Since the rotor is itself rotating within the stator at an angular velocity ω_m , the magnitude of the flux density vector $\boldsymbol{B}$ at any angle α around the stator is given by

$$B = B_M \cos (\omega t - \alpha) \quad \text{..... (4.49-b)}$$

The total voltage induced in the coil will be the sum of the voltages induced in each of its four sides. The equation for the induced voltage in a wire was shown to be

$$e_{ind} = (v \times B) \cdot l \quad \text{..... (4.15)}$$

However, this equation was derived for the case of a moving wire in a stationary magnetic field. In this case, the wire is stationary and the magnetic field is moving, so the equation does not directly apply. To use it, we must be in a frame of reference where the magnetic field appears to be stationary. In such a stationary field, the sides of the coil will appear to go by at an apparent velocity v_{rel} and **Eq 4.15** can then be applied.

Fig 4.12(b) shows the vector magnetic field and velocities from the point of view of a stationary magnetic field and a moving wire. Since the velocity of the end conductors is given by $v = r\omega_m$, the flux passing through the coil can be expressed as $\phi = 2rlB_m$ and ω_m equals to $\omega_e = \omega$ for a two-pole stator, the induced voltage can be expressed as

$$e_{ind} = \phi \omega \cos \omega t \quad \text{..... (4.50)}$$

Eq 4.50 describes the voltage induced in a single-turn coil. If the coil in the stator has N_C turns of wire, then the total induced voltage of the coil will be

$$e_{ind} = N_c \phi \omega \cos \omega t \quad \text{..... (4.51)}$$

which is the same as the result obtained for the simple rotating loop in Section **4.2**. Also, the cosine term of the equations above, has no special significance compared to the sine. It resulted from the choice of reference direction for α in this derivation. If the reference direction for α had been rotated by **90°** it would have contained a sine term, as in previous equations **[2]**.

4.5.2 The Induced Voltage in a Three-Phase Set of Coils

If three coils, each of N_C turns, are placed around the rotor magnetic field as shown in **Fig 4.13**, then the voltages induced in each of them will be the same in magnitude but will differ in phase by 120°.

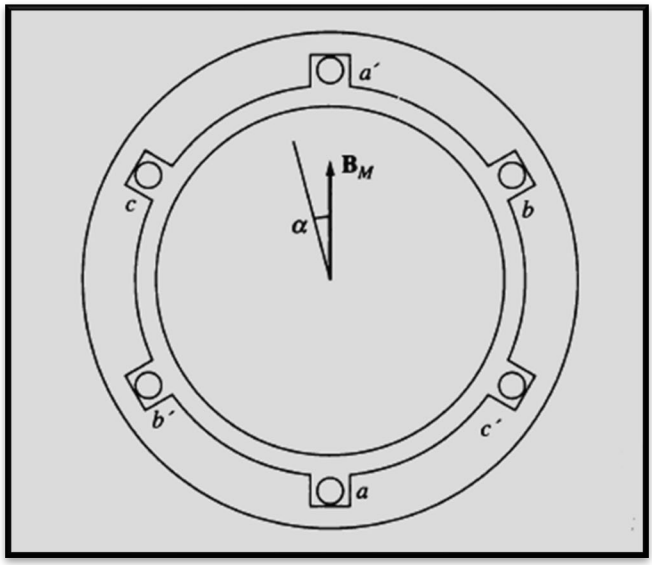

Figure 4.13 The production of three-phase voltages from three coils spaced 120° apart [2]

The resulting voltages in each of the three coils are

$$e_{aa'}(t) = N_c \phi \omega \sin \omega t \quad \text{..... (4.52-a)}$$

$$e_{bb'}(t) = N_c \phi \omega \sin (\omega t - 120°) \quad \text{..... (4.52-b)}$$

$$e_{cc'}(t) = N_c \phi \omega \sin (\omega t - 240°) \quad \text{..... (4.52-c)}$$

Therefore, a three-phase set of currents can generate a uniform rotating magnetic field in a machine stator, and a uniform rotating magnetic field can generate a three-phase set of voltages in such a stator.

4.5.3 The RMS Voltage in a Three-Phase Stator

The peak voltage in any phase of a three-phase stator of this sort is

$$E_{max} = N_c \phi \omega \quad \text{..... (4.53)}$$

Since $\omega = 2\pi f$, this equation can also be written as

$$E_{max} = 2\pi N_c \phi f \quad \text{..... (4.54)}$$

Therefore, the rms voltage of any phase of this three-phase stator becomes

$$E_A = \sqrt{2}\, \pi N_c \phi f \quad \text{..... (4.55)}$$

The rms voltage at the terminals of the machine will depend on whether the stator is Y- or Δ-connected. If the machine is Y-connected, then the terminal voltage will be $\sqrt{3}$ times E_A, if the machine is Δ-connected, then the terminal voltage will just be equal to E_A **[2]**.

4.6 Induced Torque In An AC Machine

In ac machines under normal operating conditions, there are two magnetic fields present, a magnetic field from the rotor circuit and another magnetic field from the stator circuit **[37]**. The interaction of these two magnetic fields produces the torque in the machine, just as two permanent magnets near each other will experience a torque which causes them to line up. **Fig 4.14(a)** shows a simplified ac machine with a sinusoidal stator flux distribution that peaks in the upward direction and a single coil of wire mounted on the rotor.

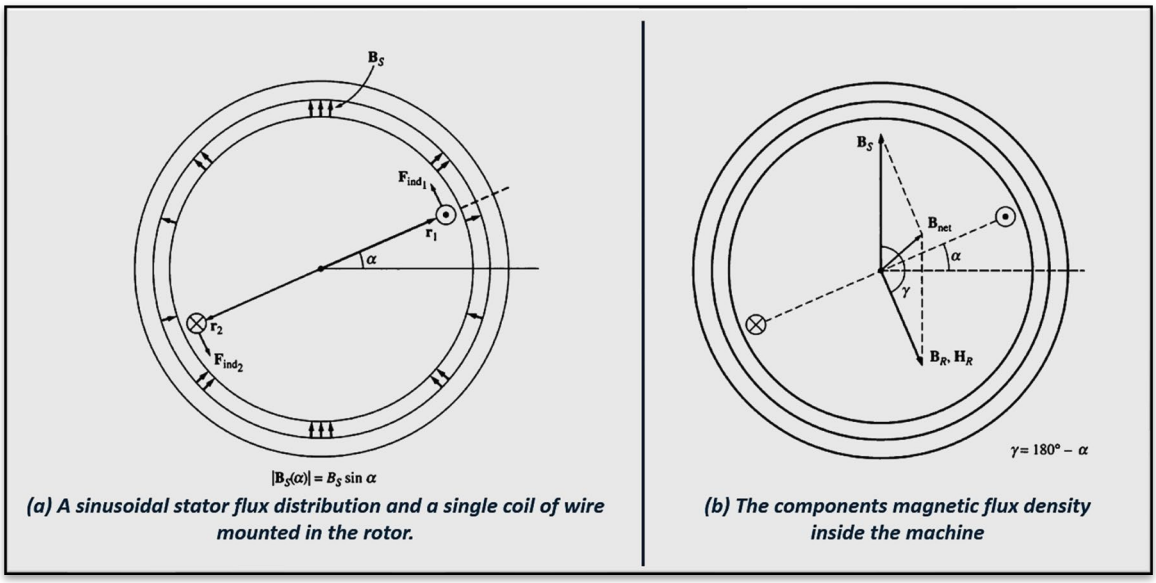

Figure 4.14 - A simplified ac machine with a sinusoidal stator flux distribution and its component magnetic flux density [2]

The stator flux distribution in this machine is

$$B_s(\alpha) = B_s \sin \alpha \quad \text{..... (4.56)}$$

where B_S is the magnitude of the peak flux density. $B_s(\alpha)$ is positive when the flux density vector points radially outward from the rotor surface to the stator surface. The induced force on conductor 1 is according to **Eq 4.14** *(F = i l B sin θ)*;

$$F_{ind,1} = i\, l\, B_s \sin \alpha \quad \text{..... (4.57)}$$

with direction as shown. The torque on the conductor is

$$\tau_{ind,1} = r\, i\, l\, B_s \sin \alpha \qquad \text{counterclockwise} \quad \text{..... (4.58)}$$

Similarly, the same results arise for induced force $F_{ind,2}$ and torque $\tau_{ind,2}$ on conductor 2, with direction as shown, and therefore, the resulting torque on the rotor loop is

$$\tau_{ind} = 2r\, i\, l\, B_s \sin \alpha \qquad \text{counterclockwise} \quad \text{..... (4.59)}$$

Eq 4.59 can be expressed in a more convenient form by examining **Fig 4.14(b)** and noting two facts:

(a) The current i flowing in the rotor coil produces a magnetic field of its own. The direction of the peak of this magnetic field is given by the right-hand rule, and the magnitude of its magnetizing intensity H_R is directly proportional to the current flowing in the rotor **[2]**:

$$H_R = C\,i \quad \text{..... (4.60)}$$

where C is a constant of proportionality.

(b) The angle between the peak of the stator flux density B_S and the peak of the rotor magnetizing intensity H_R is γ. Furthermore,

$$\gamma = 180° - \alpha \Rightarrow \sin\gamma = \sin(180° - \alpha) = \sin\alpha \quad \text{..... (4.61)}$$

By combining these two observations, the torque on the loop can be expressed as

$$\tau_{ind} = K\,H_R\,B_s \sin\alpha \qquad \text{counterclockwise} \quad \text{..... (4.62)}$$

where K is a constant, dependent on the construction of the machine. Note that both the magnitude and the direction of the torque can be expressed by the equation

$$\tau_{ind} = K\,H_R \times B_s \quad \text{..... (4.63)}$$

Finally, since $B_R = \mu\,H_R$, this equation can be reexpressed as

$$\tau_{ind} = k\,B_R \times B_s \quad \text{..... (4.64)}$$

where $k = K/\mu$. Note that in general k will not be constant, since the magnetic permeability μ varies with the amount of magnetic saturation in the machine.

Eq 4.64 is just the same as **Eq 4.33**, which was derived for the case of a single loop in a uniform magnetic field. It can be applied to any ac machine, not just to the simple one-loop rotor just described. Only the constant k will differ from machine to machine. The net magnetic field in this machine is the vector sum of the rotor and stator fields (assuming no saturation):

$$B_{net} = B_R + B_s \quad \text{..... (4.65)}$$

This fact can be used to produce an equivalent (and sometimes more useful) expression for the induced torque in the machine. From **Eq 4.64** and **Eq 4.65** , the induced torque can also be expressed as a cross product of B_R and B_{net} with the same constant k as before. Eventually, the magnitude of this expression results in

$$\tau_{ind} = k\,B_R \times B_{net} \sin\delta \quad \text{..... (4.66)}$$

where δ is the angle between B_R and B_{net} **[2]**.

5. AC MACHINES (INDUCTION MOTORS)

5.1 Introduction of Induction Motors

Induction motors are known as the workhorse of industry because of their low cost and rugged construction **[7]**. The distinguishing feature of an induction motor is that no dc field current is required to run the machine. The rotor voltage, which produces the rotor current and the rotor magnetic field, is induced in the rotor windings rather than being physically connected by wires. Although it is possible to use an induction machine as either a motor or a generator, it has many disadvantages as a generator and so is only used as a generator in special applications **[2]**. They are also used as servo motors in vector control drive systems, in cases where significant application requirements or where low installation costs are required. However, they are not sufficient enough to compete with **synchronous permanent magnet motors** in servo drives for applications where priority is given to high precision and really fast performance of the dynamics of speed control. **Fig 5.1** below, shows a cutaway diagram of these two types of ac motors, both of which contain a typical two-pole stator.

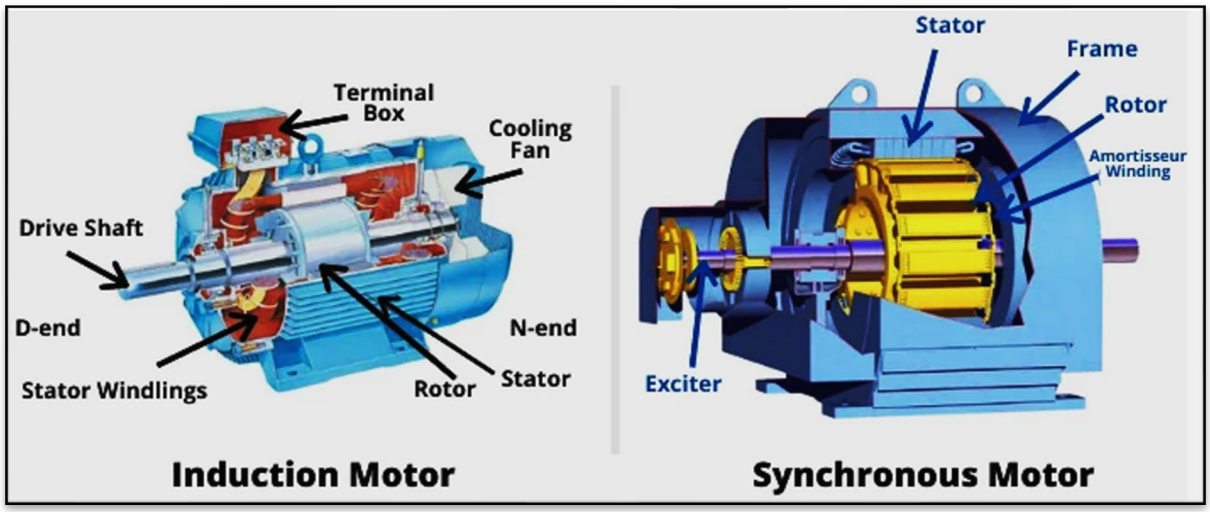

Figure 5.1 - Cutaway Diagram of the two major classes of AC motors [38]

The stator of the induction motor has the same structure as a synchronous machine, while its rotor has a different structure. **Fig 5.2** shows the two different types of induction motor rotors which can be placed inside the stator. One is called a **cage rotor**, while the other is called a **wound rotor.**

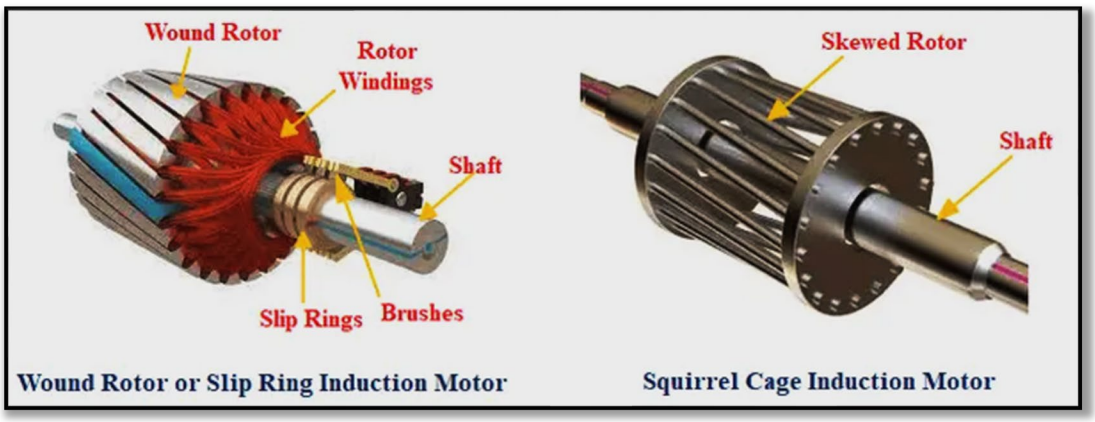

Figure 5.2 - Design of the two types of induction motor rotors [39]

A cage induction motor rotor consists of a series of conducting bars laid into slots carved in the face of the rotor and shorted at either end by large shorting rings. This design is mostly referred to as a **squirrel-cage rotor** because the conductors, if examined individually, would look like one of the exercise wheels that squirrels or hamsters run on **[2]**.

A **wound rotor** has a complete set of three-phase windings that are similar to the windings on the stator. The three phases of the rotor windings are usually Y-connected and the endings of the three rotor wires are tied to slip rings on the rotor's shaft, mainly in skewed way in order to eliminate slot harmonics. The rotor windings are shorted through brushes riding on the slip rings. Wound-rotor induction motors therefore have their rotor currents accessible at the stator brushes, where they can be examined and where extra resistance can be inserted into the rotor circuit. It is possible to take advantage of this feature to modify the torque-speed characteristic of the motor. Thus, due to their construction associated with brushes and slip rings components, wound-rotor induction motors are rarely used, since they are more expensive than squirrel-cage induction motors and require much more maintenance **[2]**.

5.1.1 The Development of Induced Torque in an Induction Motor

Fig 5.3 shows a cage rotor induction motor. A three-phase set of voltages has been applied to the stator and a three-phase set of stator currents is flowing. These currents produce a magnetic field $\boldsymbol{B_s}$, which is rotating in a counterclockwise direction. The speed of the magnetic field's rotation is given by

$$n_{sync} = \frac{120 f_{se}}{P} \quad \text{..... (5.1)}$$

where $\boldsymbol{f_{se}}$ is the system frequency applied to the stator in hertz and $\boldsymbol{P}$ is the number of poles in the machine.

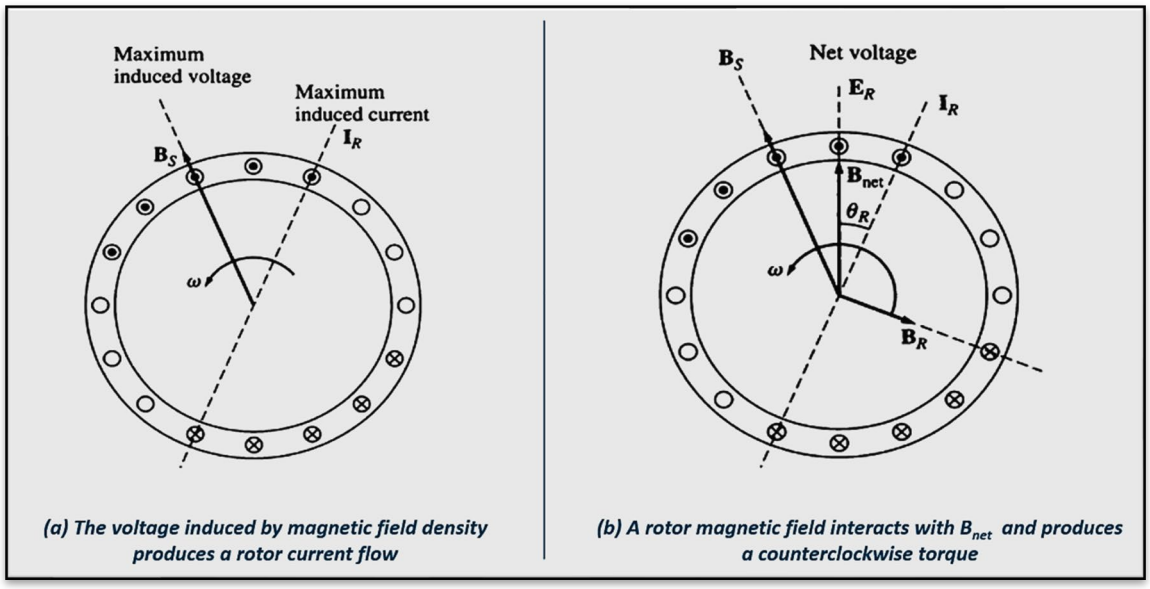

Figure 5.3 - A cage rotor producing magnetic field density by a three-phase set of stator currents [2]

This rotating magnetic field $\boldsymbol{B_S}$ passes over the rotor bars and induces a voltage $\boldsymbol{e_{ind}}$ in them ($\boldsymbol{v_s \cdot B_s \cdot l}$ according to **Eq 4.15** for the induced voltage). It is the relative motion of the rotor compared to the stator magnetic field that produces induced voltage in a rotor bar. The velocity of the upper rotor bars relative to the magnetic field is to the right, so the induced voltage in the upper bars is out of the page, while the induced voltage in the lower bars is into the page. This results in a current flow out of the upper bars and into the lower bars. However, since the rotor assembly is inductive, the peak rotor current $\boldsymbol{I_R}$ lags behind the peak rotor voltage $\boldsymbol{V_R}$ as shown in **Fig 5.3(b)**. The rotor current flow produces a rotor magnetic field $\boldsymbol{B_R}$.

Finally, since the resulting torque in the machine is counterclockwise ($\tau_{ind} = k\, B_R \times B_s$, according to **Eq 4.64** for the induced torque), the rotor induced torque is also counterclockwise and accelerates in that direction.

There is a finite upper limit to the motor's speed, however. If the induction motor's rotor was turning at **synchronous speed**, then the rotor bars would be stationary relative to the magnetic field and there would be no induced voltage **[9]**. If e_{ind} was equal to zero, then there would be no rotor current and no rotor magnetic field. With no rotor magnetic field, the induced torque would be zero, and the rotor would slow down as a result of friction losses. An induction motor can thus speed up to near-synchronous speed, but it can never exactly reach synchronous speed. In normal operation both the rotor and stator magnetic fields B_R and B_s rotate together at synchronous speed n_{sync}, while the rotor itself turns at a slower speed **[2]**.

5.1.2 The Concept of Rotor Slip

The voltage induced in a rotor bar of an induction motor depends on the speed of the rotor relative to the magnetic fields. Since the behavior of an induction motor depends on the rotor's voltage and current, it is often more logical to talk about this relative speed. Two terms are commonly used to define the relative motion of the rotor and the magnetic fields. One is **slip speed**, defined as the difference between synchronous speed and rotor speed **[2]**:

$$n_{slip} = n_{sync} - n_m \quad \text{…….. (5.2)}$$

where n_{slip} is the slip speed of the machine, n_{sync} is the speed of the magnetic fields and n_m is the mechanical shaft speed of motor. The other term used to describe the relative motion is **slip**, which is the relative speed expressed on a per-unit or a percentage basis. Thus, the slip s is defined as

$$s = \frac{n_{slip}}{n_{sync}} (\times 100)$$

$$\Rightarrow s = \frac{n_{sync} - n_m}{n_{sync}} (\times 100) \quad \text{…….. (5.3)}$$

This equation can also be expressed in terms of angular velocity ω (radians per second) as

$$s = \frac{\omega_{sync} - \omega_m}{\omega_{sync}} (\times 100) \quad \text{…….. (5.4)}$$

Notice that if the rotor turns at synchronous speed then slip $s = 0$, while if the rotor is stationary, $s = 1$. All normal motor speeds fall somewhere between those two limits. It is possible to express the mechanical speed of the rotor shaft in terms of synchronous speed and slip. Solving **Eq 5.3** and **Eq 5.4** for mechanical speed yields

$$n_m = (1 - s) n_{sync} \quad \text{…….. (5.5)}$$

or

$$\omega_m = (1 - s) \omega_{sync} \quad \text{…….. (5.6)}$$

These equations are really useful in the derivation of induction motor torque and power relationships.

5.1.3 The Electrical Frequency on the Rotor

An induction motor works by inducing voltages and currents in the rotor of the machine, and for that reason it has sometimes been called a **rotating transformer**. Like a transformer, the primary (stator) induces a voltage in the secondary (rotor), but unlike a transformer, the secondary frequency is not necessarily the same as the primary frequency. If the rotor of a motor is locked so that it cannot move, then the rotor will have the same frequency as the stator. On the other hand, if the rotor turns at synchronous speed, the frequency on the rotor will be zero. The rotor frequency, eventually, is proved to be directly proportional to the difference between the speed of the magnetic field n_{sync} and the speed of the rotor n_m and so, for any speed in between it can be expressed as

$$f_{re} = s\, f_{se} \quad \text{…….. (5.7)}$$

where f_{re} is the rotor frequency and f_{se} the stator frequency.

Several alternative forms of this expression exist that are sometimes useful. One of the most common is the expression:

$$f_{re} = \frac{n_{sync} - n_m}{n_{sync}}\, f_{se}$$

Since $n_{sync} = 120\, f_{se} / P$ (according to **Eq 5.1**), therefore

$$f_{re} = \frac{P}{120}\,(n_{sync} - n_m) \quad \text{…….. (5.8)}$$

5.2 Losses, Power and Torque in Induction Motors

An induction motor can be basically described as a rotating transformer. Its input is a three-phase system of voltages and currents. For an ordinary transformer, the output is electric power from the secondary windings. The secondary windings in an induction motor (the rotor) are shorted out, so no electrical output exists from normal induction motors. Instead, the output is mechanical. The relationship between the input electric power P_{in} and the output mechanical power P_{out} of this motor is shown in the power-flow diagram in **Fig 5.4**.

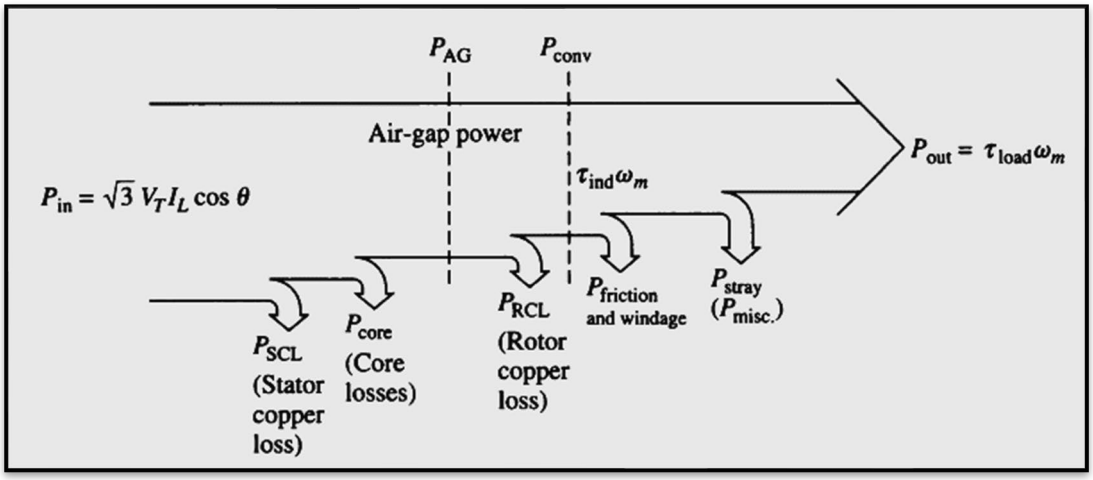

Figure 5.4 - Power – Flow diagram of an induction motor [2], [40]

The **input power** to an induction motor is in the form of three-phase electric voltages and currents. The first losses encountered in the machine are I^2R **losses in the stator windings (the stator copper loss** P_{SCL} **)**. Then, some amount of power is **lost as hysteresis and eddy currents in the stator (**P_{core}**)**. The power remaining at this point is transferred to the rotor of the machine across the air gap between the stator and rotor. This power is called the **air-gap power** P_{AG} of the machine. After the power is transferred to the rotor, some of it is lost as I^2R losses (the **rotor copper loss** P_{RCL}), and the rest is converted from electrical to mechanical form (P_{conv}). Finally, friction and windage losses $P_{F\&W}$ and stray losses P_{misc} are subtracted. The remaining power is the output of the motor P_{out} **[2]**.

Fig 5.5 shows the per-phase equivalent circuit of an induction motor. If the equivalent circuit is examined closely, it can be used to derive the power and torque equations governing the operation of the motor.

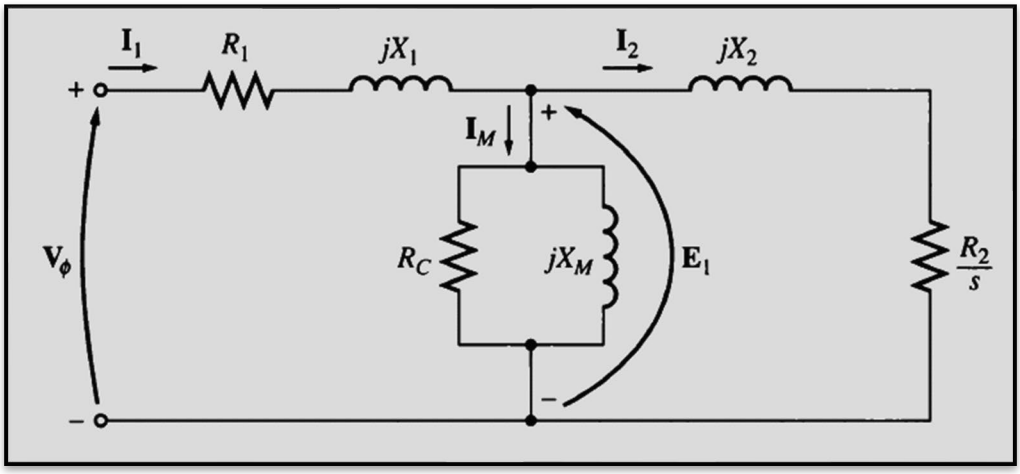

Figure 5.5 - The per-phase equivalent circuit of an induction motor [2]

The input current to a phase of the motor can be found by dividing the input voltage V_φ by the total equivalent impedance:

$$I_1 = \frac{V_\varphi}{Z_{eq}} \quad \text{…….. (5.9)}$$

where

$$Z_{eq} = R_1 + jX_1 + \frac{1}{R_C - jB_M + \frac{1}{V_2/s + jX_2}} \quad \text{…….. (5.10)}$$

Therefore, the stator copper losses, the core losses, and the rotor copper losses can be found. The stator copper losses in the three phases are given by

$$P_{SCL} = 3I_1^2 R_1 \quad \text{…….. (5.11)}$$

The core losses are given by

$$P_{core} = 3E_1^2 R_C \quad \text{…….. (5.12)}$$

so, the air-gap power can be found as

$$P_{AG} = P_{in} - P_{SCL} - P_{core} \quad \text{…….. (5.13)}$$

The only element in the equivalent circuit of **Fig 5.5**, where the air-gap power can be consumed, is in the resistor R_2 / s. Therefore, the air-gap power can also be given by

$$P_{AG} = 3I_2^2 \frac{R_2}{s} \quad \text{…….. (5.14)}$$

The actual resistive losses in the rotor circuit are given by the equation

$$P_{RCL} = 3I_R^2 R_R \quad \text{…….. (5.15)}$$

or

$$P_{RCL} = 3I_2^2 R_2 \quad \text{…….. (5.16)}$$

since the power is unchanged when referred across an ideal transformer. After stator copper losses, core losses, and rotor copper losses are subtracted from the input power to the motor, the remaining power is converted from electrical to mechanical form. This converted power, which is sometimes called **developed mechanical power**, is given by

$$P_{conv} = P_{AG} - P_{RCL}$$

$$= 3I_2^2 \frac{R_2}{s} - 3I_2^2 R_2$$

$$= 3I_2^2 R_2 \left(\frac{1}{s} - 1\right)$$

$$P_{conv} = 3I_2^2 R_2 \left(\frac{1-s}{s}\right) \quad \text{…….. (5.17)}$$

Notice from **Eq 5.14** and **Eq 5.16** that the rotor copper losses are equal to the air-gap power times the slip:

$$P_{RCL} = sP_{AG} \quad \text{…….. (5.18)}$$

Therefore, the lower the slip of the motor, the lower the rotor losses in the machine. Note also that if the rotor is not turning, the slip $s = 1$ and the air-gap power is entirely consumed in the rotor. This is logical, since if the rotor is not turning, the output power $P_{out} (= \tau_{load} \omega_m)$ must be **zero**. Since $P_{conv} = P_{AG} - P_{RCL}$, this also gives another relationship between the air-gap power and the power converted from electrical to mechanical form:

$$P_{conv} = P_{AG} - P_{RCL}$$

$$= P_{AG} - sP_{AG}$$

$$P_{conv} = (1 - s)P_{AG} \quad \text{…….. (5.19)}$$

Finally, if the friction and windage losses and the stray losses are known, the output power can be found as

$$P_{out} = P_{conv} - P_{F\&W} - P_{misc} \quad \text{…….. (5.20)}$$

The **induced torque** τ_{ind} in a machine was defined as the torque generated by the internal electric-to-mechanical power conversion. This torque differs from the torque actually available at the terminals of the motor by an amount equal to the friction and windage torques in the machine. The induced torque is given by the equation

$$\tau_{ind} = \frac{P_{conv}}{\omega_m} \quad \text{…….. (5.21)}$$

This torque is also called the **developed torque** of the machine. The induced torque of an induction motor can be expressed in a different form as well. **Eq 5.6** expresses actual speed in terms of synchronous speed ω_s and slip s, while **Eq 5.19** expresses P_{conv} in terms of P_{AG} and slip s. Substituting these two equations into **Eq 5.21** yields

$$\tau_{ind} = \frac{(1-s)P_{AG}}{(1-s)\omega_{sync}}$$

$$\tau_{ind} = \frac{P_{AG}}{\omega_{sync}} \quad \text{…….. (5.22)}$$

The last equation is especially useful because it expresses induced torque directly in terms of air-gap power and synchronous speed, which does not vary. A knowledge of P_{AG} consequently, directly yields τ_{ind}.

5.3 Introduction To Single-Phase Induction Motors

Three-phase induction motors are by far the most common ones in larger commercial and industrial settings. However, most homes and small businesses do not have three-phase power available. For such locations, all motors must run from single-phase power sources **[2]**. One common single-phase motor is the single-phase version of the induction motor. The rotor stays the same, but the stator has only a single distributed phase. An induction motor with a single-phase stator is shown with respect to the stator of a three-phase induction motor in **Fig 5.6**.

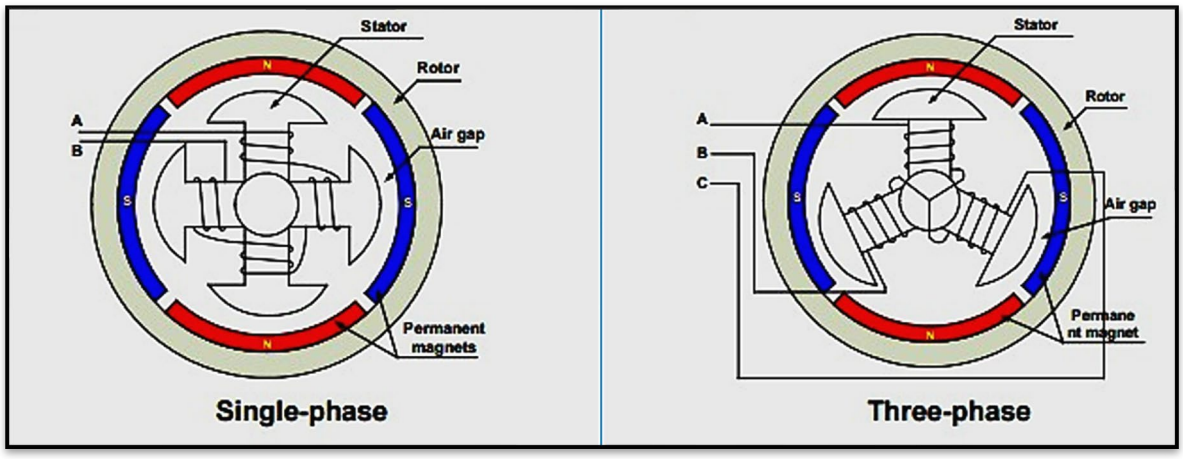

Figure 5.6 A single-phase and a three-phase distribution in induction motors [41]

Single-phase induction motors, as the one in **Fig 5.7(a)** below, suffer from a severe handicap. Since there is only one phase on the stator winding, the magnetic field in a single-phase induction motor does not rotate. It pulses instead, getting first larger and then smaller, but always remaining in the same direction. Because there is no rotating stator magnetic field B_S, a single-phase induction motor has no starting torque **[2]**.

This fact is easy to see from an examination of the motor when its rotor is stationary. The stator flux of the machine first increases and then decreases, but it always points in the same direction. Since the stator magnetic field does not rotate, there is no relative motion between the stator field and the bars of the rotor. Therefore, there is no induced voltage due to relative motion in the rotor, no rotor current flow due to relative motion, and no induced torque. Actually, a voltage is induced in the rotor bars by transformer action ($d\varphi/dt$) and since the bars are short-circuited, current flows in the rotor **[2]**. However, this magnetic field $\boldsymbol{B_R}$ is lined up with the stator magnetic field, and it produces no net torque on the rotor,

$$\tau_{ind} = k\, B_R \times B_S \quad \ldots\ldots\ldots (4.64)$$

$$= k\, B_R\, B_S \sin \gamma$$

$$= k\, B_R\, B_S \sin 180^\circ = 0$$

At stall conditions, the motor looks like a transformer with a short-circuited secondary winding as shown in **Fig 5.7(b)**.

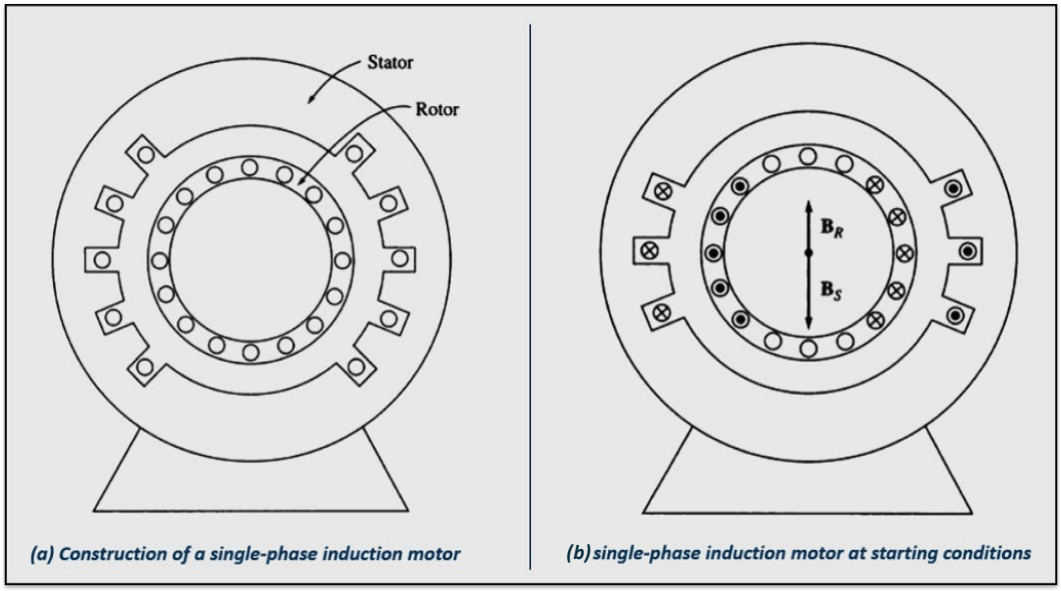

Figure 5.7 - An induction motor with a squirrel-cage rotor and a single-phase stator [2]

The fact that single-phase induction motors have no intrinsic starting torque was a serious impediment to early development of the induction motor. When induction motors were first being developed in the late 1880s and early 1890s, the first available ac power systems were 133 Hz, single-phase. With the materials and techniques then available, it was impossible to build a motor that worked well. The induction motor did not become an off-the-shelf working product until three-phase, 25 Hz power systems were developed in the mid-1890s **[2]**.

However, once the rotor begins to turn, an induced torque will be produced in it. There are two basic theories which explain why a torque is produced in the rotor once it is turning. One is called the **double-revolving-field theory** of single-phase induction motors, and the other is called the **cross-field theory** of single-phase induction motors.

5.3.1 The Double-Revolving-Field Theory of Single-Phase Induction Motors

The double-revolving-field theory of single-phase induction motors basically states that a stationary pulsating magnetic field can be resolved into two rotating magnetic fields, each of equal magnitude but rotating in opposite directions. The induction motor responds to each magnetic field separately, and the net torque in the machine will be the sum of the torques due to each of the two magnetic fields.

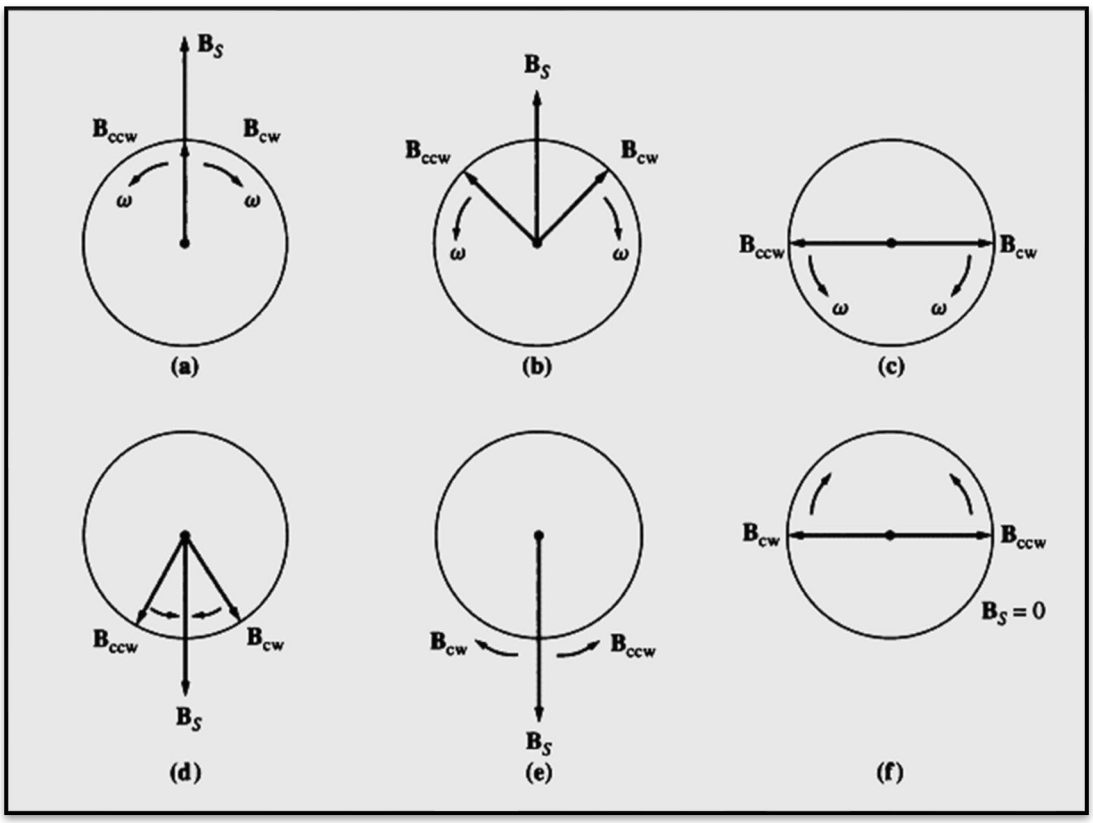

Figure 5.8 - Resolution of a single pulsating magnetic field [2]

Fig 5.8 shows how a stationary pulsating magnetic field can be resolved into two equal and oppositely rotating magnetic fields **[2]**. The flux density of the stationary magnetic field is given by

$$B_s(t) = (B_{max} \cos \omega t)\, \hat{j} \quad \ldots\ldots\ldots (5.23)$$

A clockwise-rotating magnetic field can be expressed as

$$B_{CW}(t) = \left(\frac{1}{2} B_{max} \cos \omega t\right) \hat{\imath} - \left(\frac{1}{2} B_{max} \sin \omega t\right) \hat{j} \quad \ldots\ldots\ldots (5.24)$$

and a counterclockwise-rotating magnetic field can be expressed as

$$B_{CCW}(t) = \left(\frac{1}{2} B_{max} \cos \omega t\right) \hat{\imath} + \left(\frac{1}{2} B_{max} \sin \omega t\right) \hat{j} \quad \ldots\ldots\ldots (5.25)$$

Notice that the sum of the clockwise and counterclockwise magnetic fields is equal to the stationary pulsating magnetic field B_S and lies in the vertical plane at all times as:

$$B_s(t) = B_{CW}(t) + B_{CCW}(t) \quad \ldots\ldots\ldots (5.26)$$

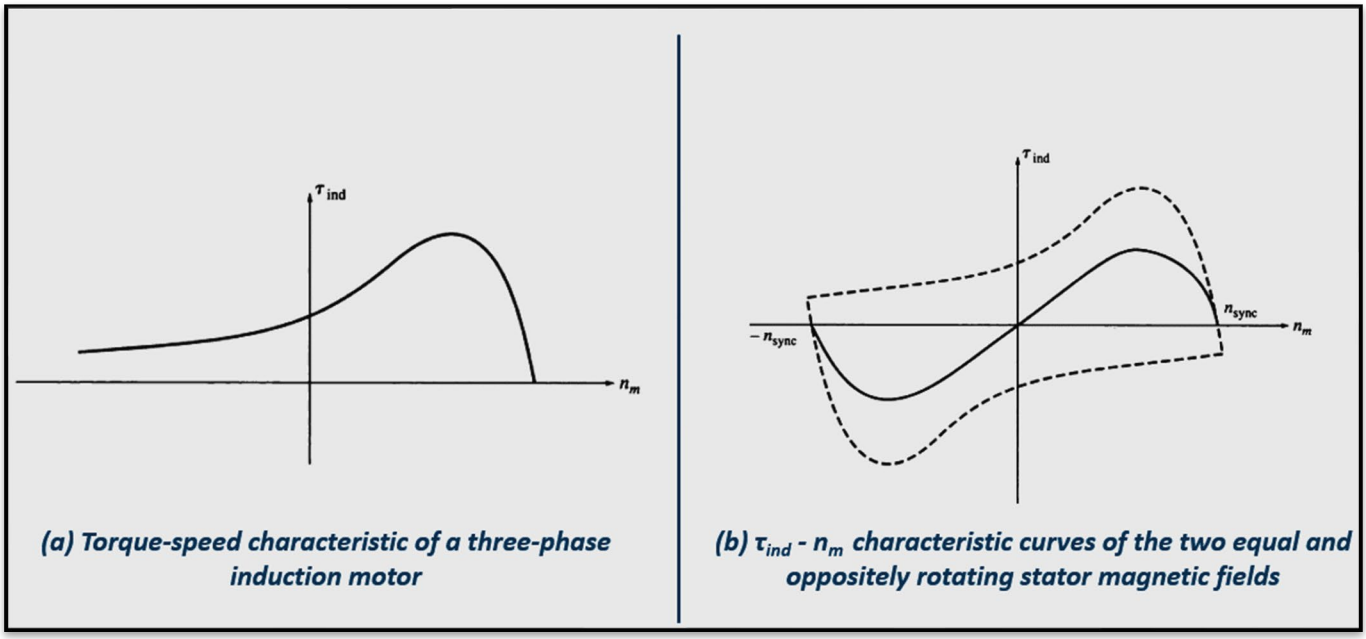

Figure 5.9 - Torque-Speed characteristic of a three-phase induction motor (corresponding to its single rotating magnetic field) [2]

The torque-speed characteristic of a three-phase induction motor in response to its single rotating magnetic field is shown in **Fig 5.9(a)**. A single-phase induction motor responds to each of the two magnetic fields present within it, so the net induced torque in the motor is the difference between the two torque-speed curves, shown in **Fig 5.9(b)**. Notice that there is no net torque at zero speed, so this motor has no starting torque. However, it is not quite an accurate description of the torque in a single-phase motor. It was formed by the superposition of two three-phase characteristics and ignored the fact that both magnetic fields are present simultaneously in the single-phase motor.

If power is applied to a three-phase motor while it is forced to turn backward, its rotor currents will be very high (shown in **Fig 5.10(b)**).

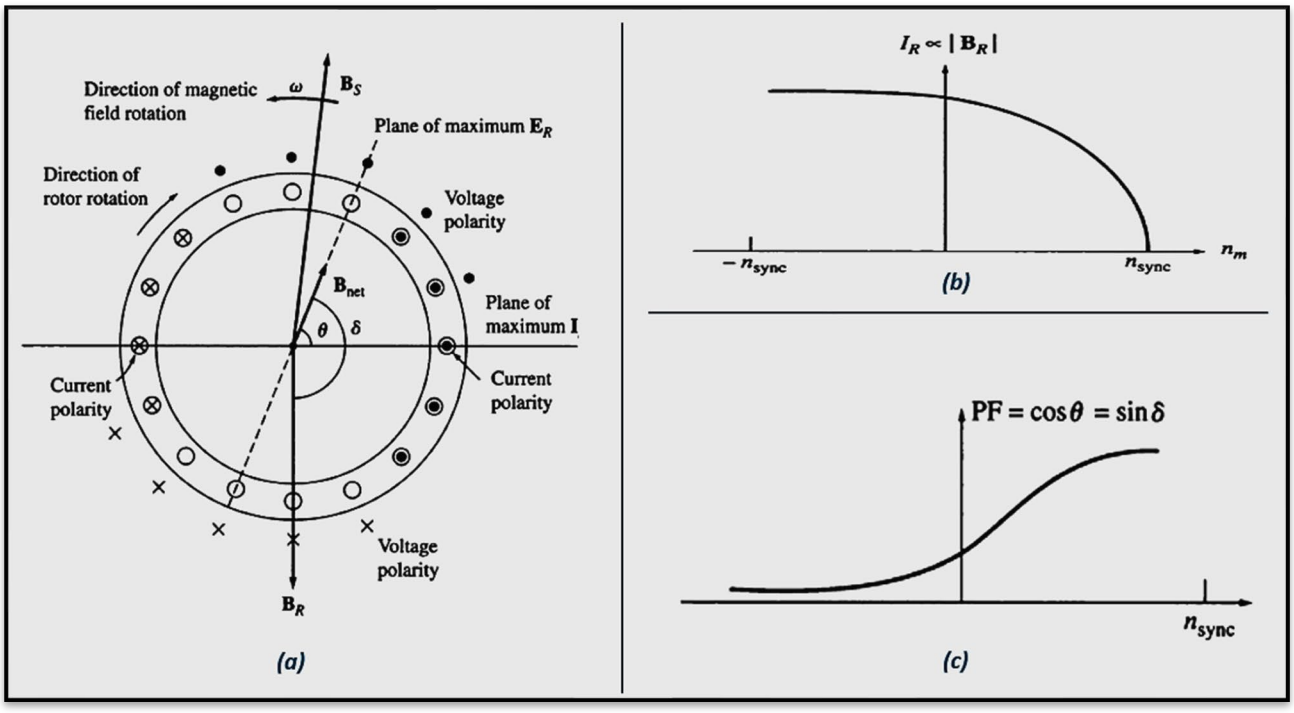

Figure 5.10 - A three-phase motor forced to turn backwards [2]

However, the rotor frequency is also very high, making the rotor's reactance much larger than its resistance. Since the rotor's reactance is so very high, the rotor current lags the rotor voltage by almost 90°, producing a magnetic field that is nearly 180° from the stator magnetic field as in **Fig 5.10(a)**. The induced torque in the motor is proportional to the sine of the angle between the two fields and the sine of an angle near 180°, which is a very small number. The motor's torque would be very small, except that the extremely high rotor currents partially offset the effect of the magnetic field angles, as shown in the diagram of power factor-speed characteristic in **Fig 5.10(c)**.

On the other hand, in a single-phase motor, both the forward and the reverse magnetic fields are present and both are produced by the same current. The forward and reverse magnetic fields in the motor each contribute a component to the total voltage in the stator and, in a sense, are in series with each other. Because both magnetic fields are present, the forward-rotating magnetic field (which has a high effective rotor resistance R_2 / s) will limit the stator current flow in the motor (which produces both the forward and reverse fields). Since the current supplying the reverse stator magnetic field is limited to a small value and since the reverse rotor magnetic field is at a very large angle with respect to the reverse stator magnetic field, the torque due to the reverse magnetic fields is very small near synchronous speed.

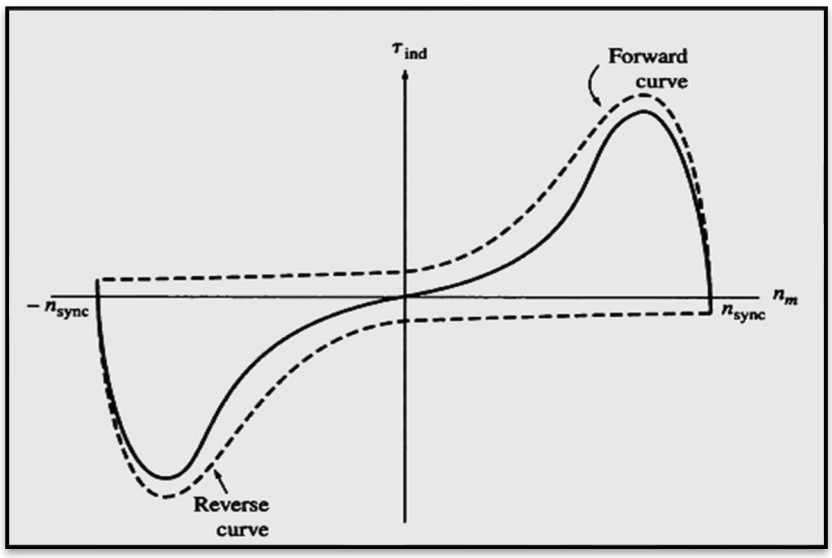

Figure 5.11 - The torque-speed characteristic of a single-phase induction motor [2]

A more accurate torque-speed characteristic for the single-phase induction motor is shown in **Fig 5.11**. In addition to the average net torque, there are torque pulsations at twice the stator frequency. These torque pulsations are caused when the forward and reverse magnetic fields cross each other twice each cycle. Although these torque pulsations produce no average torque, they do increase vibration, and they make single-phase induction motors noisier than three-phase motors of the same size. There is no way to eliminate these pulsations, since instantaneous power always comes in pulses in a single-phase circuit. A motor designer must allow for this inherent vibration in the mechanical design of single-phase motors **[2]**.

5.3.2 The Cross-Field Theory of Single-Phase Induction Motors

The cross-field theory of single-phase induction motors looks at the induction motor from a totally different point of view. This theory is concerned with the voltages and currents that the stationary stator magnetic field can induce in the bars of the rotor when the rotor is moving. Consider a single-phase induction motor with a rotor which has been brought up to speed by some external method. Such a motor is shown in **Fig 5.12(a)**.

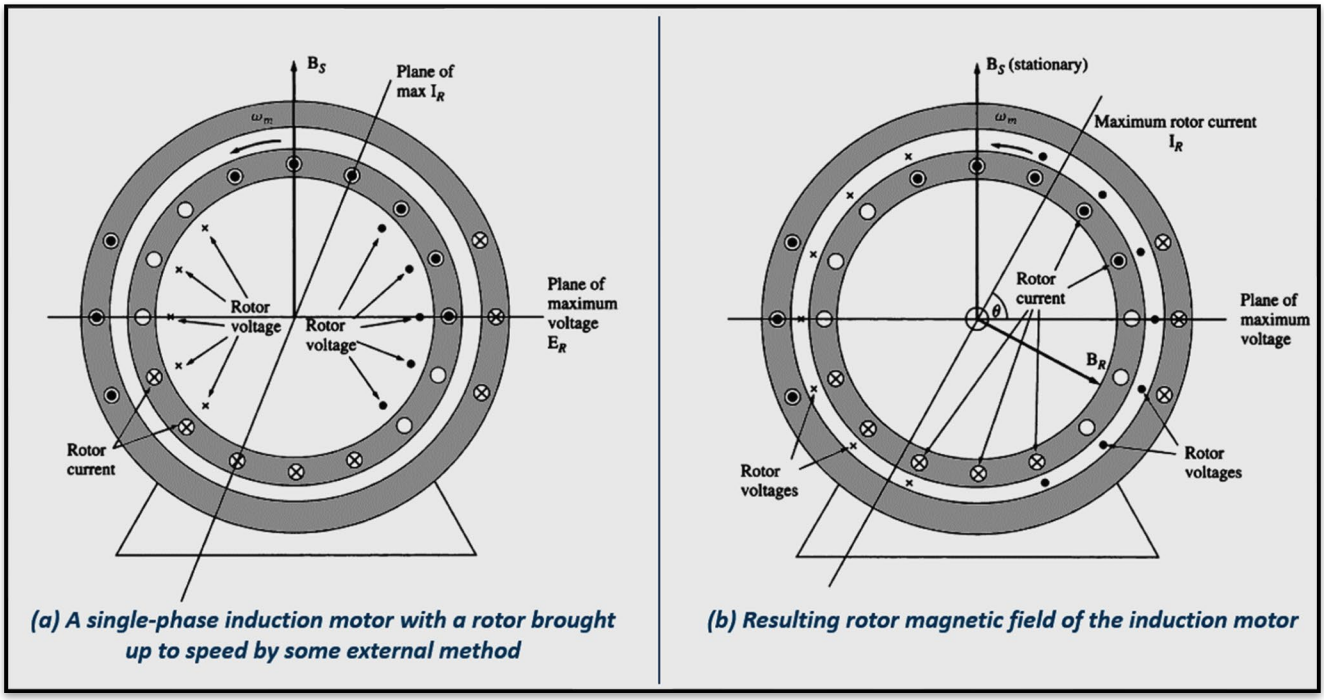

Figure 5.12 - The development of induced torque in a single-phase induction motor, explained by the cross- field theory [2]

Voltages are induced in the bars of this rotor, with the peak voltage occurring in the windings passing directly under the stator windings. These rotor voltages produce a current flow in the rotor, but because of the rotor's high reactance, the current lags the voltage by almost 90°. Since the rotor is rotating at nearly synchronous speed, that 90°-time lag in current produces an almost 90° angular shift between the plane of peak rotor voltage and the plane of peak current. The resulting rotor magnetic field is shown in **Fig 5.12(b)**.

The rotor magnetic field is somewhat smaller than the stator magnetic field, because of the losses in the rotor, but they differ by nearly 90° in both space and time. If these two magnetic fields are added at different times, one sees that the total magnetic field in the motor is rotating in a counterclockwise direction as **Fig 5.13** indicates below. With a rotating magnetic field present in the motor, the induction motor will develop a net torque in the direction of motion, and that torque will keep the rotor turning. If the motor's rotor had originally been turned in a clockwise direction, the resulting torque would be clockwise and would again keep the rotor turning.

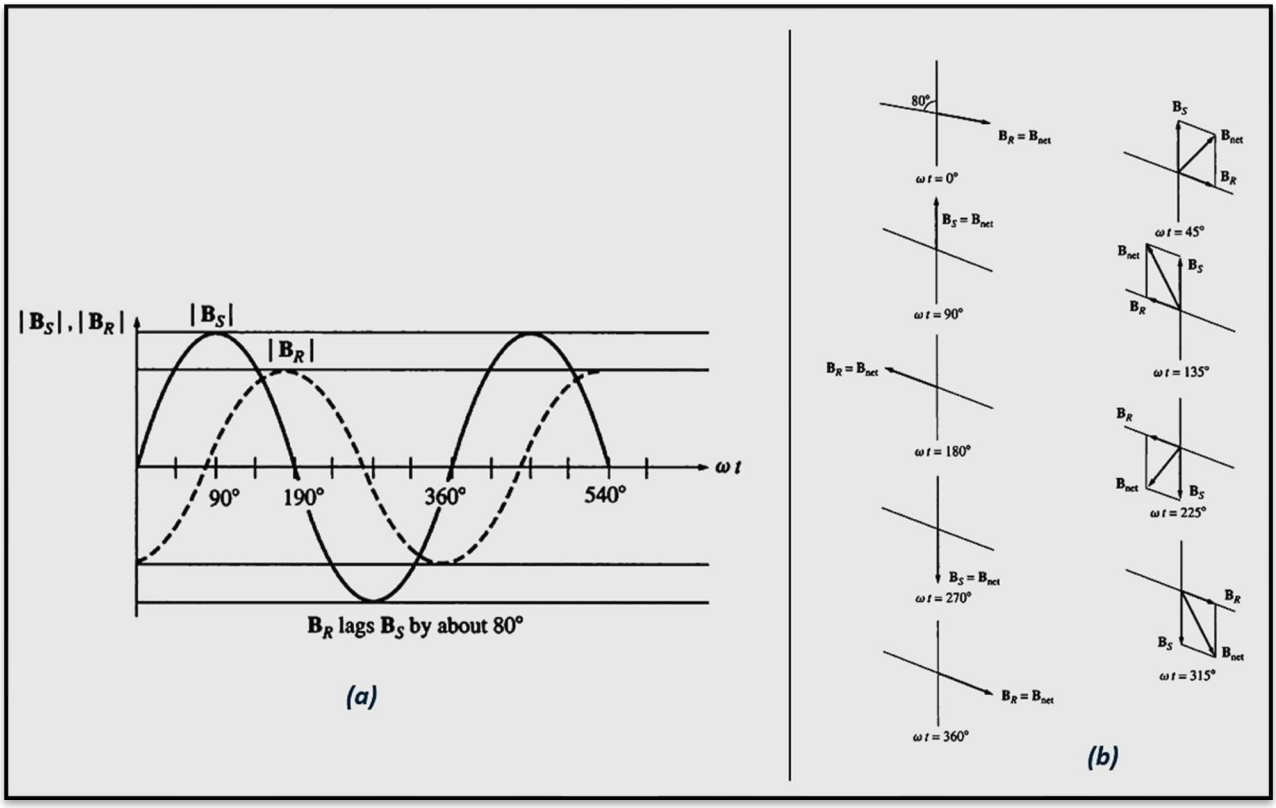

Figure 5.13 - Characteristic of the magnetic fields as a function of time and the resulting net magnetic field at various times [2]

5.4 Starting Single-Phase Induction Motors

As previously explained, a single-phase induction motor has no intrinsic starting torque. There are three techniques commonly used to start these motors and single-phase induction motors are classified according to the methods used to produce their starting torque. These starting techniques differ in cost and in the amount of starting torque produced, and an engineer normally uses the least expensive technique that meets the torque requirements in any given application. The three major starting techniques are

1. Split-phase windings
2. Capacitor-type windings
3. Shaded stator poles

All three starting techniques are methods of making one of the two revolving magnetic fields in the motor stronger than the other and so, giving the motor an initial nudge in one direction or the other.

5.4.1 Split-Phase Windings

A split-phase motor is a single-phase induction motor with two stator windings, a main stator winding ***(M)*** and an auxiliary starting winding ***(A)*** **(Fig 5.14)**. These two windings are set 90 electrical degrees apart along the stator of the motor, and the auxiliary winding is designed to be switched out of the circuit at some set speed by a centrifugal switch.

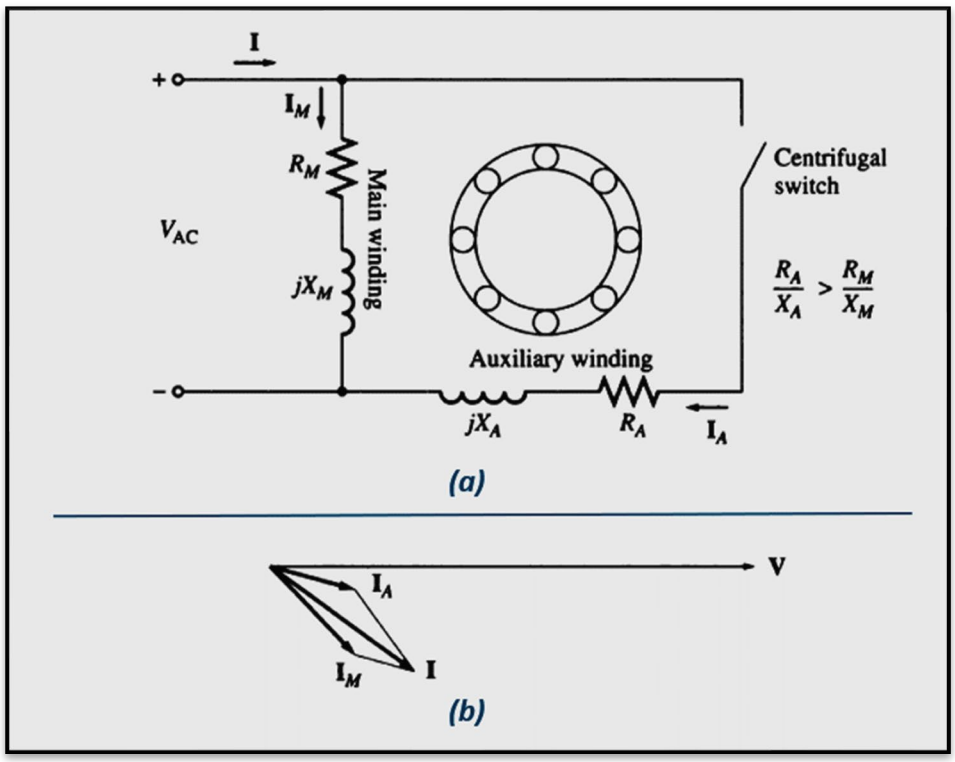

Figure 5.14 - A split-phase induction motor and its currents at starting conditions [2]

The auxiliary winding is designed to have a higher resistance/reactance ratio than the main winding, so that the current in the auxiliary winding leads the current in the main winding. This higher ***R/X*** ratio is usually accomplished by using smaller wire for the auxiliary winding. Smaller wire is permissible in the auxiliary winding, because it is used only for starting and therefore does not have to take full current continuously. **Fig 5.15 w**hich follows, indicates more properly the function of the auxiliary winding.

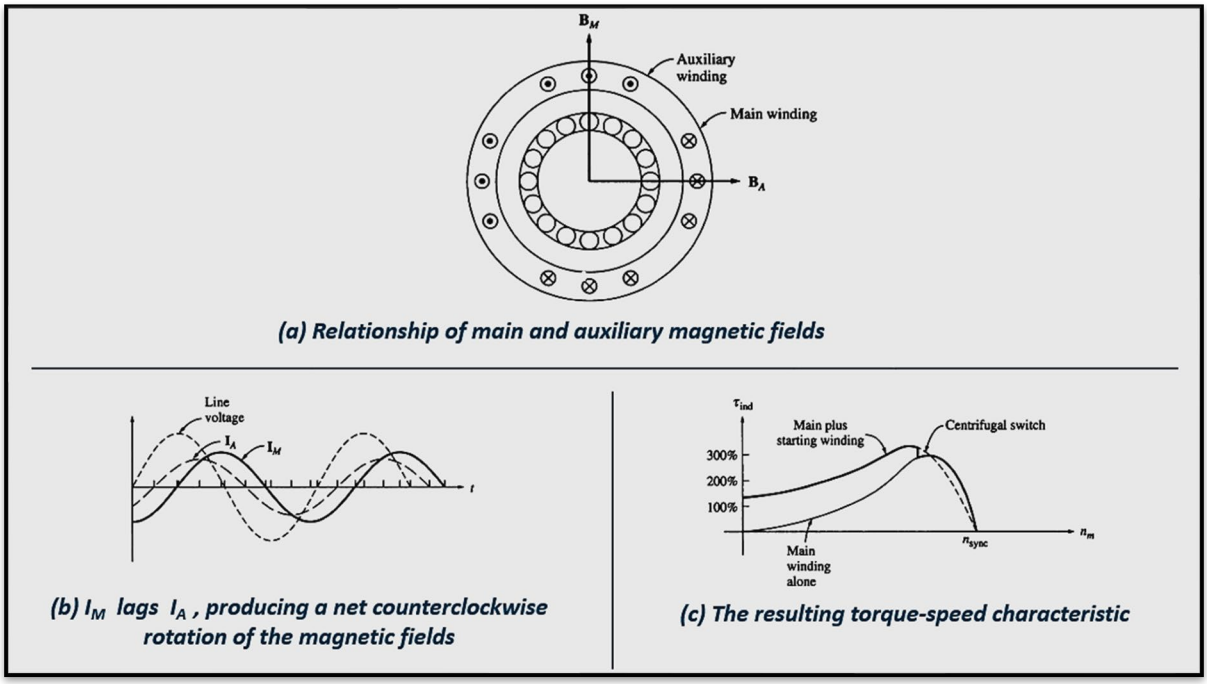

Figure 5.15 The function of the auxiliary winding in a split-phase induction motor [2]

Fig 5.15(b) shows the current in the auxiliary winding leading the current in the main winding. Thus, the magnetic field B_A peaks before the main magnetic field B_M. Since B_A peaks first and then B_M, there is a net counterclockwise rotation in the magnetic field. In other words, the auxiliary winding makes one of the oppositely rotating stator magnetic fields larger than the other one and provides a net starting torque for the motor. A typical torque-speed characteristic is shown in **Fig 5.15(c)**.

The construction and another one diagram of a split-phase motor is shown in **Fig 5.16**. It is easy to see the main and auxiliary windings (the auxiliary windings are of smaller-diameter wires) and the centrifugal switch that cuts the auxiliary windings out of the circuit when the motor approaches operating speed.

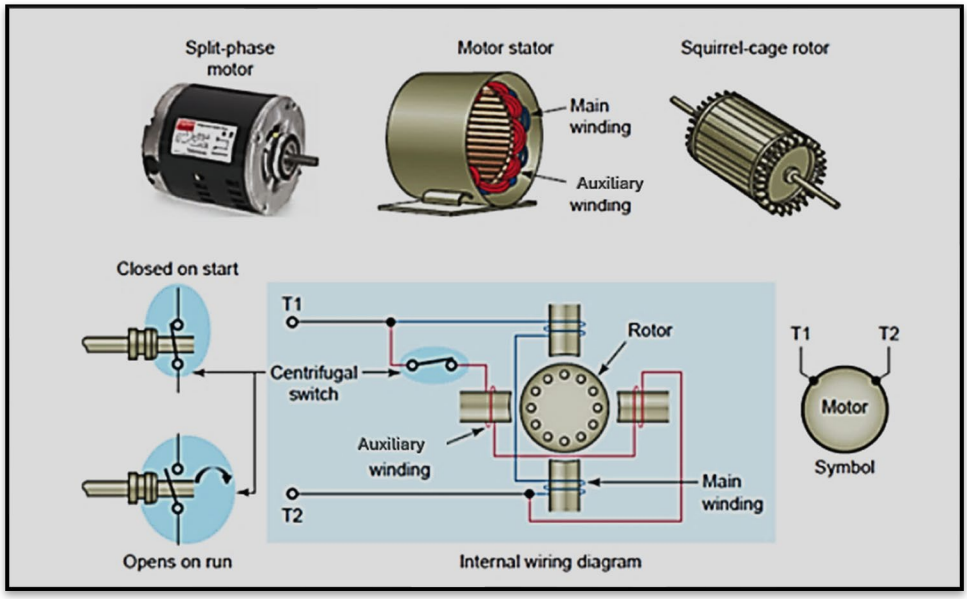

Figure 5.16 - Construction of a split-phase induction motor [42]

Split-phase motors have a moderate starting torque with a fairly low starting current. They are used for applications which do not require very high starting torques, such as fans, blowers, and centrifugal pumps. They are available for sizes in the fractional-horsepower range and are quite inexpensive.

In a split-phase induction motor, the current in the auxiliary windings always peaks before the current in the main winding and therefore, the magnetic field from the auxiliary winding always peaks before the magnetic field from the main winding. The direction of rotation of the motor is determined by whether the space angle of the magnetic field from the auxiliary winding is 90° ahead or 90° behind the angle of the main winding. Since that angle can be changed from 90° ahead to 90° behind just by switching the connections on the auxiliary winding, the direction of rotation of the motor can be reversed by switching the connections of the auxiliary winding while leaving the main winding's connections unchanged **[2]**.

5.4.2 Capacitor-Start Motors

For some applications, the starting torque supplied by a split-phase motor is insufficient to start the load on a motor's shaft. In those cases, capacitor-start motors may be used (**Fig 5.17(a)**). In a capacitor-start motor, a capacitor is placed in series with the auxiliary winding of the motor.

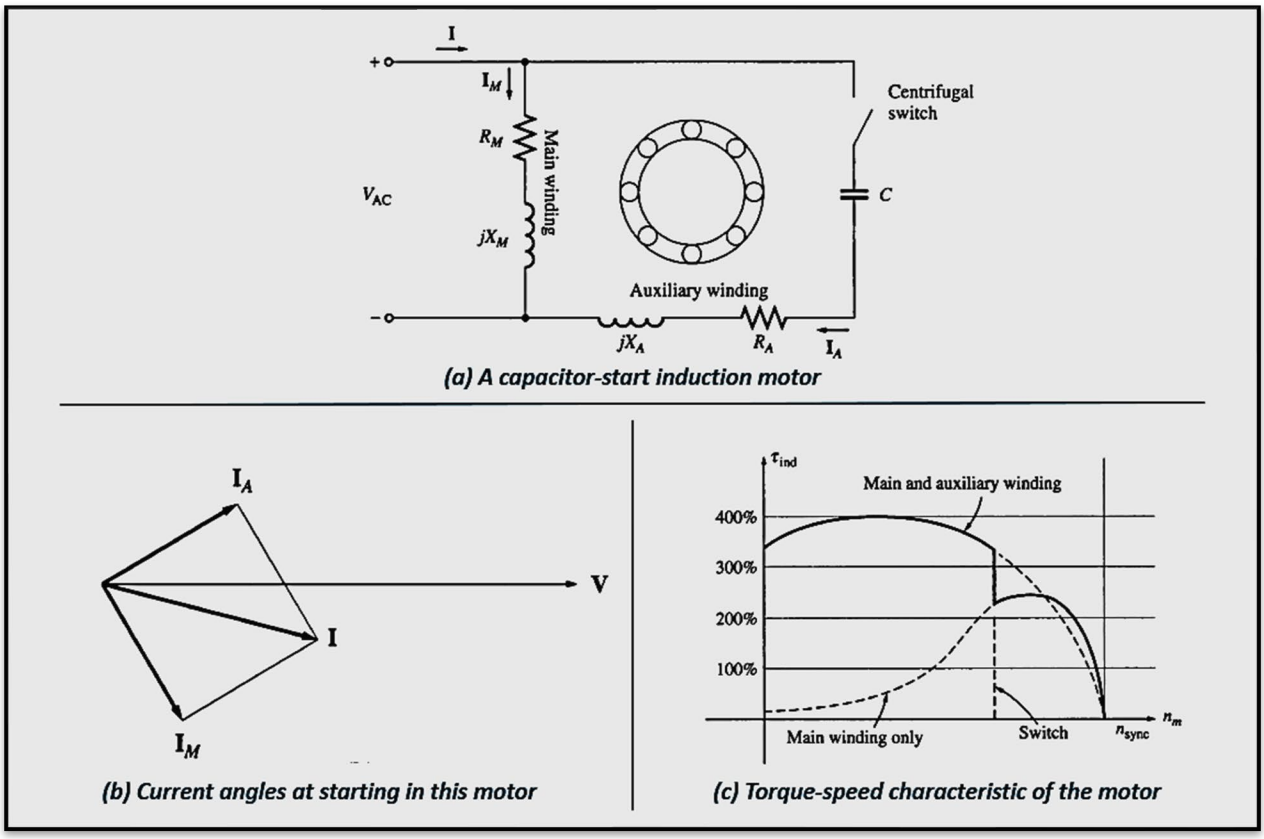

Figure 5.17 - Construction and operation of a capacitor-start induction motor [2]

By proper selection of capacitor size, the magnetomotive force of the starting current in the auxiliary winding can be adjusted to be equal to the magnetomotive force of the current in the main winding, and the phase angle of the current in the auxiliary winding can be made to lead the current in the main winding by 90° (shown in **Fig 5.17(b)**). Since the two windings are physically separated by 90°, a 90° phase difference in current will yield a single uniform rotating stator magnetic field, and the motor will behave just as though it was starting from a three-phase power source. In this case, the starting torque of the motor can be more than 300 percent of its rated value (**Fig 5.17(c)**).

Capacitor-start motors are more expensive than split-phase motors, and they are used in applications where a high starting torque is absolutely required. Typical applications for such motors are compressors, pumps, air conditioners, and other pieces of equipment that must start under a load **[2]**.

5.4.3 Permanent Split-Capacitor and Capacitor-Start, Capacitor-Run Motors

The starting capacitor does such a good job of improving the torque-speed characteristic of an induction motor that an auxiliary winding with a smaller capacitor is sometimes left permanently in the motor circuit. If the capacitor's value is chosen correctly, such a motor will have a perfectly uniform rotating magnetic field at some specific load, and it will behave just like a three-phase induction motor at that point. Such a design is called a **permanent split-capacitor** or capacitor-start- and-run motor **(Fig 5.18)**. Permanent split-capacitor motors are simpler than capacitor-start motors, since the starting switch is not needed. At normal loads, they are more efficient and have a higher power factor and a smoother torque than ordinary single-phase induction motors.

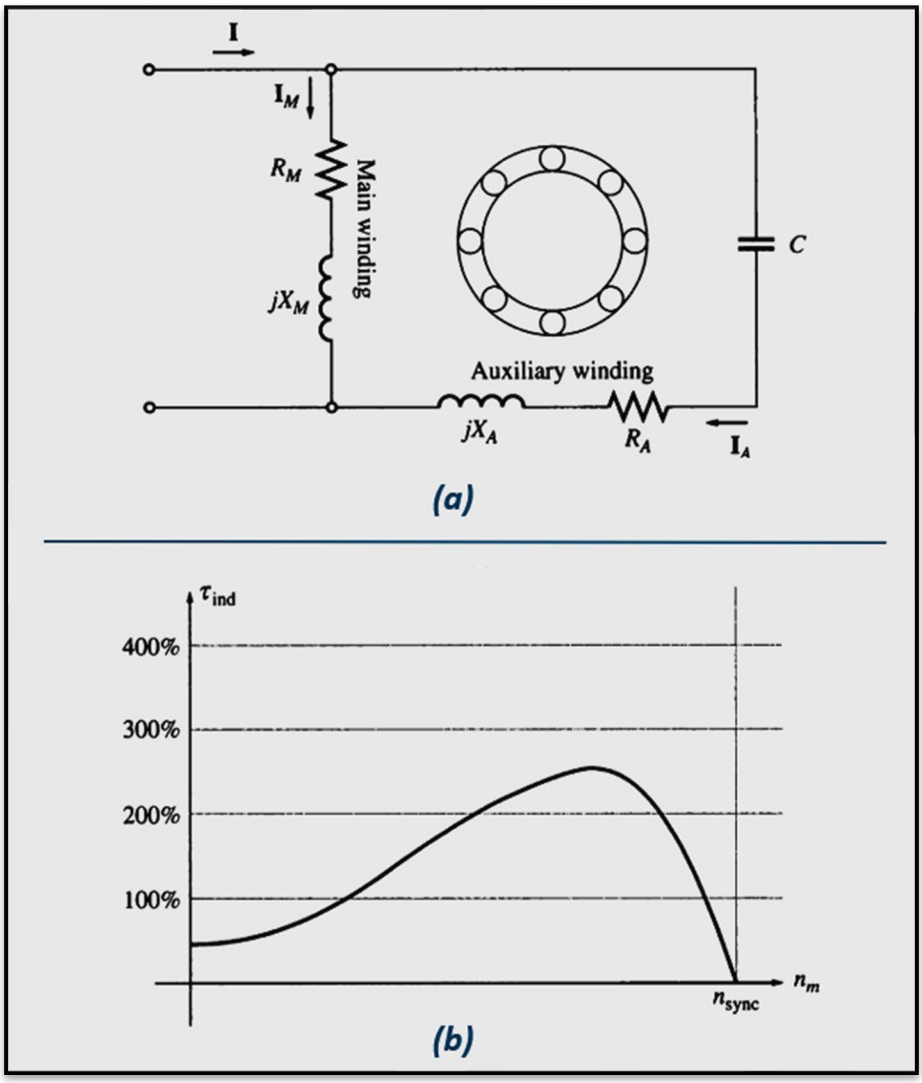

Figure 5.18 - A permanent split-capacitor induction motor and its torque-speed characteristic [2]

However, permanent split-capacitor motors have a lower starting torque than capacitor-start motors, since the capacitor must be sized to balance the currents in the main and auxiliary windings at normal-load conditions. Since the starting current is much greater than the normal-load current, a capacitor that balances the phases under normal loads leaves them very unbalanced under starting conditions. If both the largest

possible starting torque and the best running conditions are needed, two capacitors can be used with the auxiliary winding **[2]**, **[43]**.

Motors with two capacitors are called **capacitor-start, capacitor-run**, or two-value capacitor motors. The larger capacitor is present in the circuit only during starting, when it ensures that the currents in the main and auxiliary windings are roughly balanced, yielding very high starting torques. When the motor gets up to speed, the centrifugal switch opens, and the permanent capacitor is left by itself in the auxiliary winding circuit. The permanent capacitor is just large enough to balance the currents at normal motor loads, so the motor again operates efficiently with a high torque and power factor. The permanent capacitor in such a motor is typically about 10 to 20 percent of the size of the starting capacitor **[46]**.

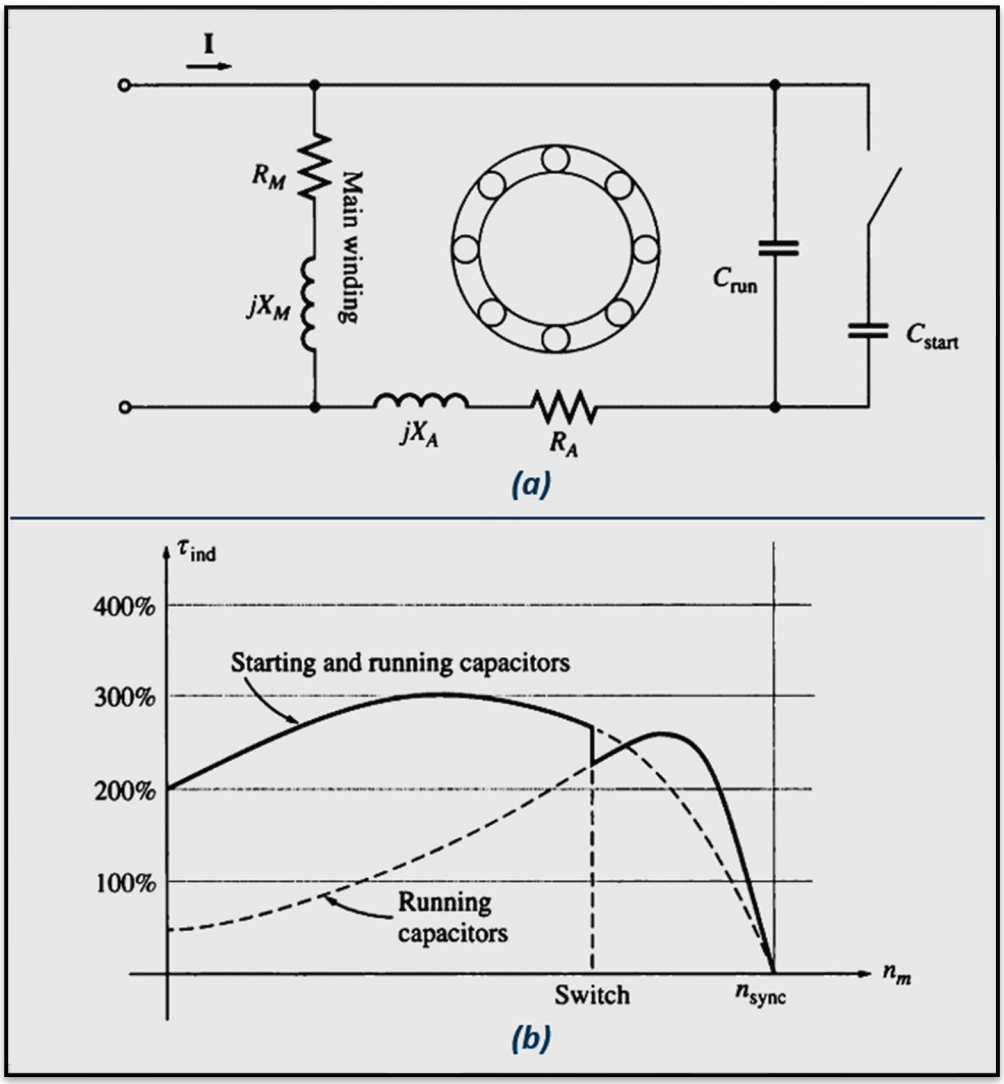

5.19 - A capacitor-start, capacitor-run induction motor and its torque-speed characteristic [2]

Fig 5.19 shows a schematic diagram of such a capacitor-start, capacitor run motor along with the torque-speed characteristic of this motor. The direction of rotation of any capacitor-type motor may be reversed by switching the connections of its auxiliary windings.

5.4.4 Shaded-Pole Motors

A shaded-pole induction motor is an induction motor with only a main winding. Instead of having an auxiliary winding, it has salient poles, and one portion of each pole is surrounded by a short-circuited coil called a shading coil (**Fig 5.20(a)**). A time-varying flux is induced in the poles by the main winding. When the pole flux varies, it induces a voltage and a current in the shading coil which opposes the original change in flux. This opposition retards the flux changes under the shaded portions of the coils and therefore produces a slight imbalance between the two oppositely rotating stator magnetic fields. The net rotation is in the direction from the unshaded to the shaded portion of the pole face. The torque-speed characteristic of a shaded-pole motor is shown in **Fig 5.20(b)**.

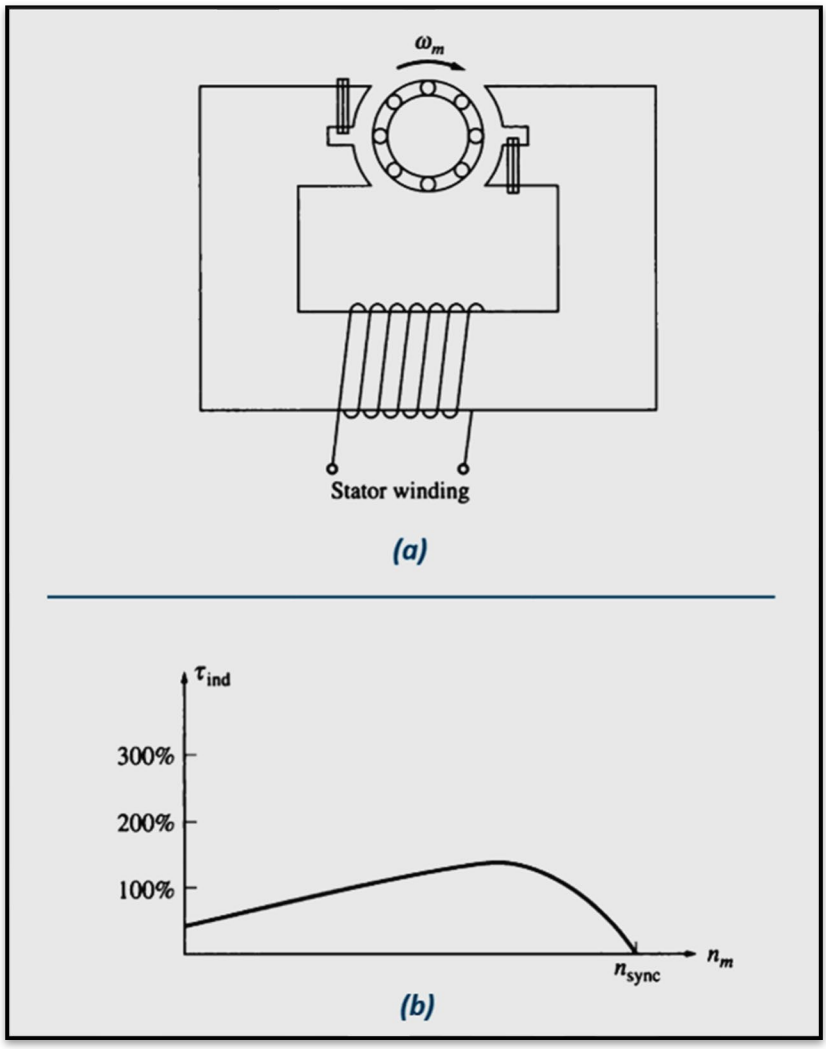

Figure 5.20 - A basic shaded-pole induction motor and its resulting torque-speed characteristic [2]

Shaded poles produce less starting torque than any other type of induction motor starting system. They are much less efficient and have a much higher slip than other types of single-phase induction motors. Such poles are used only in very small motors (1/20 hp and less) with very low starting torque requirements **[43]**. Where it is possible to use them, shaded-pole motors are the cheapest design available. Because shaded-pole motors rely on a shading coil for their starting torque, there is no easy way to reverse the direction of rotation of such a motor. To achieve reversal, it is necessary to install two shading coils on each pole face and to selectively short one or the other of them. The difference between a construction of a two-pole and a four-pole shaded-pole induction motor is indicated in **Fig 5.21** below.

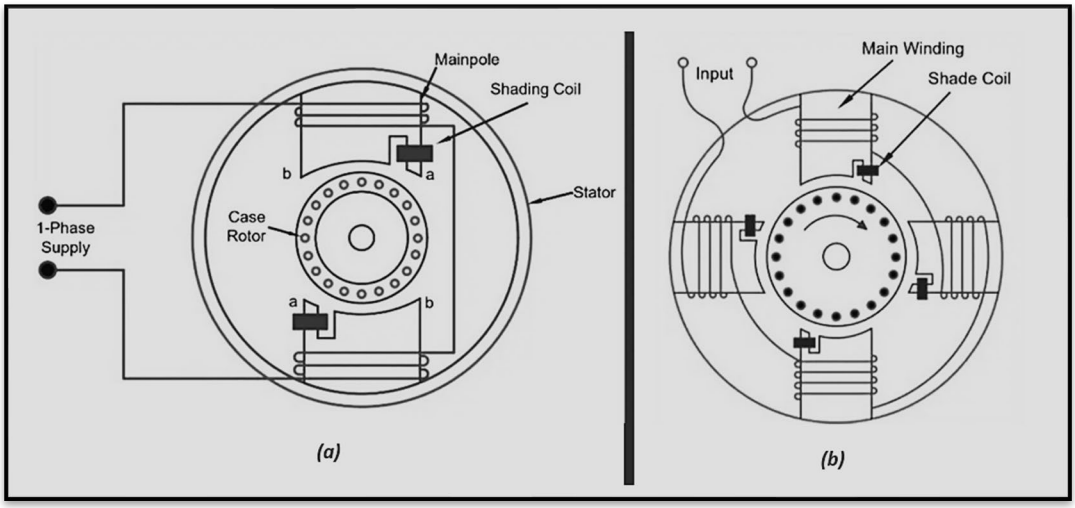

Figure 5.21 - A shaded-pole induction motor either with two-pole or four-pole shading coils [2]

5.5 Speed Control of Single-Phase Induction Motors

In general, the speed of single-phase induction motors may be controlled in the same manner as the speed of polyphase induction motors. For squirrel-cage rotor motors, the following techniques are available **[2]**:

1. Vary the stator frequency.
2. Change the number of poles.
3. Change the applied terminal voltage V_T.

In practical designs involving fairly high-slip motors, the usual approach to speed control is to vary the terminal voltage of the motor. The voltage applied to a motor may be varied in one of three ways:

1. An autotransformer may be used to continually adjust the line voltage. This is the most expensive method of voltage speed control and is used only when very smooth speed control is needed.

2. A solid-state controller circuit may be used to reduce the rms voltage applied to the motor by ac phase control. Solid-state control circuits are considerably cheaper than autotransformers and so are becoming more and more common.

3. A resistor may be inserted in series with the motor's stator circuit. This is the cheapest method of voltage control, but it has the disadvantage that considerable power is lost in the resistor, reducing the overall power conversion efficiency.

Another technique is also used with very high-slip motors, such as shaded-pole motors. Instead of using a separate autotransformer to vary the voltage applied to the stator of the motor, the stator winding itself can be used as an auto-transformer. **Fig 5.22** shows a schematic representation of a main stator winding, with a number of taps along its length. Since the stator winding is wrapped about an iron core, it behaves as an autotransformer.

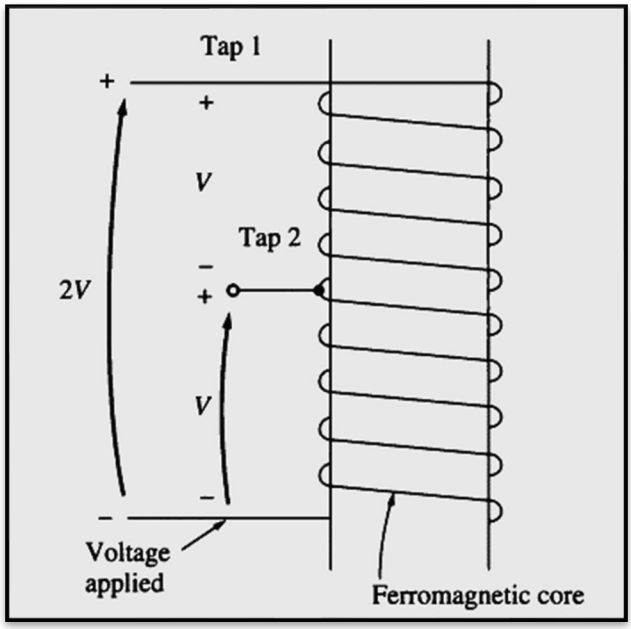

Figure 5.22 The use of a main stator winding as an autotransformer [2]

When the full line voltage V is applied across the entire main winding, then the induction motor operates normally. Suppose instead that the full line voltage is applied to tap 2, the center tap of the winding. Then an identical voltage will be induced in the upper half of the winding by transformer action, and the total winding voltage will be twice the applied line voltage. The total voltage applied to the winding has effectively been doubled.
Therefore, the smaller the fraction of the total coil that the line voltage is applied across, the greater the total voltage will be across the whole winding, and the higher the speed of the motor will be for a given load **(Fig 5.23)**.

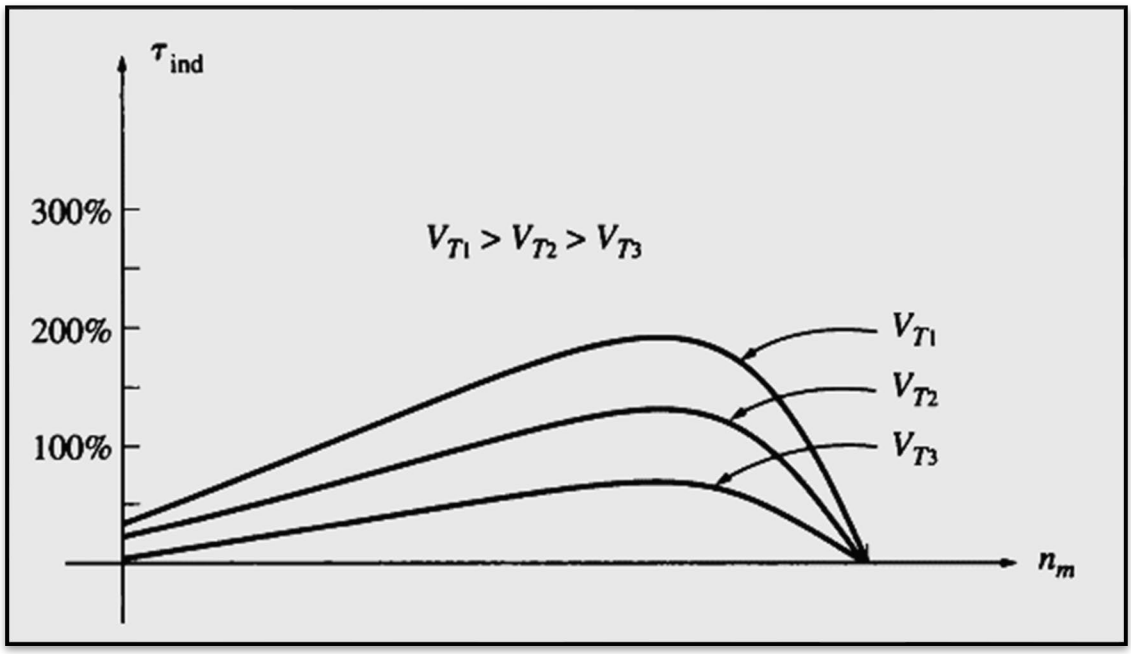

Figure 5.23 - Torque-speed characteristic of a shaded-pole induction motor as terminal voltage varies [2]

This is the standard approach used to control the speed of single-phase motors in many fan and blower applications. Such speed control has the advantage that it is quite inexpensive, since the only components necessary are taps on the main motor winding and an ordinary multiposition switch. It also has the advantage that the autotransformer effect does not consume power the way series resistors would.

5.6 The Circuit Model of A Single-Phase Induction Motor

The best way to begin the analysis of a single-phase induction motor is to consider the motor when it is stalled. At that time, the motor appears to be just a single-phase transformer with its secondary circuit shorted out, and so its equivalent circuit is that of a transformer. This equivalent circuit is shown in **Fig 5.24(a)**.

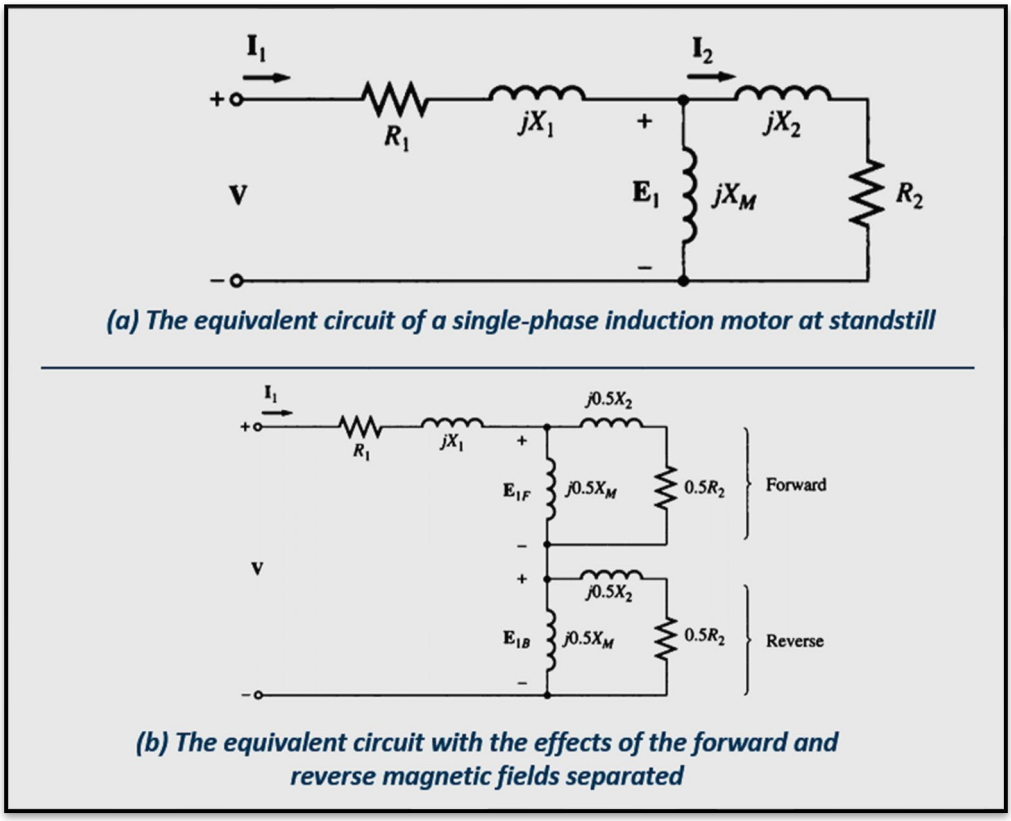

Figure 5.24 - Analysis of the equivalent circuit of a single-phase induction motor [2]

In this figure, R_1 and X_1 are the resistance and reactance of the stator winding, X_M is the magnetizing reactance, and R_2 and X_2 are the referred values of the rotor's resistance and reactance. The core losses of the machine are not shown and will be lumped together with the mechanical and stray losses as a part of the motor's rotational losses. As mentioned, the pulsating air-gap flux in the motor at stall conditions can be resolved into two equal and opposite magnetic fields within the motor. Since these fields are of equal size, each one contributes an equal share to the resistive and reactive voltage drops in the rotor circuit. It is possible to split the rotor equivalent circuit into two sections, each one corresponding to the effects of one of the magnetic fields. The motor equivalent circuit with the effects of the forward and reverse magnetic fields separated is shown in **Fig 5.24(b)**.

Now, assuming that the motor's rotor begins to turn with the help of an auxiliary winding that switches out again after the motor comes up to speed, then the effective rotor resistance of an induction motor depends on the amount of relative motion between the rotor and the stator magnetic fields. However, there are two magnetic fields in this motor, and the amount of relative motion differs for each of them.

For the forward magnetic field, the per-unit difference between the rotor speed and the speed of the magnetic field is the slip s, where slip is defined in the same manner as it was for three-phase induction

motors. The rotor resistance in the part of the circuit associated with the forward magnetic field is thus $0.5R_2/s$.

The forward magnetic field rotates at speed n_{sync} and the reverse magnetic field rotates at speed $-n_{sync}$. Therefore, the total per-unit difference in speed (on a base of n_{sync}) between the forward and reverse magnetic fields is **2**. Since the rotor is turning at a speed **s** slower than the forward magnetic field, the total per-unit difference in speed between the rotor and the reverse magnetic field is **2 - s**. Therefore, the effective rotor resistance in the part of the circuit associated with the reverse magnetic field is $0.5R_2/(2-s)$. The final induction motor equivalent circuit is shown in **Fig 5.25**.

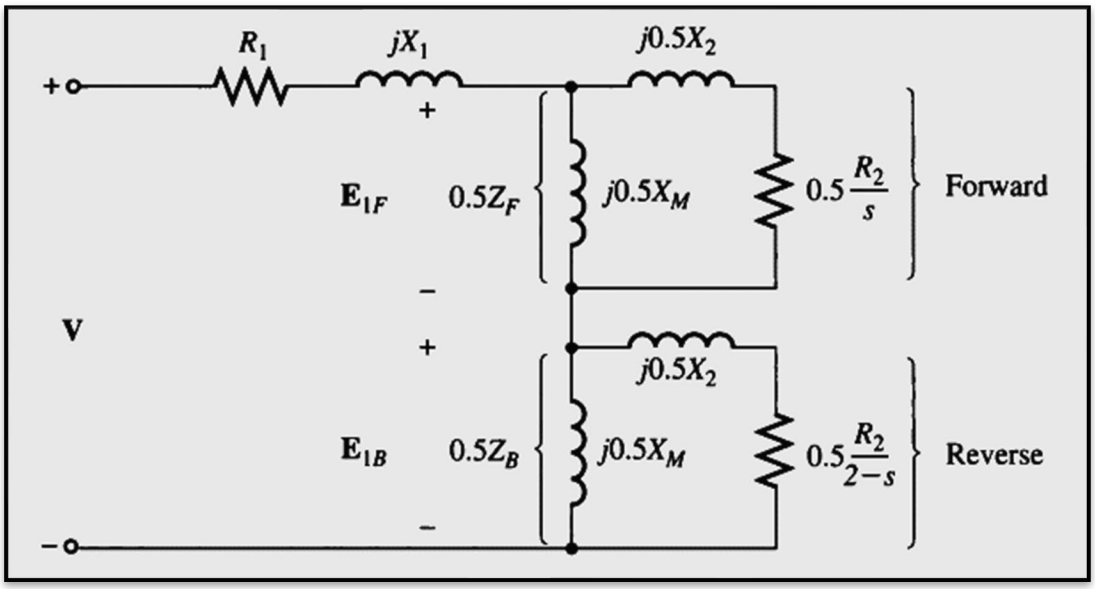

Figure 5.25 - The equivalent circuit of a single-phase induction motor running at speed with only its main windings energized [2]

5.7 Circuit Analysis with the Single-Phase Induction Motor Equivalent Circuit

The single-phase induction motor equivalent circuit in **Fig 5.25** is similar to the three-phase equivalent circuit, except that there are both forward and back-ward components of power and torque present. The same general power and torque relationships that applied for three-phase motors also apply for either the forward or the backward components of the single-phase motor, and the net power and torque in the machine is the difference between the forward and reverse components. The power-flow diagram of an induction motor is repeated in **Fig 5.26** for easy reference.

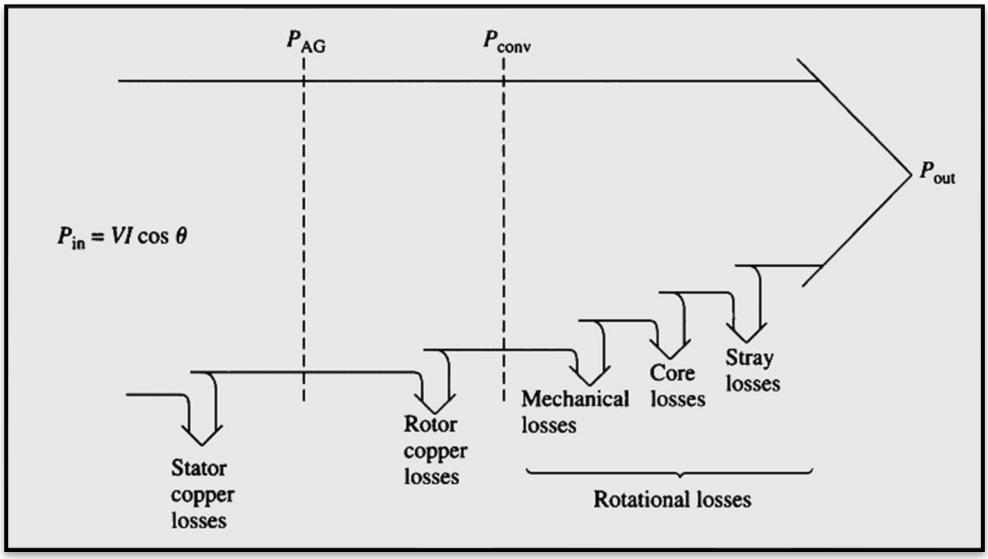

Figure 5.26 - The power-flow diagram of a single-phase induction motor

To make the calculation of the input current flow into the motor simpler, it is customary to define impedances Z_F and Z_B, where Z_F is a single impedance equivalent to all the forward magnetic field impedance elements and Z_B is a single impedance equivalent to all the backward magnetic field impedance elements (shown in **Fig 5.27**).

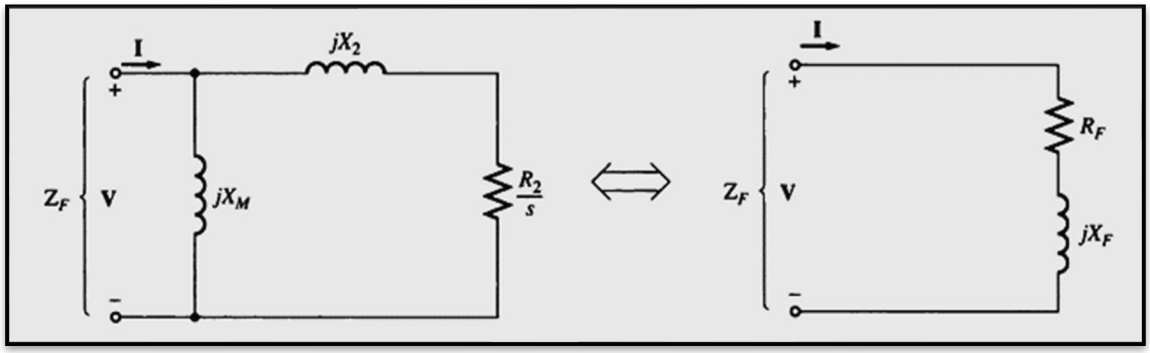

Figure 5.27 - A series combination of R_F and jX_F yields the Thevenin equivalent of the forward-field impedance elements [2]

These impedances are given by

$$Z_F = R_F + jX_F = \frac{(R_2/s + jX_2)(jX_M)}{(R_2/s + jX_2) + jX_M} \quad \text{..... (5.27)}$$

and

$$Z_B = R_B + jX_B = \frac{[R_2/(2-s) + jX_2](jX_M)}{[R_2/(2-s) + jX_2] + jX_M} \quad \text{..... (5.28)}$$

In terms of Z_F and Z_B, the current flowing in the induction motor's stator winding is

$$I_1 = \frac{V}{R_1 + jX_1 + 0.5Z_F + 0.5Z_B} \quad \text{..... (5.29)}$$

The per-phase air-gap power of a three-phase induction motor is the power consumed in the rotor circuit resistance $0.5R_2 / s$. Similarly, the forward air-gap power of a single-phase induction motor is the power consumed by $0.5R_2 / s$, and the reverse air-gap power of the motor is the power consumed by $0.5R_2 /(2- s)$. Therefore, the air-gap power of the motor could be calculated by determining the power in the forward resistor $0.5R_2 / s$, determining the power in the reverse resistor $0.5R_2 /(2- s)$, and subtracting one from the other.

The most difficult part of this calculation is the determination of the separate currents flowing in the two resistors. Fortunately, a simplification of this calculation is possible. Notice that the only resistor within the circuit elements composing the equivalent impedance Z_F is the resistor R_2 / s. Since Z_F is equivalent to that circuit, any power consumed by Z_F must also be consumed by the original circuit, and since R_2 / s is the only resistor in the original circuit, its power consumption must equal that of impedance Z_F. Therefore, the air-gap power for the forward magnetic field can be expressed as

$$P_{AG,F} = I_1^2 (0.5 R_F) \quad \text{..... (5.30)}$$

Similarly, the air-gap power for the reverse magnetic field can be expressed as

$$P_{AG,B} = I_1^2 (0.5 R_B) \quad \text{..... (5.31)}$$

The advantage of these two equations is that only the one current I_1 needs to be calculated to determine both powers. The total air-gap power P_{AG} in a single-phase induction motor is thus

$$P_{AG} = P_{AG,F} - P_{AG,B} \quad \text{..... (5.32)}$$

The induced torque in a three-phase induction motor can be found from the equation

$$\tau_{ind} = \frac{P_{AG}}{\omega_{sync}} \quad \text{..... (5.33)}$$

The rotor copper losses can be found as the sum of the rotor copper losses due to the forward field and the rotor copper losses due to the reverse field.

$$P_{RCL} = P_{RCL,F} + P_{RCL,B} \quad \text{..... (5.34)}$$

The rotor copper losses in a three-phase induction motor were equal to the per- unit relative motion between the rotor and the stator field (the slip) times the air-gap power of the machine. Similarly, the forward rotor copper losses, as well as the reverse rotor copper losses of a single-phase induction motor are given by

$$P_{RCL,F} = s P_{AG,F} \quad \text{and} \quad P_{RCL,B} = s P_{AG,B} \quad \text{..... (5.35)}$$

Since these two power losses in the rotor are at different frequencies, the total rotor power loss is just their sum.

The power converted from electrical to mechanical form in a single-phase induction motor is given by the same equation as Pconv for three-phase induction motors. This equation is

$$P_{conv} = \tau_{ind} \omega_m \quad \text{..... (5.36)}$$

Since $\omega_m = (1 - s)\omega_{sync}$, this equation can be reexpressed as

$$P_{conv} = \tau_{ind}(1 - s)\omega_{sync} \quad \text{…….. (5.37)}$$

From **Eq 5.33**, P_{conv} can also be expressed as

$$P_{conv} = (1 - s) P_{AG} \quad \text{…….. (5.38)}$$

As in the three-phase induction motor, the shaft output power is not equal to P_{conv}, since the rotational losses must still be subtracted. In the single-phase induction motor model used here, the core losses, mechanical losses, and stray losses must be subtracted from P_{conv} in order to get P_{out}.

6. CONTROL STRATEGIES OF AC MOTOR DRIVE SYSTEMS

The control of AC motor drive systems is generally more complex than that of DC motor drive systems and the complexity increases as the required performance of the machine increases. The requirement for variable frequency, the complex dynamic characteristics of AC motors and the difficulty of processing feedback signals are some of the reasons for this complexity. In the last decades, the control methodologies of AC machines are in great development, increasing in this way, their competitiveness. In addition to classical control methods, new techniques have also been developed in recent years, based on predictive control, fuzzy logic and neural networks **[12]**.

6.1 Introduction to Basic Control Methods of Induction Motors

As it was described in the previous chapter, the control of induction motors is obtained in general, by controlling the torque, the speed, the rotation and the position. The choice of control method should be made according to the needs of the specific application and always in relation to the cost. The main control methods are the **scalar control (V/f =** constant**)**, **space vector control (field - oriented)** and **direct torque control (DTC).**

Scalar Control: This technique is one of the most traditional ones, considering only the machine's steady-state relationships. The requiring quantities in this control are the RMS value of the stator supply voltage and its frequency. The operating principle is to vary the stator supply voltage and frequency in such a way that the V/f ratio is kept constant. This technique does not achieve a high performance and finds application in systems where power is low and simplicity is more important than performance. The present thesis report was based on this particular type of motor control for simulation results, which are to follow in the next chapter.

Field Oriented Control (FOC): This control is of a different philosophy, as it uses the dynamic model of the machine, instead of the steady state model. In cases where precision control and fast system response are required, the vector control method is used. In induction motors the implementation of vector control is quite complex and depends on factors such as temperature and magnetic saturation. However, this method shows reliable results regarding the steady state and the changes in the mechanical load of the engine, as well as good dynamic behavior in the changes of the desired speed. Two subcategories of vector control are the Direct Field Oriented Control (**DFOC**) and the Indirect Field Oriented Control (**IFOC**). In case of the first, the basic magnitude of the angle of the rotating reference frame with respect to the stationary frame, is calculated by means of the feedback of the output, while in case of the second, it is calculated directly from the input.

Direct torque control (DTC): This is an emerging technique for controlling PWM inverter-fed induction motor (**IM**) drives. It allows the precise and quick control of the IM flux and torque without calling for complex control algorithms. In principle, it requires only the knowledge of the stator resistance, resulting into less dependency on the system’s control unit, in comparison with the two foregoing techniques.

6.2 Scalar Control with Constant Voltage to Frequency Ratio (*V/f*)

The scalar control, as already mentioned, is the simplest and most widespread method induction motor control. This control is based on the variation of the frequency always in proportion to the supply voltage of the motor stator and can be used in an open or closed loop. A simple scalar control (V/f) arrangement is shown in **Fig 6.1** below **[7]**, **[43]**.

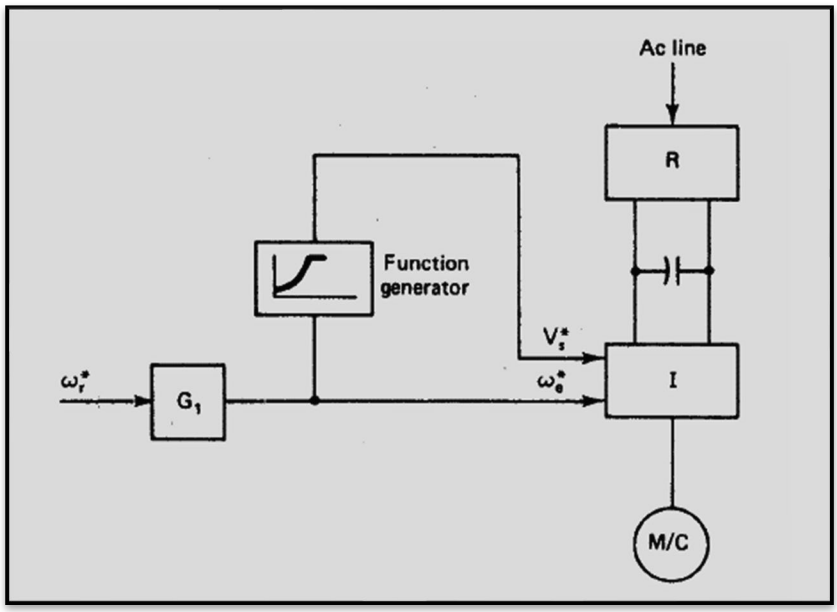

Figure 6.1 - A simple scalar V/f control of an Induction Motor [43]

In cases where precise control of speed and position is not required, an open loop control system is used. The above control system of **Fig 6.1** is quite simple and economical, as it does not require the installation of a tachogenerator. However, precise control of the motor speed is not achieved when there is a change in the mechanical load on the motor shaft and in addition, the drive system does not respond quickly to changes in the desired speed.

6.2.1 Open-Loop Control Circuit in PWM-VSI Drives

Same as before, in VSI drives (both PWM and square-wave type), the speed can also be controlled without a speed feedback loop necessarily, where there may be a slower acting feedback loop through the processor controller. **Fig 6.1** shows such a control. The frequency of the inverter output voltages is controlled by the input speed reference signal ω_{ref}. The input command ω_{ref} is modified for protection and improved performance and the required control inputs (ω_s or f and V_s signals) to the PWM controller in **Fig 6.1** are calculated. The PWM controller can be realized by analog components, as discussed in Chapter 3. The control signals can be calculated from the f and V_s signals and by knowing V_d and $\hat{V}_{tri}$ **[7]**.

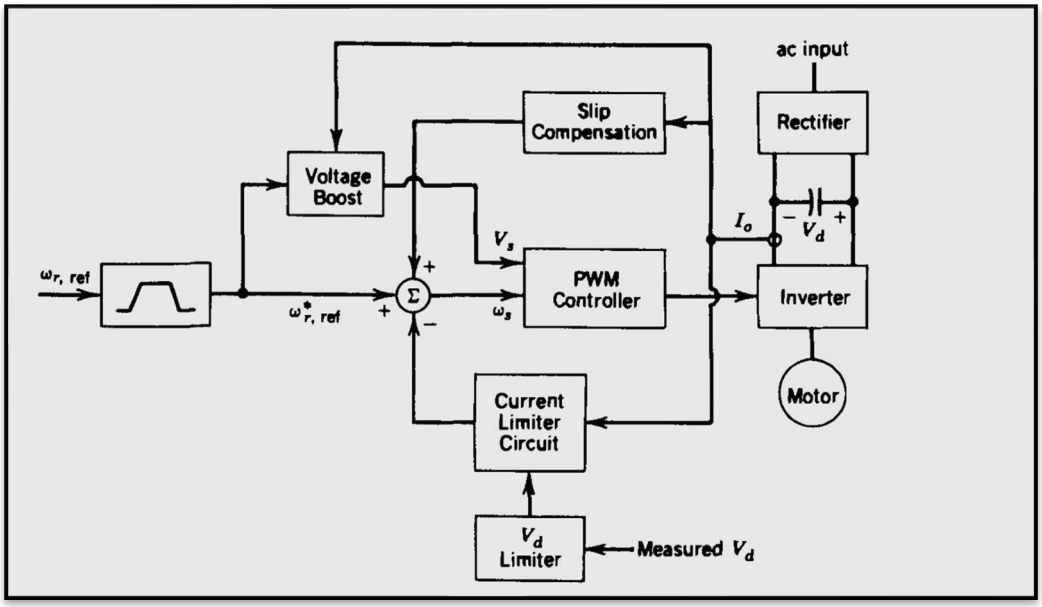

Figure 6.2 – Open-loop circuit for V/f control of an Induction Motor [7]

For protection and better speed accuracy, current and voltage feedback may be employed. These signals are required anyway for starting/stopping of the drive, to limit the maximum current through the drive during acceleration/deceleration or under heavy load conditions, and to limit the maximum dc link voltage during braking of the induction motor. Because of slip, the induction motor operates at a speed lower than the synchronous speed. It is possible to approximately compensate for this slip speed, which increases with torque, without measuring the actual speed. Moreover, a voltage boost is required at lower speeds. It should be noted that, if needed, the speed can be precisely controlled by measuring the actual speed and thereby using the actual slip in the block diagram of **Fig 6.2**. By knowing the slip, the actual torque can be calculated, thereby allowing the voltage boost to be calculated more accurately. To meet these objectives, the motor currents and the dc link voltage V_d across the capacitor are measured. To represent the instantaneous ac motor currents, a current i_o at the inverter input, as shown in **Fig 6.2**, is measured. The following control options are described **[7]**:

1. Speed control circuit. The above speed control circuit accepts the speed reference signal $\omega_{r,ref}$ as the input that controls the frequency of the inverter output voltages. By the ramp limiter, the maximum acceleration/deceleration rates can be specified by the user through potentiometers that adjust the rate-of-change allowed to the speed reference signal. During the acceleration/deceleration condition, it is necessary to keep the motor current i_o and the dc-bus voltage V_d within limits. If the speed regulation is to be improved, to be more independent of the load torque, it also accepts an input from the slip compensation subcircuit, as shown in **Fig 6.2** and explained in item 3 below.

2. Current-limiting circuit. A current-limiting circuit is necessary if a speed ramp limiter is not used. In the motoring mode, if ω_s is increased too fast compared to the motor speed, then ω_{slip} and, hence, i_o would increase. To limit the maximum rate of acceleration so that the motor current stays below the current limit, the actual motor current is compared with the current limit, and the error, through a controller, acts on the speed control circuit by reducing the acceleration rate (i.e., by reducing ω_s).

In the braking mode, if ω_s is reduced too fast, the negative slip would become large in magnitude and would result in a large braking current through the motor and the inverter. To restrict this current to the current limit during the braking, the actual current is compared with the current limit, and the error, fed through a controller, acts on the speed control circuit by decreasing the deceleration rate (i.e., by increasing ω_s). During braking, the dc-bus capacitor voltage must be kept within a maximum limit. If there is no regenerative braking, a dissipation resistor is switched on in parallel with the dc-bus capacitor to provide a

dynamic braking capability. If the energy recovered is larger than that lost through various losses, the capacitor voltage could become excessive. Therefore, if the voltage limit is exceeded, the control circuit decreases the deceleration rate (by increasing ω_s).

3. Compensation for slip. To keep the rotor speed constant, a term must be added to the applied stator frequency, which is proportional to the motor torque T_{em} :

$$\omega_s = \omega_{r,ref} + kT_{em} \quad \text{..... (6.1)}$$

The second term (with k as a constant of proportionality) in **Eq 6.1** is calculated by the slip compensation block of **Fig 6.2**. One option is to estimate T_{em} . This can be done by measuring the dc power to the motor and subtracting the losses in the inverter and in the stator of the motor to get the air-gap power P_{ag}. From **Eq 4.45** and **Eq 5.22**, T_{em} can be calculated.

4. Voltage boost. To keep the air gap flux constant, the motor voltage must be

$$V_s = k\omega_s + kT_{em} \quad \text{..... (6.2)}$$

Using T_{em} as calculated in item 3 above and knowing ω_s , the required motor voltage can be calculated. This provides the necessary voltage boost in **Fig 6.2**.

It should be noted that, if needed, the speed can be precisely controlled by measuring the actual speed and thereby using the actual slip in the block diagram. By knowing the slip, the actual torque can be calculated, thereby allowing the voltage boost to be calculated more accurately.

6.2.2 Scalar Control in a Closed-loop Circuit

Accuracy in speed control can be improved with a closed loop system in which a feedback loop of the speed signal is added. The control unit along with the comparator of the reference signal and the feedback signal is what creates the closed loop of the system. As a control unit, a PI controller is usually used because it is simple and easy to implement and in addition, it gives satisfactory results in the dynamic response of the system and in the rejection of disturbances. Thus, the control unit, combined with the applied PWM-controller, is implemented by PI controllers and corresponds properly to the dynamic response of the system. However, to apply a PI controller, the system should be linear, time-invariant, which the engine model is not. However, using constant voltage-to-frequency ratio technique, nearly constant magnetic flux within the engine is achieved. The choice of controller parameters and the design of the control unit play a decisive role in optimizing the response of the motor drive system **[43]**. **Fig. 6.3** below, shows such a closed-loop control circuit.

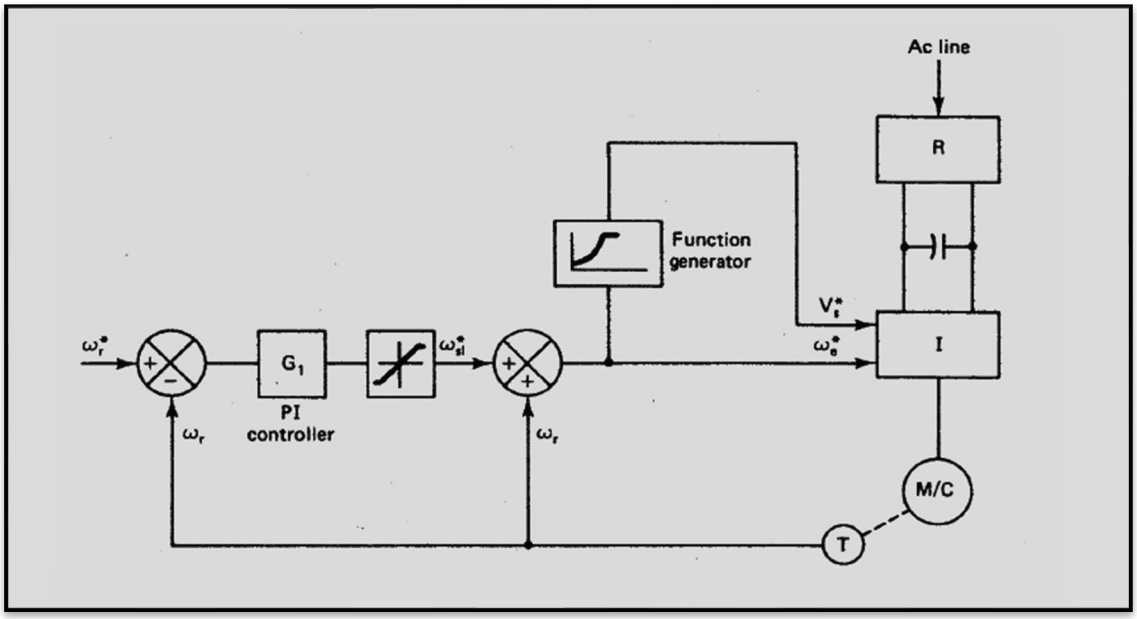

Figure 6.3 – Closed-loop circuit for V/f control of an Induction Motor [7]

The mechanical speed of the engine ω_r is converted into a control signal through a tachogenerator or a position encoder and fed back to the controller. Then, this signal is subtracted from the reference speed ω_s, resulting in the error, which is then passed through the controller and the limiter, resulting in the desired slip frequency ω_{slip} . In this signal, the actual speed of the engine is added, and consequently, the result is the desired electrical frequency of the voltage with which the engine should be supplied **[12]**.

When a speed change command is given, the engine will accelerate at a maximum rate defined by the limiter, corresponding to a limit of the engine concerning the stator currents or the developed torque. As the engine speed approaches the desired one, the slip stabilizes at some value that defines a certain operating point of the engine. The torque corresponding to this point will be equal to the load torque, while its actual speed will differ from the desired, during slip. In the case of an acceleration command, slip takes positive values, whereas in the case of deceleration, negative ones.

The behavior of this system and its response are clearly superior to that of the open-loop, as it takes into account the actual rotational speed and tries to eliminate the error (excluding slip error, of course) **[12]**.

7. IMPLEMENTATION AND SIMULATION RESULTS

The following chapter presents the simulation results which took place for the purposes of this paper, and can be distinguished into three general experiments. In the first one, a single-phase VSI is constructed, and a comparative analysis is carried out between bipolar and unipolar SPWM voltage switching modulation, operating under the same resistive load with an LC filter. Next, based on the conclusions drawn from the first experiment, the SPWM inverter is fed to an asynchronous induction motor, in order to conduct a complete motor drive system model. In the second experiment, the reliability of the system is tested, using scalar control in open-loop circuit configuration, under various circumstances, while in the final experiment, the control is applied to a closed-loop circuit, for a complete motor drive system speed control. The implementations and the simulations were carried out with the use of the Simulink package included in the MATLAB software from MathWorks company.

7.1 A Single-Phase SPWM-VSI with Bipolar and Unipolar Voltage Switching Technique

The two inverter models with bipolar and unipolar SPWM are illustrated below:

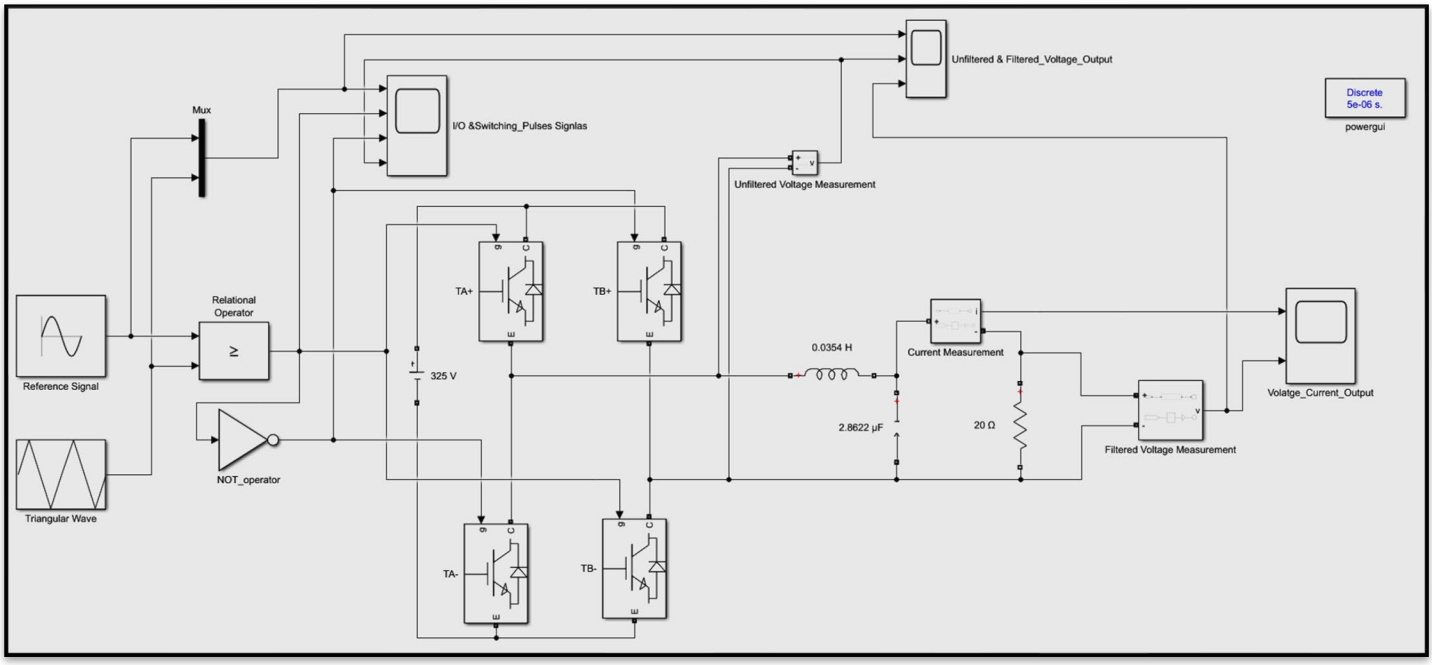

Figure 7.1 – Construction of a Single-Phase bipolar SPWM Voltage Source Inverter

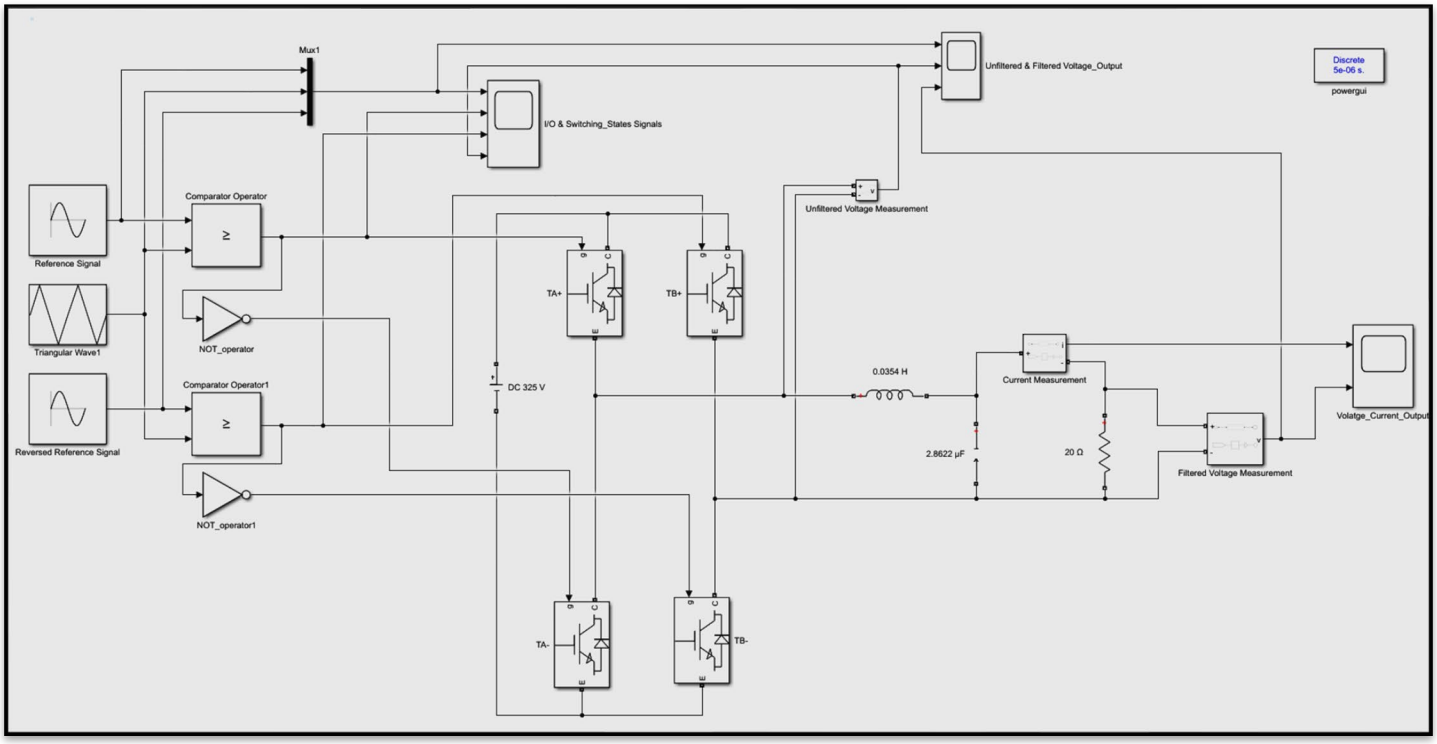

Figure 7.2 – Construction of a Single-Phase unipolar SPWM Voltage Source Inverter

For the implementation purposes of **Fig 7.1** and **Fig 7.2**, the following components were included: a DC voltage source, a sine wave (and an equal negative signal for the unipolar SPWM) which represents the reference signal, a repetitive wave in a triangular form to represent the carrier signal which produces the switching frequency of the inverter, four IGBT-type-switches which establish the inverter in a full-bridge topology and comparators as well as NOT-gate operators. A resistive load with a low-pass LC filter made by a capacitor and an inductor in parallel series, were also used to represent the inductive load, in order to get a decent sinusoidal result at the inverter output terminals, just like the behavior of an induction machine. The chosen parameter values for the secondary components of the implementation (DC voltage source, inductor, capacitor, resistor) are shown on the block diagrams above.

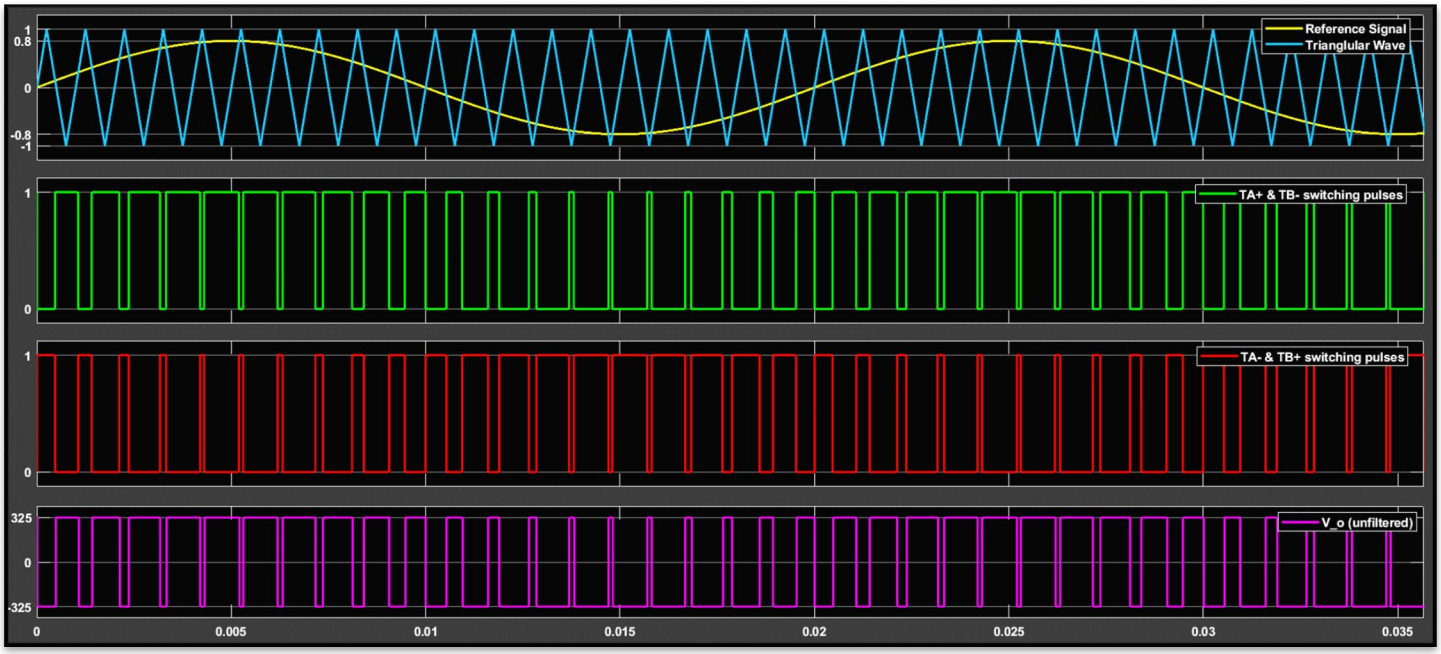

7.3 – Comparator, Switching Pulses & Voltage Output Signals of a VSI using Bipolar SPWM

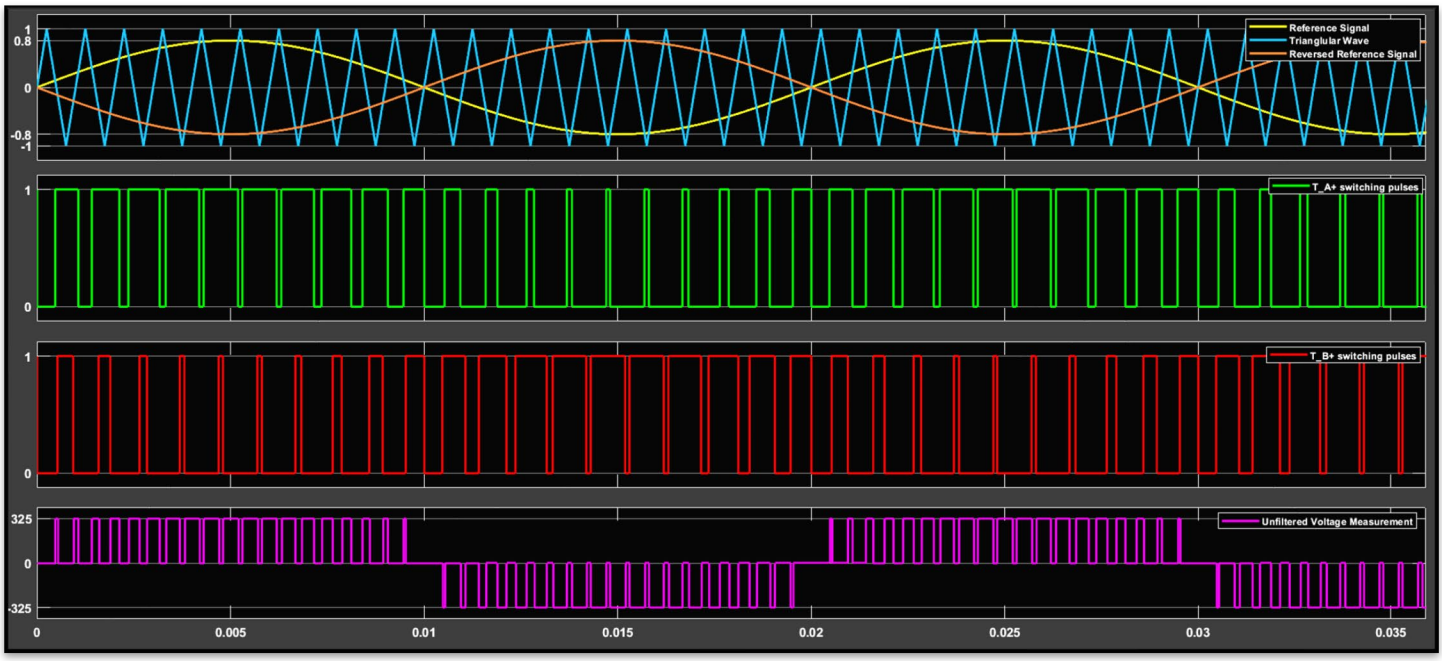

7.4 – Comparator, Switching Pulses & Voltage Output Signals of a VSI using Unipolar SPWM

Figures 7.3 and **7.4** display all the inputs and output signals for the SPWM technique in an inverter, both in bipolar and in unipolar configuration. In this simulation, the inverter is running with a switching frequency at $f_s = 1000\ Hz$ to study the impact of low switching frequency on both models. The sine waveform and its inverse have an amplitude modulation ratio $m_a = 0.8$. The fundamental frequency f_{ref} is at $50\ Hz$.

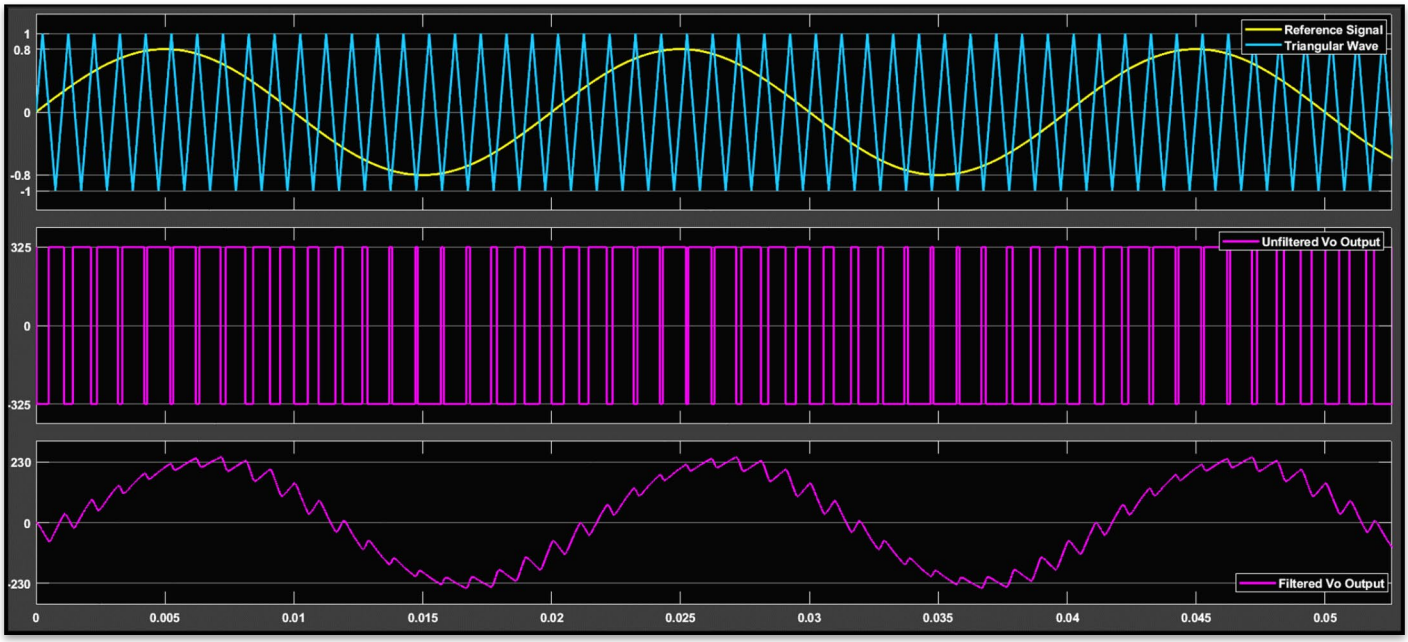

7.5 – Voltage Output of the Inverter with and without LC filter (Bipolar SPWM)

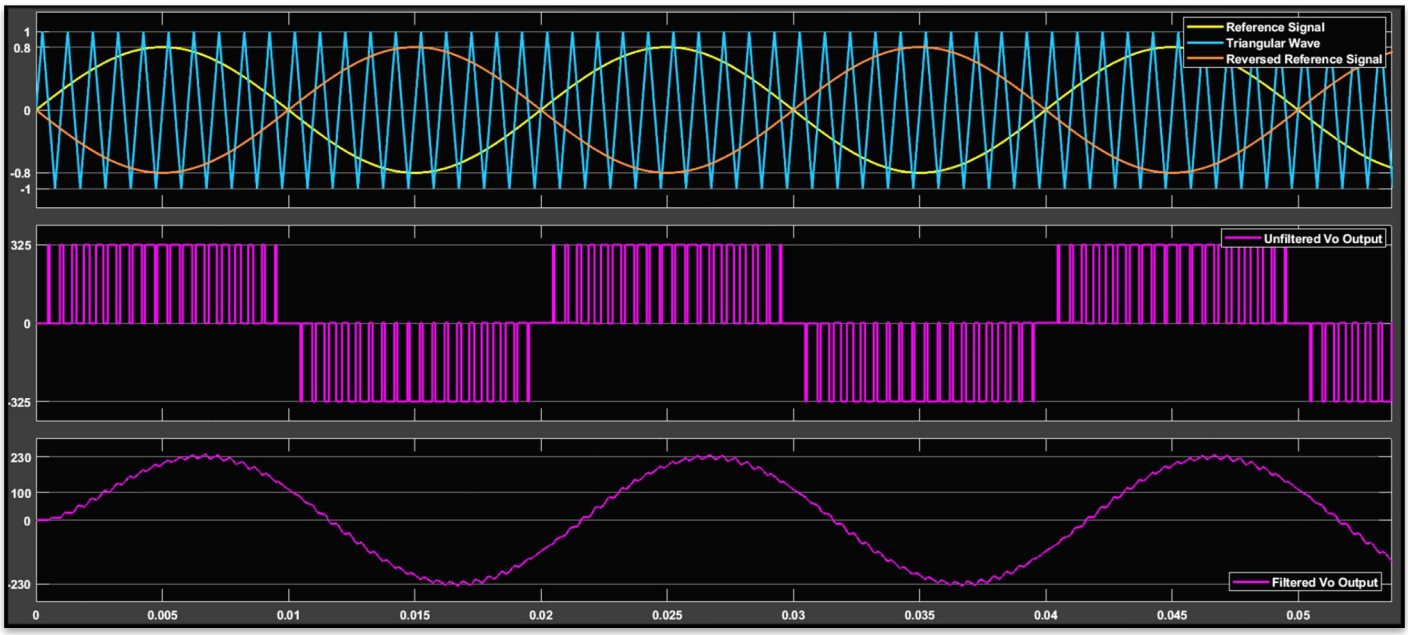

7.6 – Voltage Output of the Inverter with and without LC filter (Unipolar SPWM)

At first, the inverter voltage is measured before filtering in both of the techniques. Then, the same LC filter is applied to both circuits, in order to filter out the harmonic components at the voltage and current output terminals of the inverter and to give a waveform as similar to a pure sine wave as possible. The simulation results are shown above in **Fig 7.5** and **Fig 7.6**. After the implementation of the LC filter, the resulted voltage and current outputs for both of SPWM techniques are compared and shown in the simulations of **Fig 7.7** and **Fig 7.8** below.

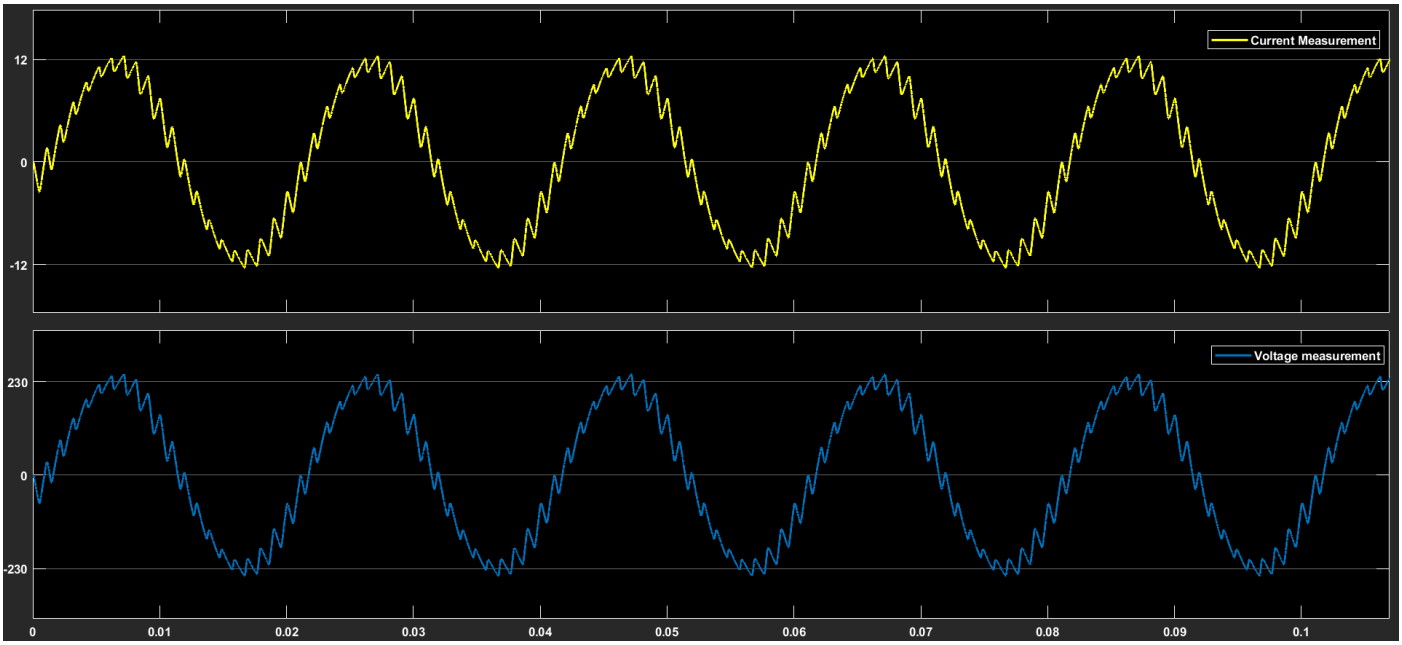

7.7 – Output voltage and current at the inverter load during 1000Hz for Bipolar SPWM

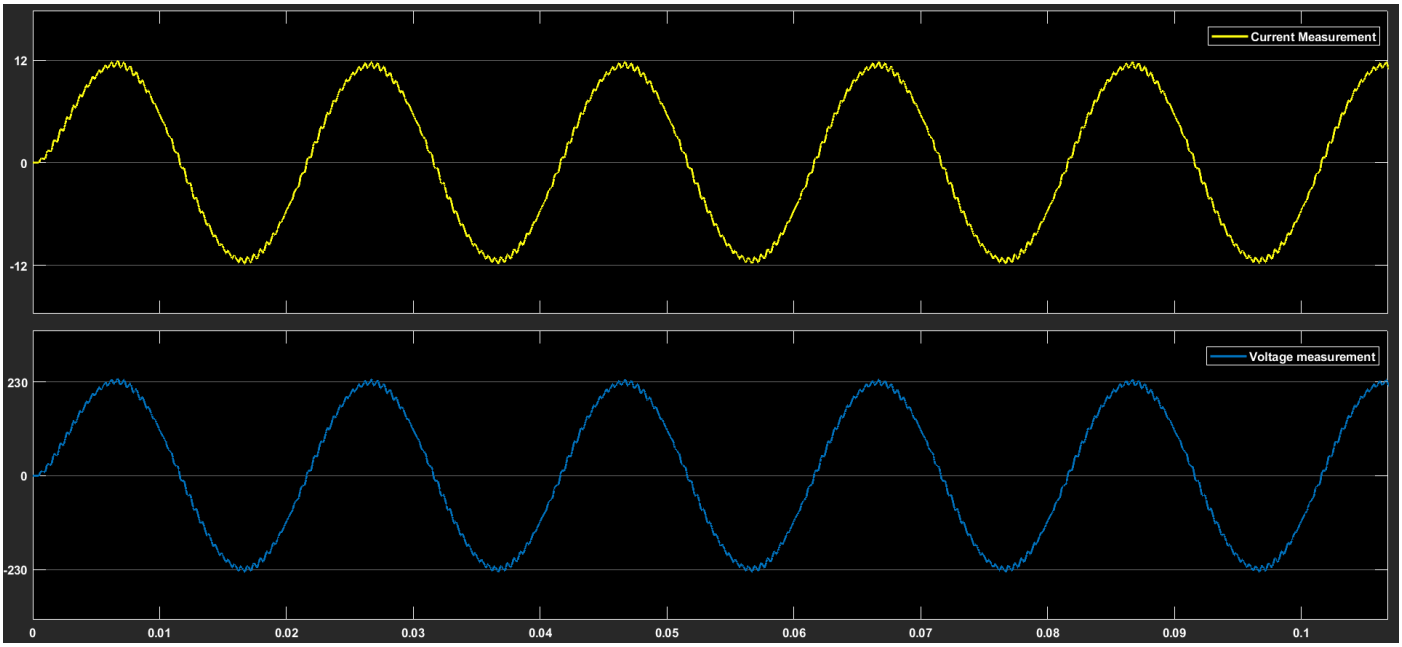

7.8 – Output voltage and current at the inverter load during 1000Hz for Unipolar SPWM

All of the foregoing results have been obtained for the lower switching frequency of **1000 Hz**. However, when the switching frequency is increased to $f_s = 15000\ Hz$, both techniques give a true sine waveform of the output voltage and current, as shown in **Fig 7.9** below. However, in practice it is really challenging to obtain pure sine wave voltages and currents outputs, unless implementing multiple loop controllers, robust control and similar other control methods.

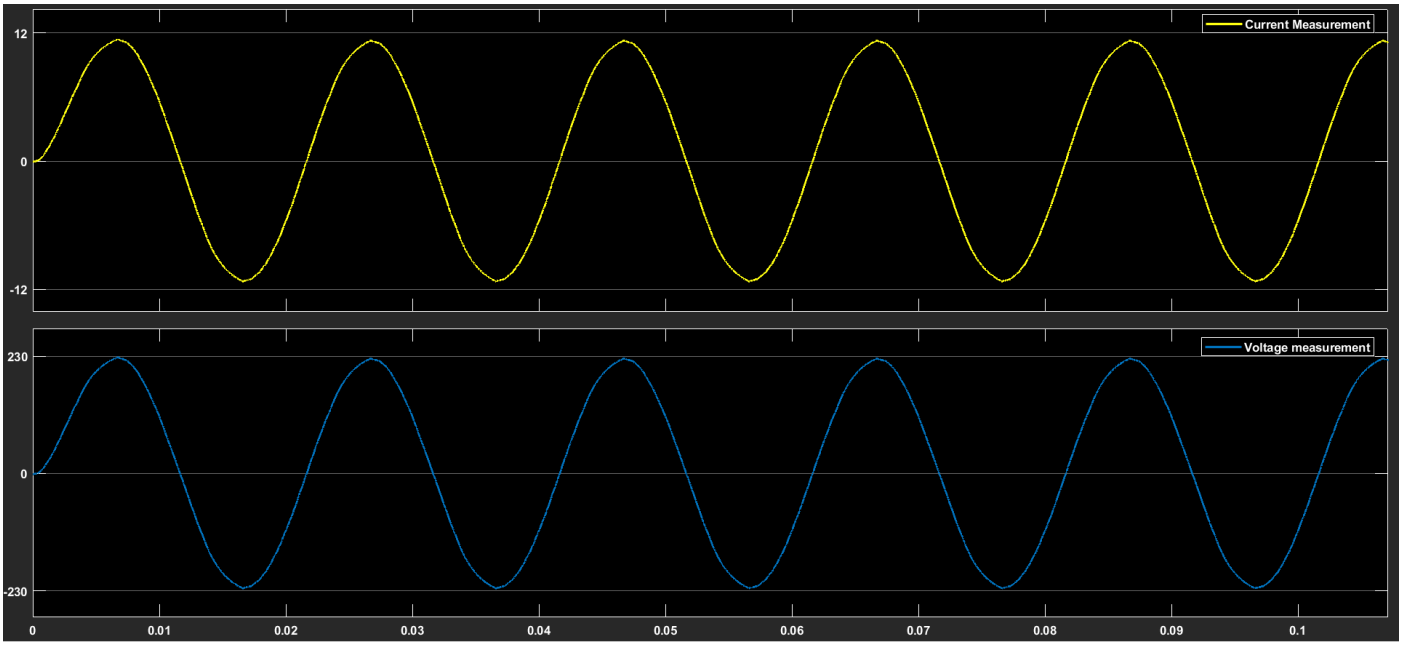

7.9 – Output voltage and current at the inverter load during 15000 Hz for both SPWM techniques

For further analysis, the frequency domain is considered with a Fast Fourier Transform (FFT) algorithm analysis. The analysis can facilitate the evaluation of the inverter output voltages and currents easily, by suppressing the different harmonic components **[44]**. In the spectrum analysis, shown in **Fig 7.10**, a switching frequency of **1 kHz** was selected at first, in order to study the impact of low frequency at the load of the inverter, as well as the impact of the chosen low pass filter at the inverter output terminals. The produced simulation results were implemented both for bipolar and unipolar SPWM techniques.

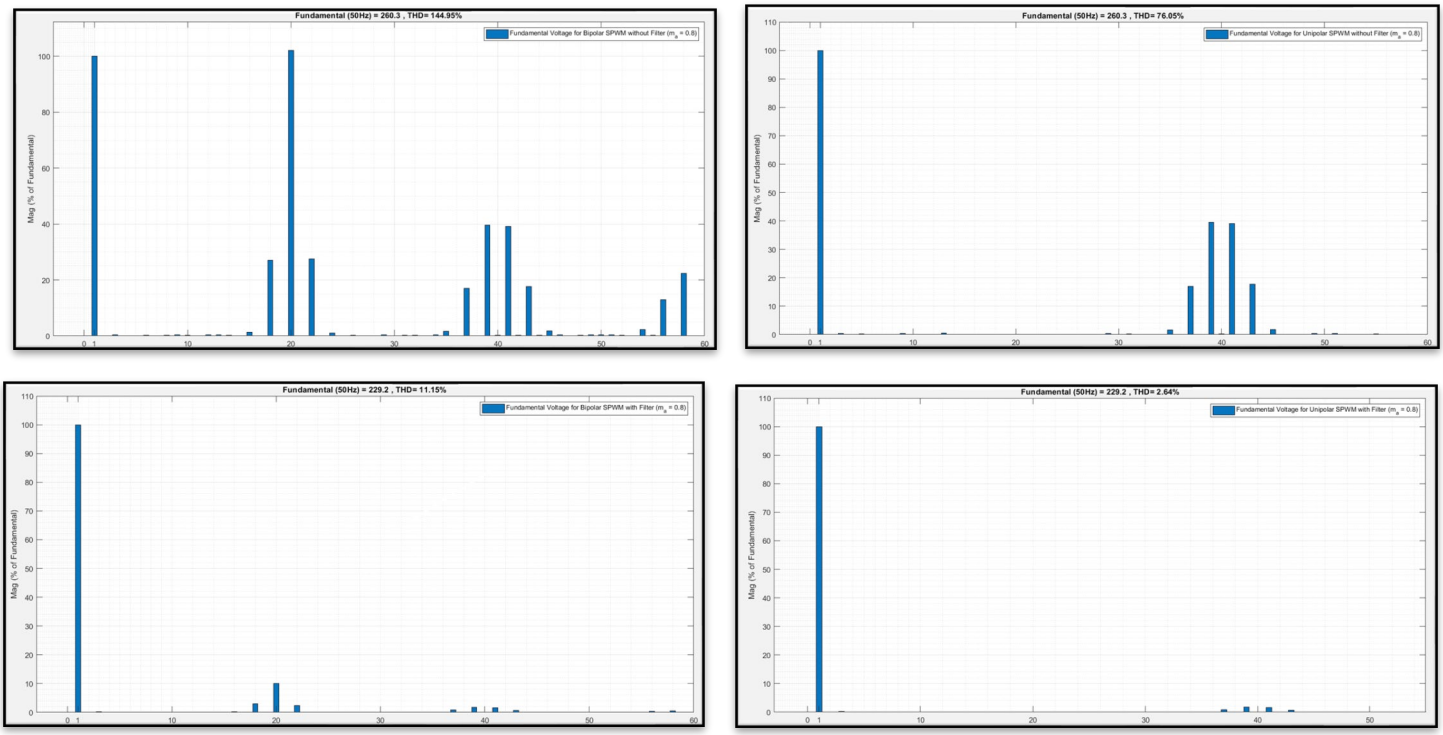

(a) Output Voltage Spectrum of Bipolar SPWM (Filtered & Unfiltered)

(b) Output Voltage Spectrum of Unipolar SPWM (Filtered & Unfiltered)

7.10 – Fundamental Frequency Component of SPWM Output Voltage for m_a = 0.8 at 1000 Hz

Fig 7.10(a) shows the spectrum of the output voltage, where the top graph is without filter, while the lower graph shows the filtered output voltage of the inverter. It can be noticed that harmonic components and their sidebands appear at **1000 Hz** and also at **2000 Hz** (or at **20** and **40**, as shown in figures, using normalized harmonic order values) of the bipolar inverter, but when the filter is applied, the dominant harmonics and their sidebands, as well as the **THD** factor are significantly reduced. Similarly, **Fig 7.10(b)** shows the spectrum analysis of unipolar SPWM output voltage of the inverter, also at **1000 Hz**. Without filter, harmonics with a small amplitude are noticed only at **2000 Hz**, while after the filter is applied, there are almost no harmonic components except the fundamental harmonic voltage at 50 Hz, which is the desired one.

However, in reality, the switching frequency should be much higher than 1 kHz. Thus, f_s is increased at the high-performance frequency of ***15000 Hz***, with the same amplitude modulation ratio m_a **= 0.8** for reference signal, in both types of SPWM inverter, exactly as before. The simulated results are illustrated in **Fig 7.11** below.

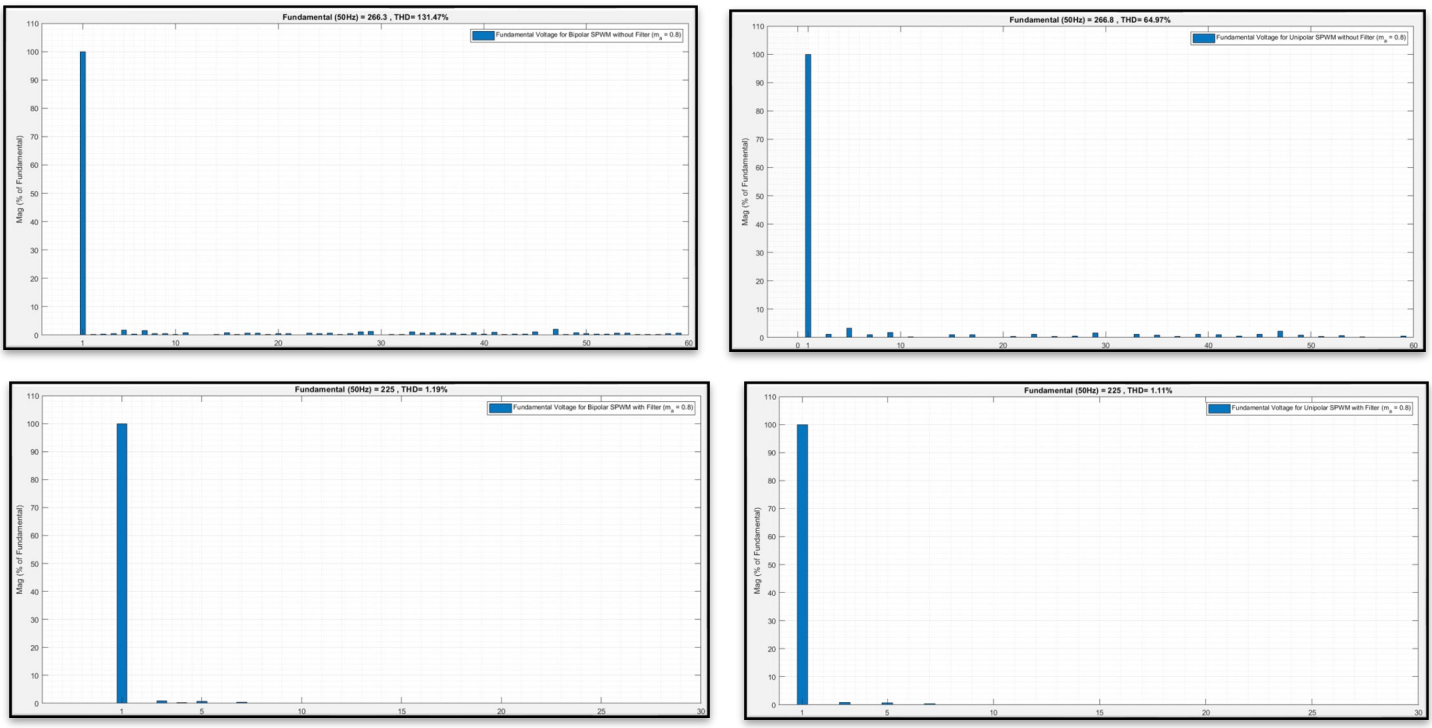

(a) Output Voltage Spectrum of Bipolar SPWM (Filtered & Unfiltered)

(b) Output Voltage Spectrum of Unipolar SPWM (Filtered & Unfiltered)

7.11 – Fundamental Frequency Component of SPWM Output Voltage for m_a = 0.8 at 15000 Hz

The lower graphs of filtered fundamental voltages in **Fig 7.11(a)** and Fig **7.11(b)** for bipolar and unipolar configuration respectively, provide significantly accurate results for high switching frequencies, resulting, as shown previously at **Fig 7.9**, in a true sine waveform of the voltage output. Even so, it is clear that in general, the unipolar inverter gives a better waveform and less distortion compared to the bipolar inverter.

7.2 Scalar Control of an SPWM Single-Phase VSI Motor Drive System (open-loop)

Now, by having selected the unipolar SPWM inverter from the previous experiment, we feed its outputs into an asynchronous machine. The selection of the machine is a single-phase asynchronous motor, based on capacitor start-capacitor run type configuration. The overall AC drive system is figured below.

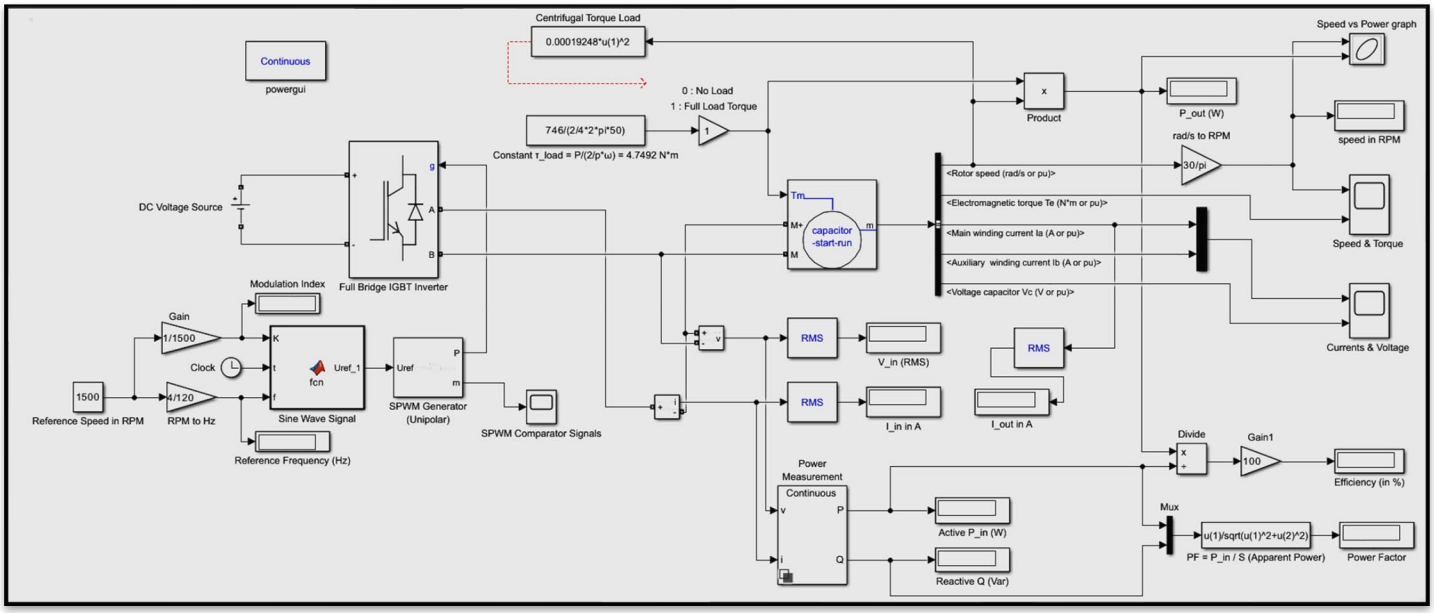

7.12 – Simulation Model of a SPIM drive circuit model (V/f control)

The construction of this open loop system of **Fig 7.12** consists of the following main components: a DC voltage source supply, a universal bridge block, a PWM generator, the asynchronous machine block and a MATLAB function to produce the desired reference signal as a true sine wave input and always in relation to the V/f ratio. Measurement blocks of power, voltage and current, calculating blocks of product, gain and division, as well as a defined function caller block are considered as secondary components and are used to extract several useful measuring data, such as the power factor(PF) and the efficiency of the overall system.

The universal bridge block comes along with the PWM generator and the MATLAB function of the reference signal to represent precisely the single-phase SPWM unipolar inverter, which was used in the previous experimental simulation (that was a two-legged bridge inverter of 4 IGBT switches, with triangular carrier signal and a total of two reference signals (the function-generated sine wave and its inverse), performing in unipolar SPWM voltage switching method). The switching frequency of the carrier signal was set to be at $f_s = 3000\ Hz$, so that the transition losses of the switches be not too high. As already mentioned, higher frequencies of the triangular signal result in more comparisons with the reference sine wave signal, providing greater accuracy in the comparison process. However, the higher the frequency, the higher the switching losses of the inverter. The rest parameters of the bridge block and PWM generator have remained the same with the values MATLAB/Simulink provides on the relative block components.

The selected asynchronous induction machine is a **four-pole** motor with **nominal power** at **1** ***Hp*** (or **746** ***Watts***), **nominal phase voltage** $V_{rms} = 230\ V$ and **nominal frequency** at **50** ***Hz*** (yielding in **1500** ***RPM*** rotor speed). The DC voltage source is set at **325** V (line voltage $V_s = \sqrt{2} * V_{rms}$). Additionally, by choosing the specific type of machine, that is a single-phase induction motor with starting and running capacitors on its windings, causes high starting torque, balanced starting and line currents, as well as stability and efficient performance during all possible states of operation, eventually acting as a typical three-phase motor drive system with a balanced set of currents. The rest parameters of the motor block remain the same as the default values MATLAB Simulink provides in it.

After implementation of the system, and in order to extract efficient conclusions regarding its operation, the behavior of the system was initially studied at the desired rated speed of **1500 *RPM*** in open-loop configuration, and then at variable reference speed values, always depending on constant ratio ***V/f*** of scalar control. Subsequently, the system was examined under zero, constant, variable, and centrifugal load conditions. Below, the waveforms of speed, torque, and currents, during motor startups are shown, under various load-type transitions and speed variances.

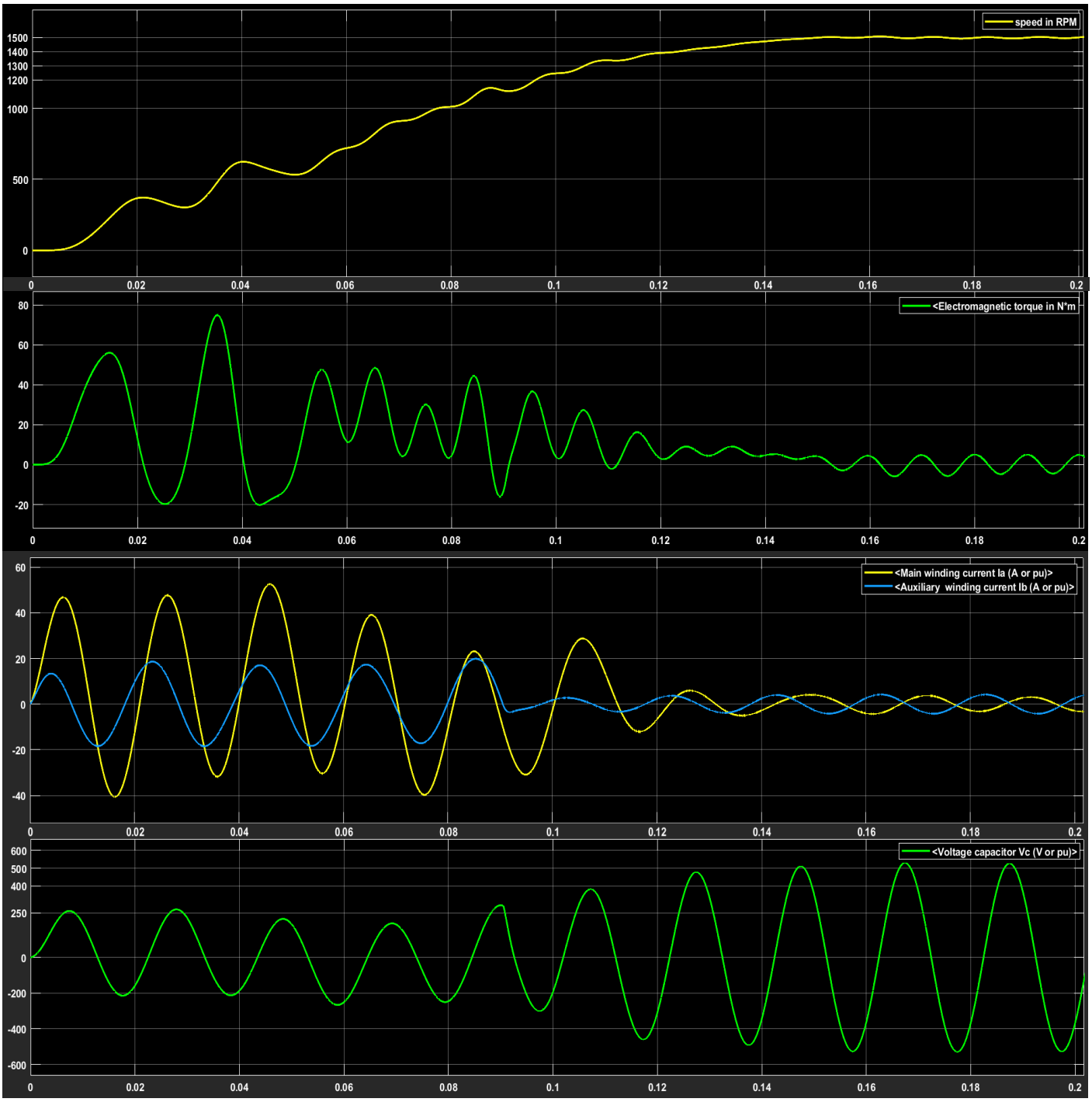

7.13 – Motor Operation for rated speed 1500 rpm, without load in open loop

Next, for various changes of the desired rated speed using scalar control, the sine wave signal function block takes different values for constant K over time, which controls the amplitude modulation index of the system's voltage **(m_a)**, as well as maintaining the v/f ratio constant. The algorithm of MATLAB function is shown below.

```
function Uref_1 = fcn(K, t, f)
  if t>0.4
      K = 0.8;
    end
  if t> 0.5
      K = 1.2;
    end
  if t>0.8
      K = 1;
    end
       Uref_1 = K*sin(2*pi*f*K*t+0.15);
```

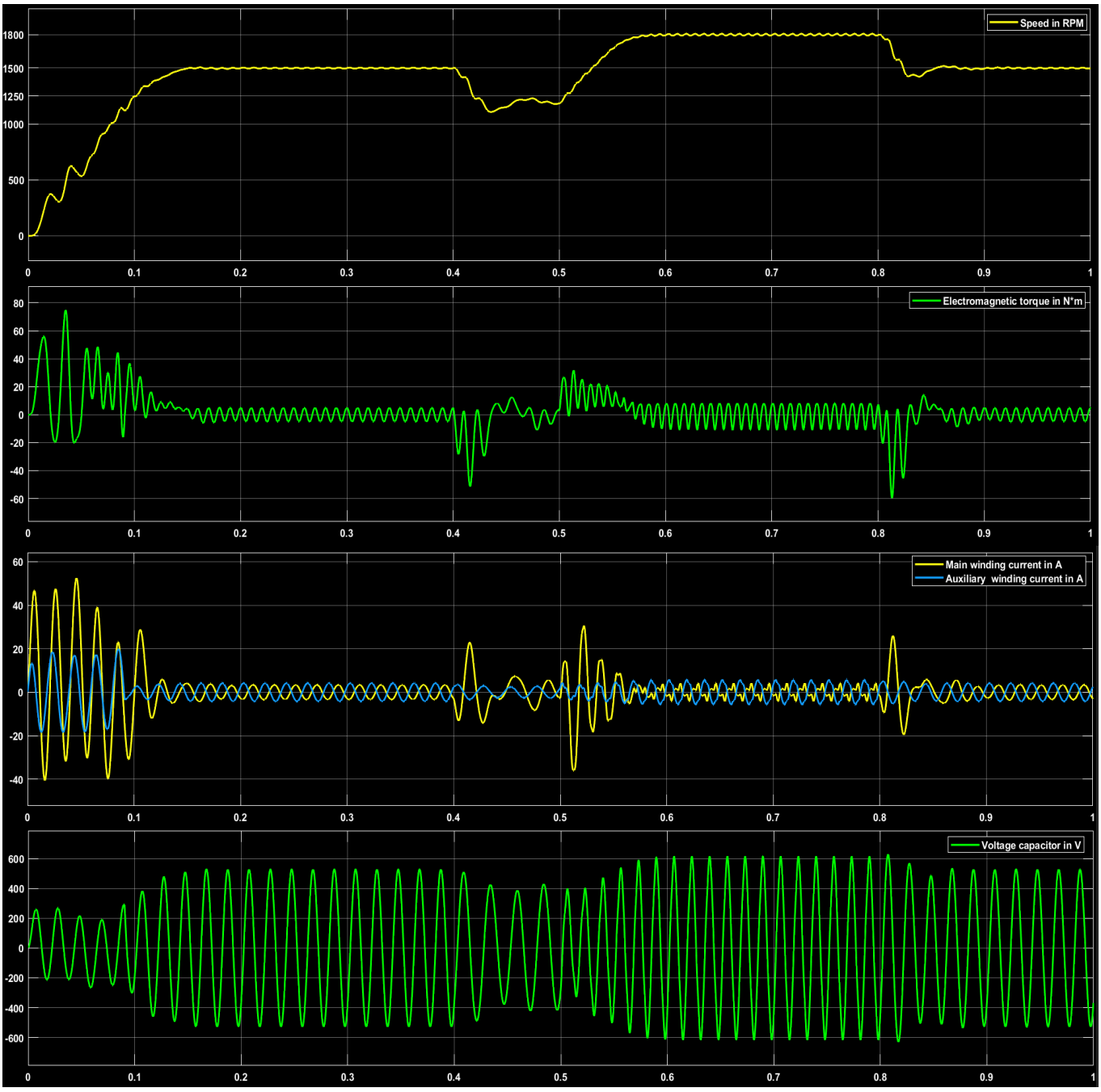

7.14 – Motor Operation for variable speed over time, without load in open loop (V/f control)

During the above motor operations, which have taken place without external load, it is observable that the overall system's responses are within acceptable standards. The machine accelerates and manages to reach the desired speed sufficiently fast. In order to describe and evaluate the dynamic response of a system, we can also use the evaluation indexes **overshoot M_p** (the percentage of the peak value of system's speed relative to the desired speed value) , **rise time t_r** (the time required for the output to reach the desired rated value for the first time) and **settling time t_s** (the time required for the output to differ from the rated value by less than ±2%). As long as these evaluation indexes are kept in small values, the system responses are capable to track the input fast and without significant overshoot, as well as to quickly dampen disturbances **[43]**. Furthermore, the SPWM inverter with v/f scalar control, leads balanced voltages and currents into the induction motor without exceeding the starting currents during speed variances, while the use of starting and running capacitors causes high torque pulsations during starting operation, as well as mitigated pulsations during steady-state operation, leading to a high power factor of the machine.

Then, in order to apply an external load to the machine, we calculate its maximum torque that can get, based on its nominal horsepower and speed, which for a 4-pole induction machine gives $\tau_{\_load} = (746VA*1Hp/2/4(2*\pi*50Hz)) =$ **4.7492** $N*m$. Thus, a constant block of this value is fed to the input of the motor in the simulation circuit, representing the 100% of the load torque of the machine. The results for constant rated speed are illustrated below in **Fig 7.15**.

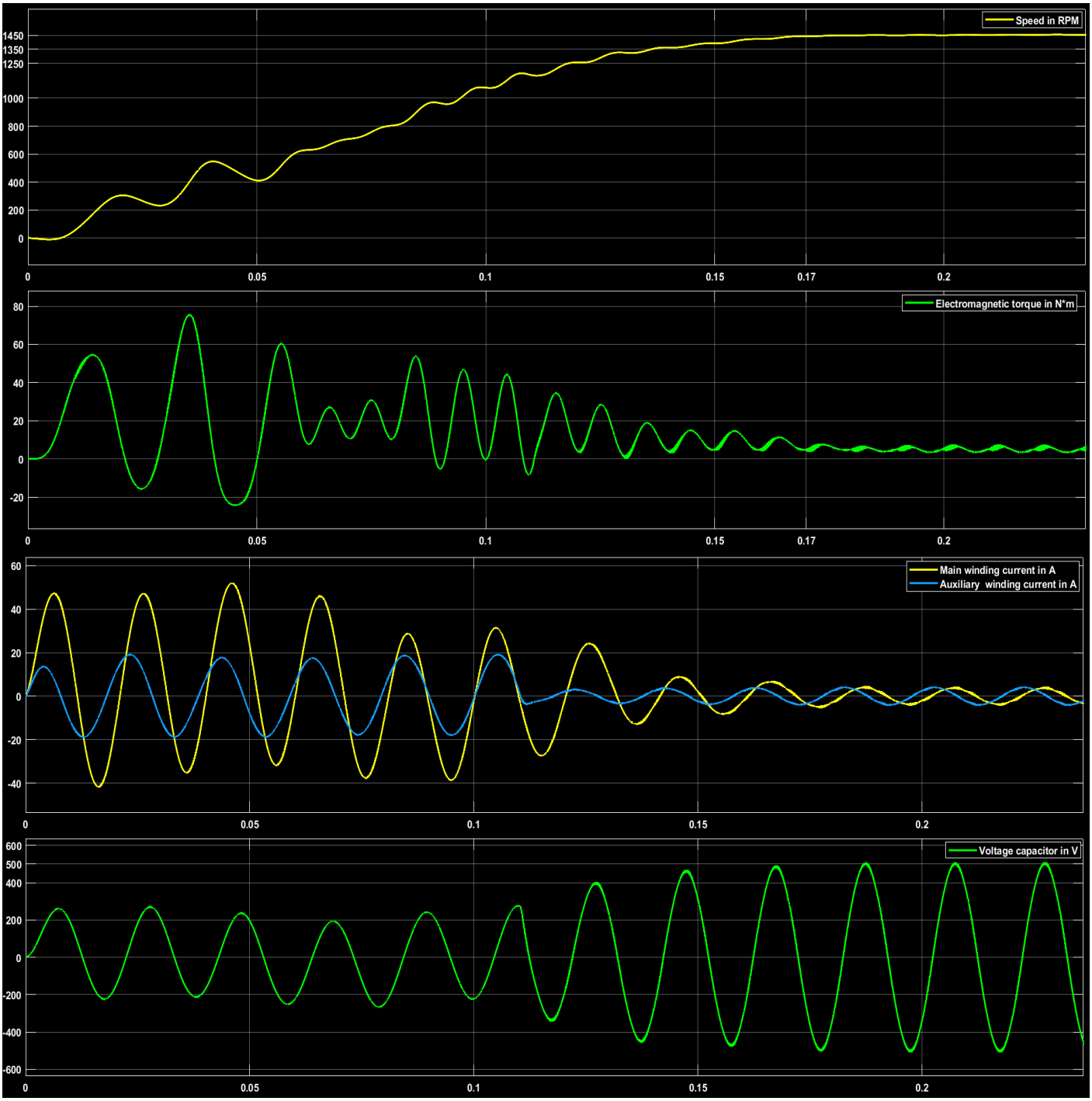

7.15 – Motor Operation for rated speed 1500 rpm, under constant nominal load in open loop

Then, load variations over time are applied to the motor, according to **Fig 7.16** below and are illustrated on percentage basis of the full load torque. As a result, **Fig 7.17** presents the behavior of the motor operation, under those load variations.

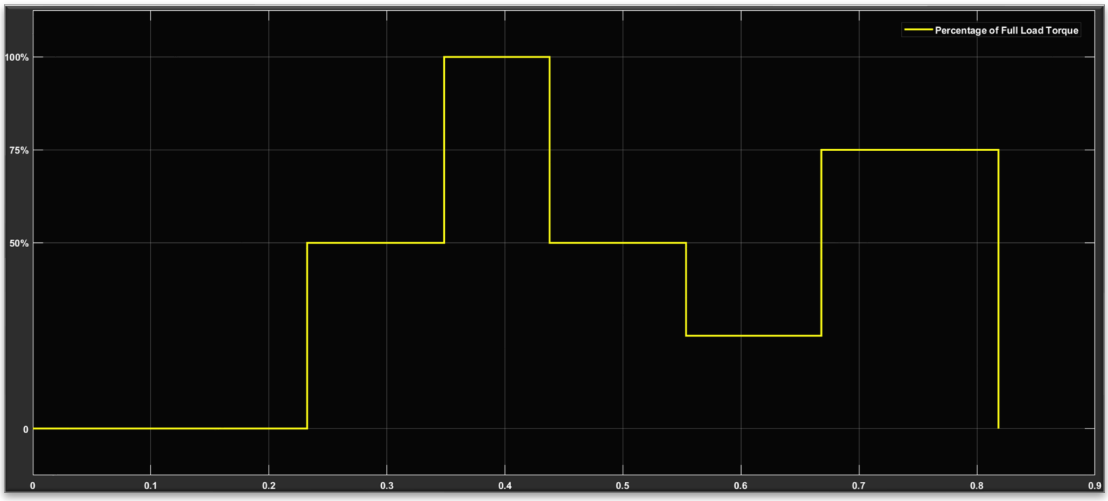

7.16 –External load variations applied to motor expressed on a percentage basis

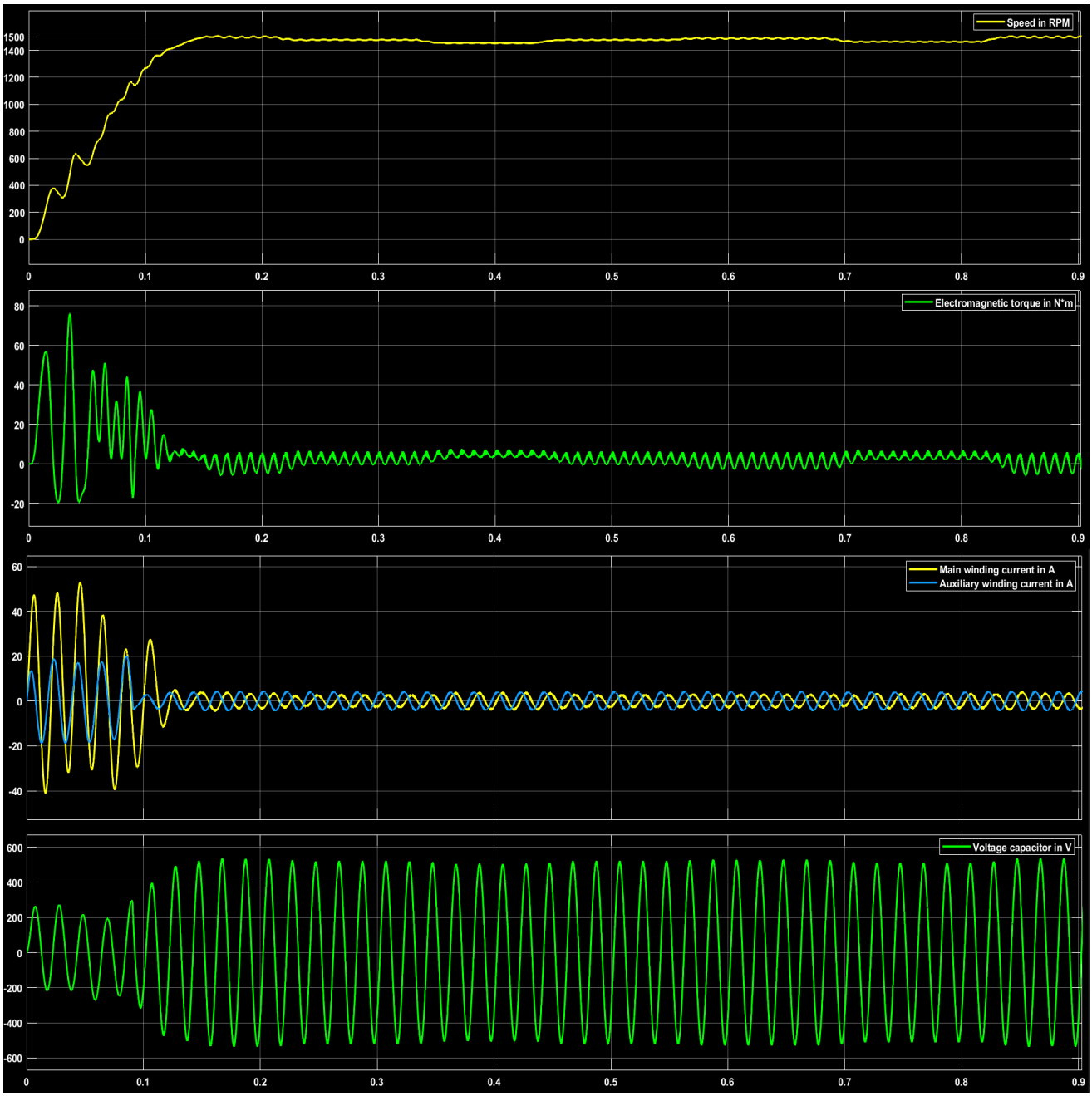

7.17 - Motor operation with constant rated power supply, under nominal load variations

Finally, the centrifugal load of **Fig 7.18** is applied to the motor's input and the results of the simulation follow on **Fig 7.19**.

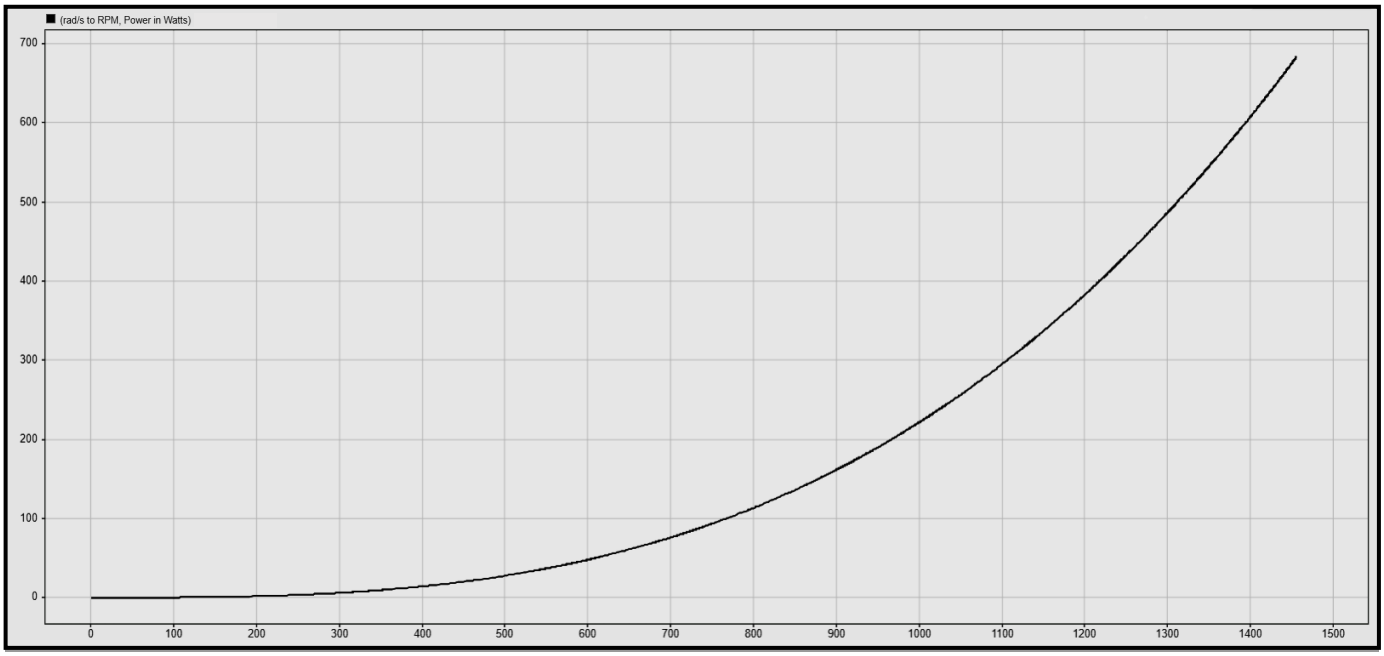

Fig 7.18 – Power-Speed Characteristic of the applied centrifugal load

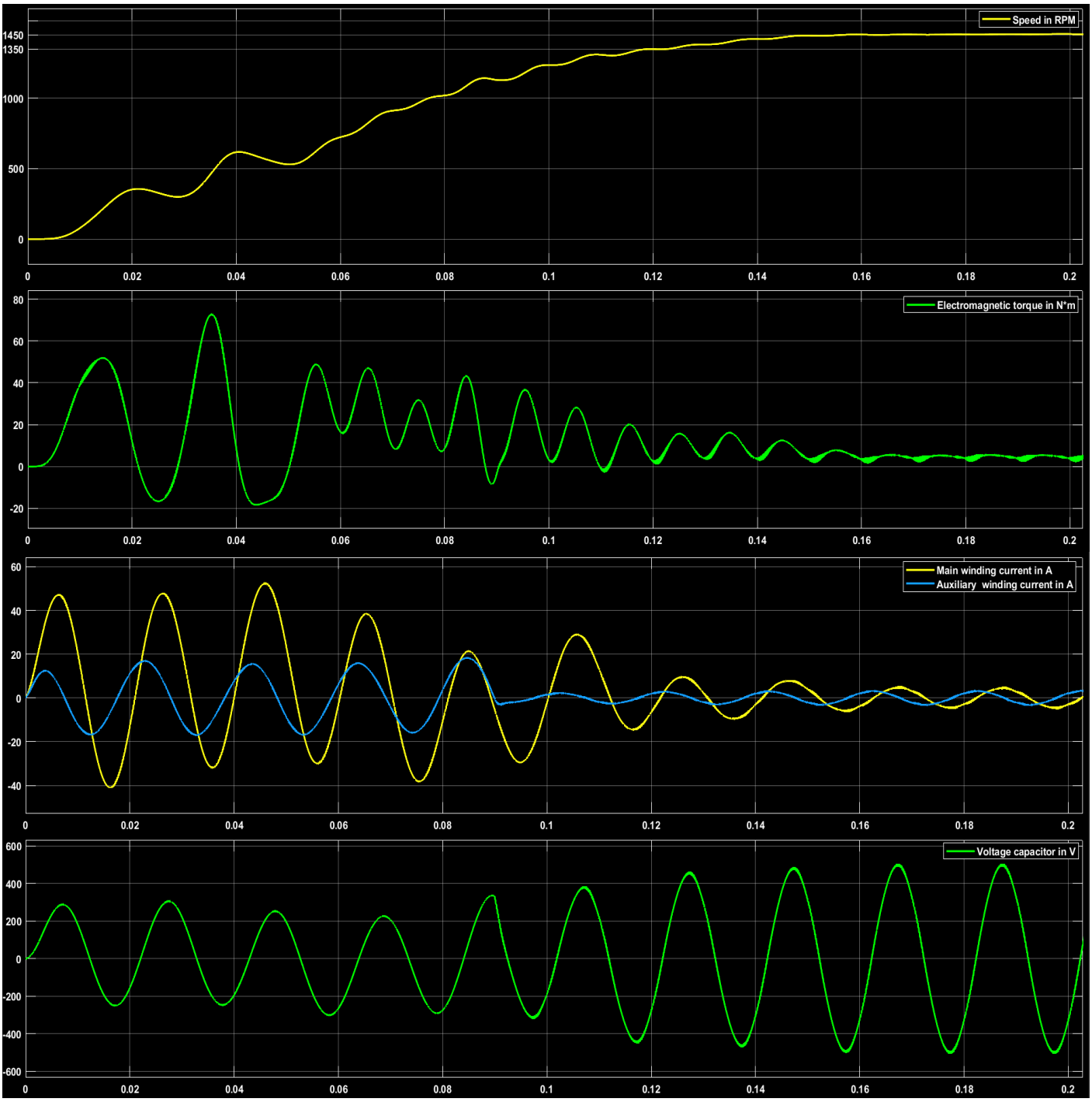

7.19 – Motor Operation with constant rated power supply, under centrifugal load in open loop

From above operations, which come up with the use of external load on the machine's shaft, it can be noted that the speed of the system is little lower than the desired speed, while evaluation indexes $\mathbf{M_p}$, $\mathbf{t_r}$ and $\mathbf{t_s}$ are still kept in sufficiently small values (even lower than operations without external load). Torque pulsations magnitude is almost 200 % of the rated torque at no load, while here, in occasions with external load, it is approximately at 4 % of the rated torque at full load. Power factor and efficiency are also higher than operation cases with no load.

7.3 Scalar Control of an SPWM Single-Phase VSI Motor Drive System (closed-loop)

Finally, the last experiment of the chapter contains a complete speed control of the overall system in closed-loop circuit, where the output of the motor is given back to the input to be compared with the reference synchronous speed and the outcome is driven to a PI controller, which in turns, controls the actual frequency and consequently the actual speed of the motor drive system. The system implementation follows below in **Fig 7.20**. It has been accomplished for centrifugal load (such as a pump load), containing the same main and secondary components of the previous simulation and by adding the PI controller along with the feedback output loop. System's responses appear in **Fig 7.21**, leading to much better performance with higher efficiency, power factor and evaluation indexes ($\mathbf{M_p}$, $\mathbf{t_r}$, $\mathbf{t_s}$) than the equivalent open-loop control circuit of the previous experiment.

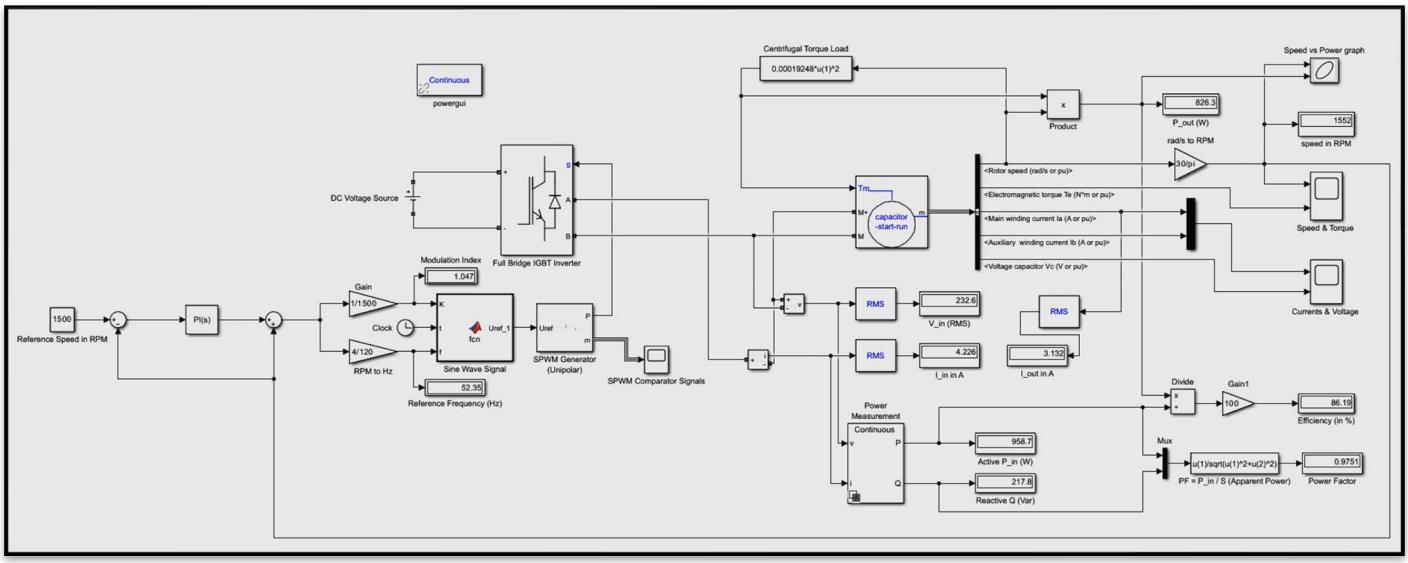

7.20 – Simulation Model of a SPIM drive circuit model with PI feedback Controller (closed-loop)

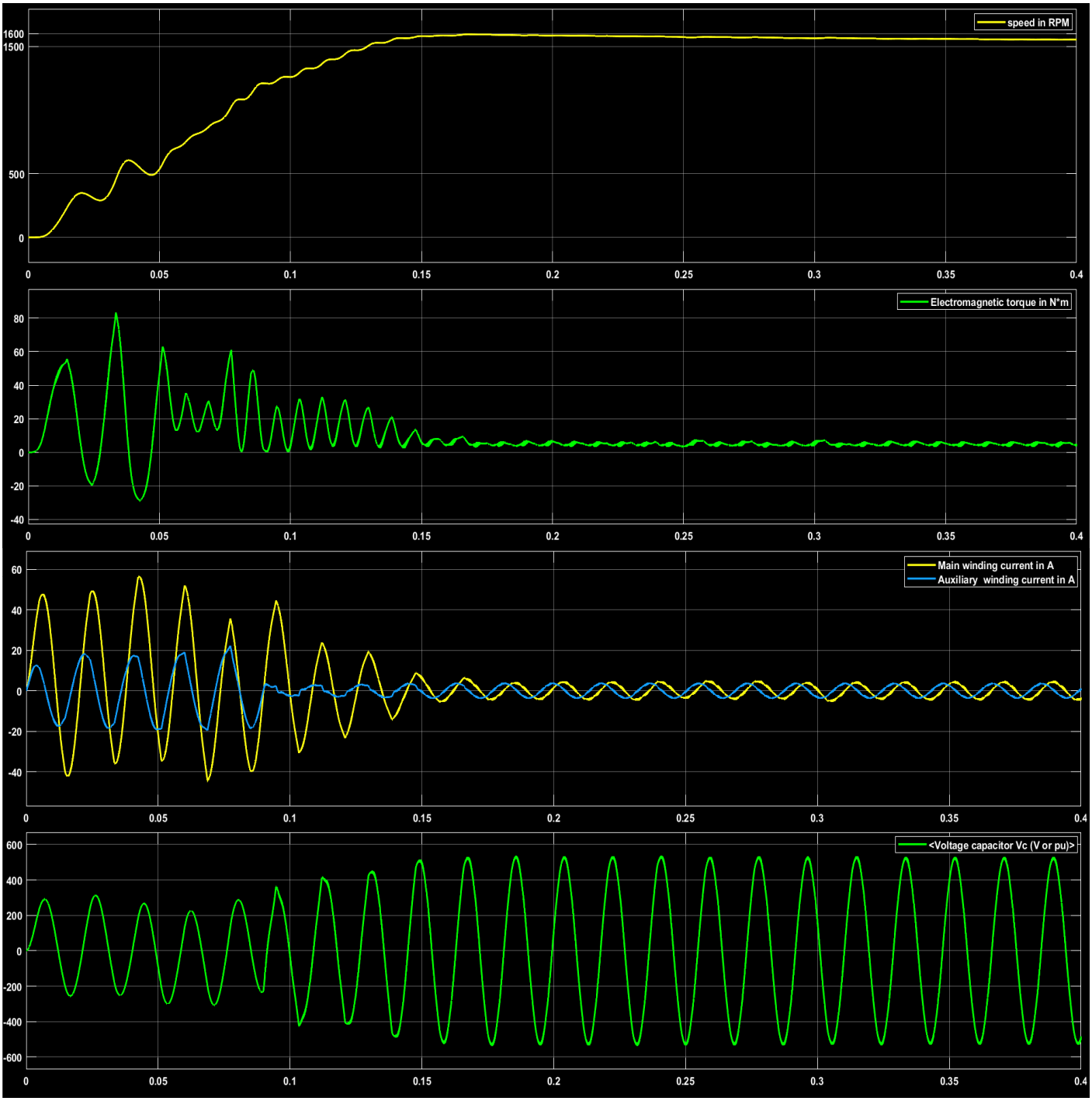

7.19 – Motor Operation with constant rated power supply, under centrifugal load in closed-loop

8. GENERAL CONCLUSIONS AND FUTURE WORK

8.1 General Conclusions According to Theory and Simulation Results

As a general conclusion, it can be noted that the control of the implemented and simulated single-phase motor driving system, as developed in this paper, is satisfactory for several everyday applications and relatively cost-effective, achieved through the use of semiconductor IGBT switches which represent the VSI of the system. The SPWM technique ensures lower Total Harmonic Distortion (THD), ultimately providing a desired sine wave output voltage and current to feed the induction motor properly. Based on the comparative analysis of the simulation, along with the relative theory of subchapters **3.5 – 3.8**, unipolar SPWM generally emerges as the better choice for most applications due to its superior harmonic performance, lower switching losses, and reduced EMI. These advantages make unipolar SPWM particularly suitable for applications where power quality and efficiency are critical, such as in renewable energy systems, electric vehicles, and high-performance motor drives.

However, in applications where simplicity and ease of implementation are more important, or where the system can tolerate higher harmonic distortion and switching losses, bipolar SPWM may still be a viable option. The choice ultimately depends on the specific requirements and constraints of the application. Thus, while unipolar SPWM is often preferred for its performance benefits, bipolar SPWM remains relevant in scenarios prioritizing simplicity and implementation ease.

From the simulation results, it is observed that the control of the induction motor using the Proportional-Integral (PI) controller produces a better response than without PI control. Thus, the open-loop constant *V/f* control method is used in low-performance applications where precise speed control is not necessary, as the speed of the motor cannot be controlled precisely. The rotor speed is not measured in this drive scheme, so the slip speed cannot be maintained, potentially leading to operation in the unstable region of the torque-speed characteristics. On the contrary, the closed-loop method offers a more precise solution for controlling speed than the open-loop method. Furthermore, the closed-loop technique controls the torque as well, which is not addressed by the open-loop control method. The closed-loop method contains a slip control loop, as the slip is proportional to the torque.

Implementing the *V/f* control strategy allowed for a more refined control over the motor's speed and torque characteristics. By maintaining a constant voltage-to-frequency ratio, the system ensured optimal performance across various operating points. The motor speed was effectively controlled over a wide range, confirming the *V/f* strategy's capability to handle different speed settings without compromising stability. The torque response was smooth and consistent, indicating precise control over the motor's electromagnetic properties. This is particularly beneficial in applications requiring variable speed and load conditions. The V/F control strategy resulted in improved overall efficiency, reducing losses and ensuring that the motor operated within its optimum performance range.

During the open-loop configuration, the VSI provided a steady voltage output modulated by the SPWM technique. The capacitor-start capacitor-run motor exhibited smooth starting characteristics and stable operation under various load conditions. The simulation results indicated a high inrush current during the starting phase, typical for capacitor-start motors. The magnitude of this current was within the expected range, demonstrating the effective engagement of the start capacitor. The power factor was observed to improve once the motor transitioned from the starting phase to the running phase, aligning with theoretical expectations. The running capacitor effectively shifted the current phase, improving the power factor. The motor efficiency under open-loop control was satisfactory, showing minimal losses and efficient power conversion by the VSI. The closed-loop configuration introduced feedback mechanisms to adjust the VSI

output based on motor performance metrics. This setup aimed to maintain desired speed and load conditions, enhancing the overall system stability and efficiency. The closed-loop control successfully maintained the motor speed within a tight tolerance range despite variations in load. This result confirms the efficacy of the feedback control algorithm in regulating motor performance. The system demonstrated robust performance under different load conditions, maintaining stable operation and quickly adapting to load changes without significant deviations in speed or torque. Closed-loop control further improved the motor efficiency and power factor by dynamically adjusting the VSI output to match the motor's operational needs.

To sum up, SPWM-based VSIs that feed single-phase induction motors have practical applications in everyday life and industrial settings. For instance, in household appliances such as washing machines and air conditioners, the control system ensures efficient and reliable operation. In industrial automation, these systems are used in conveyor belts, fans, and pumps where precise speed and torque control are crucial for optimal performance. For a system that consistently performs the same repetitive task with the expected load, both the open-loop and closed-loop control techniques can be effective as they exhibit similar performance. For an electric drive system that requires good speed control even with load variations, a closed-loop scalar speed control method with slip frequency adjustment is essential. The dynamic behavior in both cases will be quite good, and the harmonic distortion of the current will be satisfactory enough, capable to provide a proper AC current to the induction machine’s input.

8.2 Future Work

Finally, several points may be suggested for further investigation and would be interesting to study in the future. One area of potential development is the conversion of the given single-phase system into a three-phase system using a more modern switching control method, such as the Space Vector Pulse Width Modulation (SVPWM) inverter technique. This technique involves resolving the desired reference signal in its vector space, enabling the system to operate on all three phases simultaneously, whereas SPWM operates on a per-phase basis independently. Implementing SVPWM could enhance the efficiency and performance of the motor control system by providing better utilization of the DC bus voltage and reducing the switching losses.

Another area for future work is the speed control of the system using direct torque control (DTC) instead of the traditional constant V/f scalar control. DTC achieves a higher level of precision by algorithmically calculating the motor’s torque using inputs such as motor phase currents and DC bus voltage measurements, in addition to the states of the power-switching transistors within the drive. This method directly controls the motor flux and torque, eliminating the need for modulation or external feedback devices. By doing so, DTC can offer faster dynamic response and improved performance in applications requiring precise torque and speed control.

Additionally, the construction of a single board for the processor, driver, and measurement systems could streamline the overall design and improve the integration of the components. Developing a complete inverter system that includes this unified board along with the power system, and presenting it in a commercial form with detailed data specifications (datasheet), would be highly beneficial. Such a system would not only simplify the implementation process but also enhance reliability and ease of maintenance, making advanced motor control solutions more accessible and attractive for both consumer products and industrial applications. This, in turn, could lead to broader adoption and spur further innovation in the fields of power electronics and motor control technologies.

The implementation of these future enhancements could significantly improve the performance, versatility and market applicability of control systems for induction motors.

REFERENCES

[1] Bose, B. K. (2002). Modern Power Electronics and AC Drives. Prentice Hall.

[2] Chapman, S. J. (2005). Electric Machinery Fundamentals. McGraw-Hill.

[3] Holtz, J. (1992). Pulse width modulation–A survey. IEEE Transactions on Industrial Electronics, 39(5), 410-420.

[4] IEEE Std 519-1992. (1992). IEEE Recommended Practices and Requirements for Harmonic Control in Electrical Power Systems. IEEE.

[5] Holmes, D. G., & Lipo, T. A. (2003). Pulse Width Modulation for Power Converters: Principles and Practice. Wiley-IEEE Press.

[6] Carrasco, J. M., Franquelo, L. G., Bialasiewicz, J. T., Galván, E., Guisado, R. C., Prats, Moreno-Alfonso N. (2006), "Power-electronic systems for the grid integration of renewable energy sources: A survey", IEEE Transactions on Industrial Electronics, 53(4), 1002-1016.

[7] Ned Mohan, T.M. Undeland, W.P. Robbins, Power Electronics, Converters, Application and Design. 3rd Ed; Wiley Education Inc. 2003.

[8] W. M. Hamanah, A. Salem, M. A. Abido, T. G. Habetler, A. M. Qwbaiba, "Dual-axis tracking electrical drives for solar power tower", 19th International Conference on Renewable Energies and Power Quality (ICREPQ'21), at: Almeria (Spain), 28th to 30th July 2021, Volume No.19, pp. 435-440

[9] Σ.Ν. Μανιάς, «Ηλεκτρονικά Ισχύος», Εκδόσεις Συμεών, Αθήνα 2007.

[10] Κ. Βουρνάς, Γ. Κονταξής, «Εισαγωγή στα Συστήματα Ηλεκτρικής Ενέργειας», Εκδόσεις Συμμετρία, Αθήνα 2010.

[11] M. Pastorelli, S. Musumeci and F. Mandrile, "Battery Sources and Power Converters Interface in Waterborne Transport Applications," 2021 AEIT International Conference on Electrical and Electronic Technologies for Automotive (AEIT AUTOMOTIVE), Torino, Italy, 2021, pp. 1-5.

[12] Ντούρος Δ. Ευάγγελος, «Κατασκευή Τριφασικού Αντιστροφέα Για Έλεγχο Κινητήρα Επαγωγής», Διπλωματική Εργασία ΕΜΠ, Αθήνα, Οκτώβριος 2018.

[13] Gonzalez-Longatt, F. (2014). Frequency Control and Inertial Response Schemes for the Future Power Networks. In: Hossain, J., Mahmud, A. (eds) Large Scale Renewable Power Generation. Green Energy and Technology. Springer, Singapore.

[14] Ε. Τατάκης, ‹‹Σημειώσεις Ηλεκτρονικών Ισχύος ΙΙ››, Πανεπιστήμιο Πατρών.

[15] Κ. Γυφτάκης, «Σημειώσεις Ηλεκτρικών Μηχανών, Lecture 0 - Εισαγωγή», Πολυτεχνείο Κρήτης.

[16] Γ. Κιμιωνής, «Σχεδίαση φωτοβολταϊκών μετατροπέων DC/AC σε περιβάλλον Matlab/Simulink», Διπλωματική Εργασία Πολυτεχνείο Κρήτης, Χανιά, 2014.

[17] Yugendra Rao K N, "Design and Simulation of Low Pass Filter for Single phase full bridge Inverter employing SPWM Unipolar voltage switching", Int. Journal of Engineering Research and Applications, ISSN: 2248-9622, Vol. 5, Issue 9, (Part - 1) September 2015, pp.73-83.

[18] Siti Fairuz Binti Hamid, "Single Phase Motor Speed Control Using SPWM Inverter", Diploma Thesis University of Malaysia, Pahang, November 2008.

[19] Δ. Π. Γυπαράκης, «Μελέτη και κατασκευή ηλεκτρονικού μετατροπέα με στόχο τον έλεγχο κινητήρα μονίμων μαγνητών για εφαρμογές ηλεκτροκίνησης», Διπλωματική Εργασία ΕΜΠ, Αθήνα, Απρίλιος 2012.

[20] Bijoyprakash Majhi, "Analysis of Single-Phase SPWM Inverter", Diploma Thesis National Institute of Technology, Rourkela, May 2012

[21] Δ. Ζωγράφος, «Ελαχιστοποίηση Ρεύματος Γείωσης σε Αντιστροφείς Ισχύος DC/AC τύπου Πλήρους Γέφυρας χωρίς Μετασχηματιστή», Διπλωματική Εργασία Πολυτεχνείο Κρήτης, Χανιά, 2013

[22] Ν. Τσιτσόπουλος, "Βελτιστοποίηση Ελέγχου Μετατροπέων DC/AC με χρήση Γενετικών Αλγορίθμων", Διπλωματική Εργασία Πολυτεχνείο Κρήτης, Χανιά, 2006.

[23] Farhana Abdul Hamid, N., Alleef Abd Jalil, M., & Syafiqah Syahirah Mohamed, N. (2020). Design and simulation of single phase inverter using SPWM unipolar technique. Journal of Physics: Conference Series, 1432, 012021.

[24] Koutroulis, E., Chatzakis, J., Kalaitzakis, K., & Voulgaris, N. C. (2001). A bidirectional, sinusoidal, high-frequency inverter design. IEE Proceedings - Electric Power Applications, 148(4), 315.

[25] Walid Emar, Omar A. Saraereh, "Analytical and Comparative Study of Different Types of Two-Leg Chopping up Regulator", January 2019, International Journal of Advanced Computer Science and Applications Vol. 10(No. 5, 2019): pp. 115-128

[26] Κ. Γυφτάκης, «Σημειώσεις Ηλεκτρικών Μηχανών, Lecture 1 – Ηλεκτρομαγνητισμός Και Μαγνητικά Φαινόμενα, Πολυτεχνείο Κρήτης.

[27] Κ. Γυφτάκης, «Σημειώσεις Ηλεκτρικών Μηχανών, Lecture 2 – Μετασχηματιστές, Πολυτεχνείο Κρήτης.

[28] https://www.collegesidekick.com/study-guides/physics/22-7-magnetic-force-on-a-current-carrying-conductor

[29] Κ. Γυφτάκης, «Σημειώσεις Ηλεκτρικών Μηχανών, Lecture 3 – Μηχανές Συνεχούς Ρεύματος», Πολυτεχνείο Κρήτης.

[30] Κ. Φιλιππίδης, «Σημειώσεις Ηλεκτρικών Μηχανών», Πανεπιστήμιο Δυτικής Μακεδονίας

[31] https://www.physicsforums.com/threads/derivation-of-induced-voltage-in-loop.1015240/

[32] https://instrumentationtools.com/ac-generation/

[33] https://www.miniphysics.com/uy1-force-torque-on-current-loop-in-magnetic-field.html

[34] Hajiani, P., & Larachi, F. (2014). Magnetic-field assisted mixing of liquids using magnetic nanoparticles. Chemical Engineering and Processing: Process Intensification, 84, 31–37.

[35] https://www.pinterest.com/pin/alternator-or-synchronous-generator-construction-working--879609370956836421/

[36] https://www.electricaltechnology.org/2022/09/synchronous-motor.html

[37] Asanbayev, Valentin. Alternating Current Multi-Circuit Electric Machines: A New Approach to the Steady-State Parameter Determination. Germany, Springer International Publishing, 2015.

[38] https://pocketsparky.com/knowledgebase/basics-of-synchronous-ac-motors/

[39] Chen, H., Zuo, Y., Chau, K., Zhao, W., & Lee, C. (2021). modern electric machines and drives for wind power generation: a review of opportunities and challenges. Iet Renewable power generation, 15(9), pp. 1864-1887.

[40] Ramprasath, E. & Manojkumar, Purvi. (2015). Modelling and Analysis of Induction Motor using LabVIEW. International Journal of Power Electronics and Drive Systems (IJPEDS). 5. 344. 10.11591/ijpeds.v5.i3.pp344-354.

[41] https://www.xinnuomotor.com/30-kw-electric-motor/

[42] https://www.linquip.com/blog/split-phase-induction-motors/

[43] Ν. Γ. Τζέκας, «Κατασκευή Μοντέλου Για Έλεγχο Ταχύτητας Μονοφασικού Επαγωγικού Κινητήρα», Διπλωματική Εργασία Αριστοτέλειο Πανεπιστήμιο Θεσσαλονίκης, Μάρτιος 2010

[44] Algaddafi, A., Elnaddab, K., Al Ma'mari, A., & Esgiar, A. N. (2016). Comparing the performance of bipolar and unipolar switching frequency to drive DC-AC Inverter. 2016 International Renewable and Sustainable Energy Conference (IRSEC).

[45] Farhana Abdul Hamid, N., Alleef Abd Jalil, M., & Syafiqah Syahirah Mohamed, N. (2020). Design and simulation of single phase inverter using SPWM unipolar technique. Journal of Physics: Conference Series, 1432, 012021.

[46] Antar, Rakan Khalil and A. Abdulaziz. (2018). "Single-phase Induction motor Drive Circuit Based on SPWM and SVPWM Techniques." International Journal of Engineering and Innovative Technology (IJEIT). Volume 7, Issue 10.